A METHOD FOR MEASURING SMOOTH GEOMEMBRANE / SOIL INTERFACE SHEAR BEHAVIOUR UNDER UNSATURATED CONDITIONS

A thesis Submitted to the
College of Graduate Studies and Research
in Partial Fulfillment of the Requirements
for the Degree of Master's of Science
in the Department of Civil Engineering
University of Saskatchewan
Saskatoon, SK Canada

By

Manoj Jogi

Permission to Use

In presenting this thesis in partial fulfillment of the requirements for a Postgraduate degree from the University of Saskatchewan, I agree that the Libraries of this University may make it freely available for inspection. I further agree that permission for copying of this thesis in any manner, in whole or in part, for scholarly purposes may be granted by the professor or professors who supervised my thesis work or, in their absence, by the Head of the Department or the Dean of the College in which my thesis work was done. It is understood that any copying, publication, or use of this thesis or parts thereof for financial gain shall not be allowed without my written permission. It is also understood that due recognition shall be given to me and to the University of Saskatchewan in any scholarly use which may be made of any material in my thesis.

Requests for permission to copy or to make other use of material in this thesis in whole or part should be addressed to:

Head of the Department of Civil Engineering
University of Saskatchewan
Saskatoon, Saskatchewan S7N 5C5
Canada

Abstract

Geomembranes are one of the most widely used geosynthetics in various civil engineering applications. Their primary function is as a barrier to liquid or vapour flow. Smooth Geomembranes are frequently used in combination with different soils, and due to their low surface roughness, are challenging to design to ensure adequate shear strength along the smooth geomembrane-soil interface. It is important to use the appropriate values of interface shear strength parameters in the design of slopes incorporating one or more geomembranes in contact with soils. The parameters are determined by conducting direct shear test on the geomembrane-soil interface. Laboratory tests of interface shear strength for geomembranes and soil are typically carried out with no provision for measurement of pore pressures at the soil/geomembrane interface.

This thesis deals with study of smooth geomembrane-soil interfaces, particularly under unsaturated conditions. The various factors that affect the interface shear behaviour are also studied. The tests were conducted using a modified direct shear box with a miniature pore pressure transducer installed adjacent to the surface of the geomembrane. Geomembrane–soil interface shear tests were carried out with continuous measurement of suction in close proximity to the interface during the shearing process thus making it possible to analyze test results in terms of effective stresses. The method was found to be suitable for unsaturated soils at low values of matric suction.

Results of interface shear tests conducted using this method show that it is quite effective in evaluating interface shear behaviour between a geomembrane and an unsaturated soil. The results suggest that soil suction contributes to shearing resistance at low normal stress values. At lower normal stress values, the interface shear behaviour appears to be governed only by the magnitude of total normal stress.

At high normal stresses, the failure mechanism changed from soil particles sliding at the surface of geomembrane to soil particles getting embedded into the geomembrane and plowing trenches along the direction of shear. A plowing failure mechanism resulted in the mobilization

of significantly higher shear strength at the geomembrane soil interface. It was found that placement water contents near saturated conditions results in lower effective stresses, a shallower plowing mechanism and lower values of mobilized interface shear strength.

Acknowledgements

DEDICATED TO

My Family

Contents

List of Tables

List of Figures

List of Symbols

σ	Normal stress (kPa)
τ	Shear stress (kPa)
a	Adhesion in TS space (kPa)
c	Cohesion in TS space (kPa)
ϕ	Friction angle (degrees)
ϕ_G	Interface Friction angle (degrees)
τ_p	Peak shear stress (kPa)
τ_r	Residual shear stress (kPa)
R_a	Surface roughness parameter (microns)
ΔR	Change in surface roughness (%)
τ'	Effective shear stress (kPa)
u_a	Pore air pressure (kPa)
ψ	Matric suction (kPa)
u_w	Pore water pressure (kPa)
ϕ^b	Slope of failure envelope in shear stress matric suction space (degrees)
β	Parameter related to angle of shearing resistance of soil
LL	Liquid limit (%)
PL	Plastic limit (%)
PI	Plasticity index (%)
If	Flow index
It	Toughness index (%)
w_s	Saturated gravimetric water content
w_w	Gravimetric water content
nf	A fitting parameter related to rate of desaturation of the soil
mf	A fitting soil parameter related to the curvature of the function in high suction range

af	A fitting parameter corresponding to soil suction at inflection point, somewhat related to air entry value of soil
h_r	A constant parameter used to represent soil suction at residual water content
a_p	Peak adhesion in TS space (kPa)
a_r	Residual adhesion in TS space (kPa)
c_p	Peak cohesion in TS space (kPa)
c_r	Residual cohesion in TS space (kPa)
ϕ_{Gp}	Peak friction angle for soil geomembrane interface in TS space
ϕ_{Gr}	Residual friction angle for soil geomembrane interface in TS space (degrees)
ϕ'_p	Effective peak friction angle for soil only obtained by saturated tests (degrees)
ϕ'_r	Effective residual friction angle for soil only obtained by saturated tests (degrees)
ϕ'_{Gp}	Effective peak friction angle for soil geomembrane interface obtained by saturated tests (degrees)
ϕ'_{Gr}	Effective residual friction angle for soil geomembrane interface obtained by saturated tests (degrees)
ϕ''_{Gp}	Peak friction angle for soil geomembrane interface in ES space (degrees)
ϕ''_{Gr}	Residual friction angle for soil geomembrane interface in ES space (degrees)
a''_p	Peak adhesion in ES space (kPa)
a''_r	Residual adhesion in ES space (kPa)
a'_p	Effective peak adhesion obtained by saturated tests (kPa)
a'_r	Effective residual adhesion obtained by saturated tests (kPa)
c'_p	Effective peak cohesion obtained by saturated tests (kPa)
c'_r	Effective residual cohesion obtained by saturated tests (kPa)

Chapter 1   Introduction

1.1   General

Geomembranes are commonly used as barriers in waste containment facilities and landfills due to various benefits associated with their use and because of regulatory requirements. Geomembrane are also increasingly being used in reservoirs, ponds, lined canals and other geotechnical projects. Geotechnical engineers often characterize the shearing resistance along interface between geomembranes and soils using results from interface direct shear tests. The results of these tests are used in an analysis of stability against sliding along the given interface. Interface shear testing between soil and geosynthetics has now become an essential part of the design process in geotechnical and geo-environmental engineering.

1.2   Geomembranes and their applications

Geomembranes are "impervious" thin sheets of rubber or polymeric material used primarily for linings and covers of liquid or solid waste containment facilities (Figure 1.1). Geomembranes represent the largest category (by cost), of geosynthetics products used in civil engineering applications. The growth in the use of geomembranes can be attributed to the various benefits associated with their application, their relative economy and increasingly stringent environmental regulations.

The mechanism of diffusion in geomembrane is on molecular scale which is different from other porous media. Water molecules diffuse through narrow spaces between polymer molecular chains. Geomembranes cannot be regarded as totally impermeable as some amount of diffusion permeation is observed in geomembranes. A typical thermoplastic geomembrane will have diffusion permeability of the order of 10^{-11} to 10^{-13} cm/s. Because of their extremely low permeability, their primary function is as a liquid or vapour barriers. The range of applications is great and at least 30 individual civil engineering applications have been developed (Koerner, 1995).

1.2.1 Landfill side slopes

Contamination of groundwater can be minimized by providing a liner system at the base and sides of a landfill. Landfills side slopes consist of different geosynthetic and soil components (Figure 1.1). A key design element in these systems is the geomembrane in contact with a natural or processed soil. The consolidation of the waste mass in landfills induces movement of the waste relative to the geomembrane. If the geomembrane is restrained, deformation between the geomembrane and the soil may take place. As the deformation progresses, increased shear stress is mobilized at the interface between geomembrane and soil. The waste itself can be quite strong when properly compacted; and hence the stability of waste landfill slope is a function of the interface shear strength along the geomembrane surfaces.

To maximize the containment volumes, landfills are increasingly being designed and constructed with steeper side slopes. However, as the side slope becomes steeper, there is greater potential for failure along one of many interfaces. The failure potential for a particular interface is governed by shear strength between the two individual components of the interface.
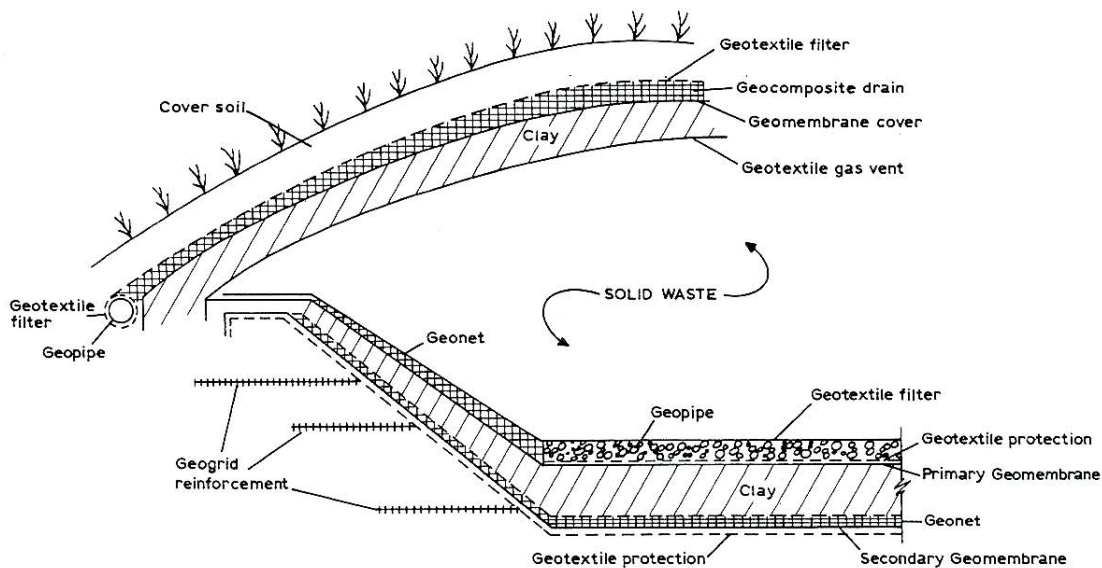
Figure 1.1 Cross-section of a domestic waste landfill showing the use of geomembranes in both the liner and the cover systems (Koerner, 1995)

1.2.2   Landfill Covers

Geomembrane landfill covers are used when it is absolutely necessary to minimize downward infiltration into the waste mass. Further soil cover is placed over the geomembrane to provide a substrate for vegetation which will release moisture back into the atmosphere through evapotranspiration. In landfill covers, the stability is largely governed by the interface friction properties between this surficial soil cover layer and the relatively thin non-woven geotextiles separating the vegetative cover layer from a synthetic drainage layer or sand drainage layer. If a geomembrane is used in a cover system, the interface friction between geomembrane and the adjacent component may govern stability.

The shear strength of the interfaces in each one of these applications governs the overall stability of the structure. The interfaces and their associated failure mechanisms have long been identified as being critical to the overall performance of the geotechnical structures. A significant number of landfills have failed in past due to interface failure. These are discussed by Seed et al. (1990), Mitchell et al. (1990), Stark et al. (2000) and Koerner and Soong (2000). With each new project failure and with ongoing difficulties of siting new landfills (Koerner and Soong 2000), stability is becoming a key issue. Due to this reason a significant amount of research work has focused on the factors that affect the interface shear mechanism. The design of the liner and cover system shown in Figure 1.1 requires the evaluation of slope stability which in turn requires knowledge of interface shear behaviour of geomembrane and soils.

1.3   Past Research Work Related to Soil-Geomembrane Interface

In March 1988, a slope stability failure occurred at the Kettleman Hills Class 1 hazardous waste treatment and storage landfill at Kettleman Hills, California (Byrne et al. 1992). This failure developed by sliding along the interfaces within the composite multilayer liner system beneath the waste fill. The landfill failures given in Table 1.1 are attributed to low friction resistance at the interface between the geosynthetic and soil. These and other similar landfill failures have led to research into the interface friction behaviour for various interfaces at the liner and cap of the landfill. Many researchers have conducted research work on the interface shear behaviour of geomembranes and soils over the last 20 years. Interface shear strength of non-textured geomembrane and soil represents a significant portion of the research work conducted related to geosynthetics.

Table 1.1 Summary of Recent Landfill Failures

Year	Location	Quantity involved	References
1988	N. America	490,000 m^3	Mitchell, et al. (1990)
1994	Europe	60,000 m^3	Koerner and Soong, (2000)
1997	N. America	100,000 m^3	Evans, et al. (1998) & Stark et. al, (2000)
1997	Africa	300,000 m^3	Koerner and Soong, (2000)
1997	S. America	1,200,000 m^3	Koerner and Soong, (2000)

1.4   Need for Further Research

Although considerable research has been conducted into interface shear strength, there is a general lack of sufficient knowledge or control over the primary factors that affect the measured values of interface shear strength parameters. Consensus has yet to be reached regarding the relative importance of various factors that control the interface shear behaviour. Even the standard testing method, ASTM D5321-02 (ASTM 2002), is not adequate since it does not address the existence and effect of initial capillary suction on test results (Bemben and Schulze 1995).

It is worth noting that all the researchers (e.g. Ling et al. 2001, Mitchell et al. 1990) have expressed interface shear strength parameters in terms of total normal stresses instead of effective normal stresses at the interfaces. The soil component of a composite liner system is usually unsaturated, particularly beneath side slopes where the interface shear strength is mobilized. Therefore, there is uncertainty regarding the conditions of the interface in the field and a need for a study that focuses on the behaviour of interfaces between geomembranes and unsaturated soils, with the measurement of negative pore pressures on the geomembrane surface during shearing.

Typically, geomembrane-soil interface shear tests are conducted at several different normal stresses. For each normal stress, the shear stress increases with increasing shear displacement and reaches a peak value. As shearing is continued, there is a reduction in shear stress until a constant or residual value is reached. These peak and residual shear stresses are then plotted against relevant normal stresses to obtain a failure envelope. Curved failure envelopes are obtained for both the drained and the undrained interface shear tests, (e.g. Jones and Dixon, 1998;

Esterhuizen et al., (2001). For the undrained interface shear tests, the failure envelope is more non-linear at low normal stresses as shown in Figure 1.2.

The failure envelope flattens and approaches a limiting value of shear strength as normal stress increases (Figure 1.2). Usually, for the range of normal stresses expected in the field, a linear Coulomb-type failure envelope is drawn through the data points. This failure envelope is defined in terms of two interface shear strength parameters: friction angle (δ) representing its inclination in the shear stress-normal stress space, and adhesion (α) representing the intercept of the failure envelope with the shear stress axis (Figure 1.2). The stability of any slope containing a geomembrane can be assessed using these interface shear strength parameters.
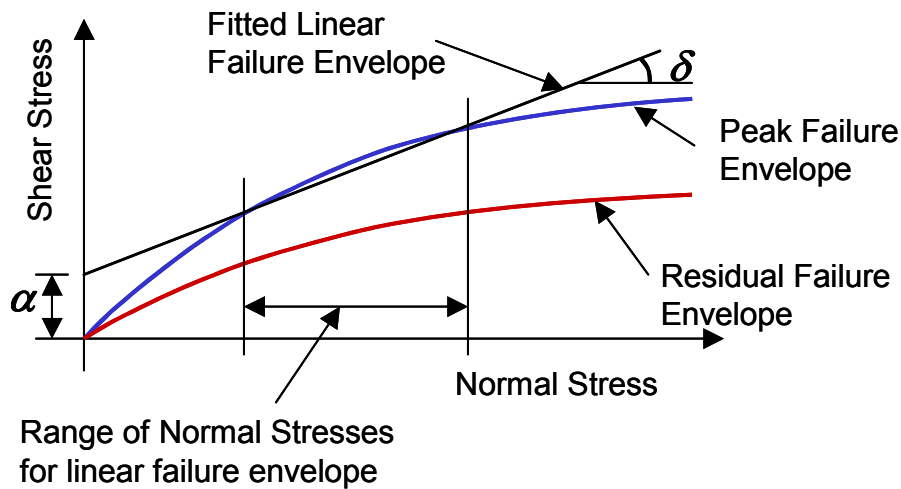
Figure 1.2 Typical undrained failure envelopes for geomembrane-soil interface

While it is possible to simulate a fully drained response by selecting a sufficiently slow shearing rate, it is often difficult to ensure a fully undrained response merely by selecting a very fast shearing rate. Pore-water pressure fluctuates during shearing at the geomembrane-soil interface. Jones and Dixon (1998) have pointed out that such fluctuations could be positive or negative (i.e. suction), depending on the degree of saturation of the soil. In case of an unsaturated soil, negative pore-water pressures are likely to be present at the geomembrane-soil interface. Thus, the measurement of pore-water pressures during shearing is crucial to a correct interpretation of the interface shear strength. Without these measurements, it is quite difficult to establish the magnitude of normal effective stress acting on the geomembrane-soil interface.

A detailed review of published literature on geomembrane-soil interface shear testing has revealed that there have been no previous attempts to measure the pore-water pressure at or near the geomembrane-soil interface. It is, therefore, not surprising to see interface shear strength interpreted in terms of total stresses instead of effective stresses. This is also true for interface shear tests involving smooth geomembranes and unsaturated cohesive soils (Seed and Boulanger, 1991; Fishman and Pal, 1994; Ling et al., 2001). Fishman and Pal (1994), using interface shear strength envelopes plotted in terms of total normal stresses, concluded that higher interface shear strength is mobilized in tests involving unsaturated clays than those involving saturated clays. For the interface shear strength envelopes reported by Fishman and Pal (1994), it is likely that the presence of negative pore-water pressures at the geomembrane-soil interface resulted in a higher effective stress (and therefore, higher shear strength) at the interface. Fisherman and Pal (1994) did not measure pore-water pressures at the interface, and therefore, were unable interpret interface shear strength in terms of effective stresses. Clearly, there is a need to examine geomembrane-soil interface shear behaviour using effective stresses and on the basis of unsaturated soil mechanics principles.

1.5   Objectives of the Research

The main objectives of the research are given below:

1. To develop an apparatus/method to evaluate the effect of soil suction on interface shear behaviour.
2. To analyze the test results in terms of total stress space and effective stress space.
3. To analyze the test results using principles of unsaturated soil mechanics and the feasibility of applying these principles for analysis.
4. To study various other mechanisms controlling the interface shear behaviour of smooth geomembranes and soils. This includes study of interface shear behaviour from Tribological (the science of the mechanisms of friction, and wear of interacting surfaces) point of view

1.6   Scope of the Research

Interface shear strength of geomembrane and soils involves many aspects which include equipments and experimental set up, factors affecting interface shear behaviour, analysis of the

data and the interpretation of the results. Each one of these topics covers many aspects. The presence of geomembrane in contact with soil makes the study even more complicated and it demands study of the interfaces from the point-of-view of tribology (the science of the mechanisms of friction, and wear of interacting surfaces).

However, the scope of this thesis shall be limited to developing a new method for testing interface of geomembrane and soil under unsaturated conditions and preliminary analysis of the test data. The thesis attempts to evaluate feasibility of applying effective stress and Unsaturated Soil Mechanics principles for analysis of interface shear study. It also briefly covers other possible mechanisms that may govern interface shear behaviour of geomembrane and soil.

1.7   Organization of the Thesis

The thesis is divided into six chapters. Chapter 2 provides literature review and basic theory that is related to this research. Chapter 3 outlines the laboratory testing program along with the materials and equipments used for this research work. Chapter 4 presents the experimental results while Chapter 5 presents a detailed analysis of these results. Finally chapter 6 presents conclusions that can be drawn from this study and the recommendations that can be made based on this study. This chapter also discusses future research programs that may be undertaken based on this work.

Chapter 2   Background and Previous Work

2.1   Introduction

This chapter presents background information related to interface shear strength of smooth geomembrtanes and soils. This chapter also presents a comprehensive review of the published literature work related to the geomembrane-soil interface shear behaviour. This also includes the study of various factors that may influence the interface shear behaviour of geomembrane soil interfaces. Further some basic theory related to interface shear strength of unsaturated soils is described.

2.2   Soil-Geomembrane Interface Shear Strength

The shear strength of a smooth geomembrane and soil interface is measured in terms of limiting resistance to sliding deformations and all other mechanisms offered by the soil and geomembrane when the plane of failure passes through the interface. Until the 1990s, there was no generally accepted standard for measuring interface shear strength. Common methods included tilt table, small shear boxes and pull out boxes—all in various sizes and different levels of sophistication. The direct shear box is considered most reliable among the available methods for interface shear testing (Bachus et al., 1993). In 1992, the Geosynthetic Research Institute at Drexel University in Philadelphia, USA adopted the first standard method for measuring interface shear strength (Smith and Criley, 1995).

There are two types of stresses considered in interface shear testing.

1. Normal stress, which act in a direction normal to the plane of cross section being considered. They are referred to as normal stresses or direct stresses. A normal stress in a body resists the tendency either to compress or elongate.

2. Shear stress which act parallel to the plane being considered and are initialized when applied forces tend to cause the successive soil layers to slide over the surface of geomembrane.

2.3 Shear Testing of Interface using Direct Shear Box

The direct shear box is a traditional device used to determine the shear strength of soils in the laboratory. The direct shear box consists of two square or rectangular boxes placed one above the other. The principle of direct shear box is very simple. A normal load N is applied to the top box to produce a vertical normal stress $\sigma = N/A$, where A is the cross-sectional area of the direct shear box. A steadily increasing displacement, which causes an increasing shear force F, is applied to one half of the direct shear box, while the other half is restrained and equipped with a load measuring device.

Similar to direct shear testing, if a mass of soil is made to slide on the surface of a geosynthetic while a load is applied normal to the sliding surface, a test similar to that described above can be carried out to determine the frictional characteristics of a geosynthetic- soil interface. This forms the basis of interface shear test which can be used to measure the angle of interface shearing resistance.

The horizontal displacement of soil in the bottom half of the box relative to that in top half takes place gradually while the force F is increasing. Eventually a maximum shear stress (point B in Figure 2.1) is reached, which is termed the peak shear stress. After the peak, the shear resistance falls off as shown by region BC, at this stage it is considered that the failure of the interface has occurred.
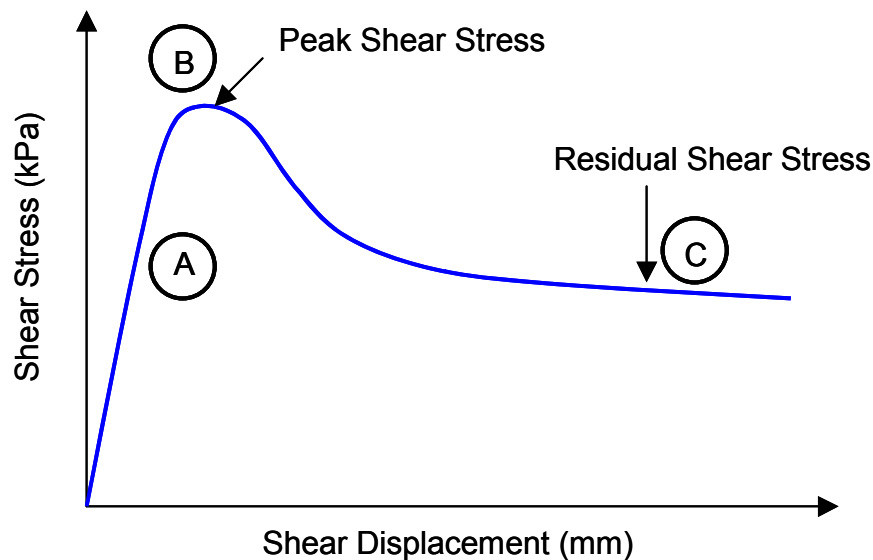
Figure 2.1 Typical plot of shear stress vs. shear displacement obtained using a direct shear box

Generally, several tests can be carried out on the same soil-geosynthetic interface combination by varying the normal load and repeating the test, giving different values of normal stresses. For each normal load, the maximum shear stress can be read off and plotted against the corresponding value of σ_n as shown in Figure 2.2. This graph generally approximates a straight line, with its inclination to the normal stress axis interpreted as the angle of interface shearing resistance (δ) and its intercept with the shear stress axis interpreted as the apparent adhesion (α).
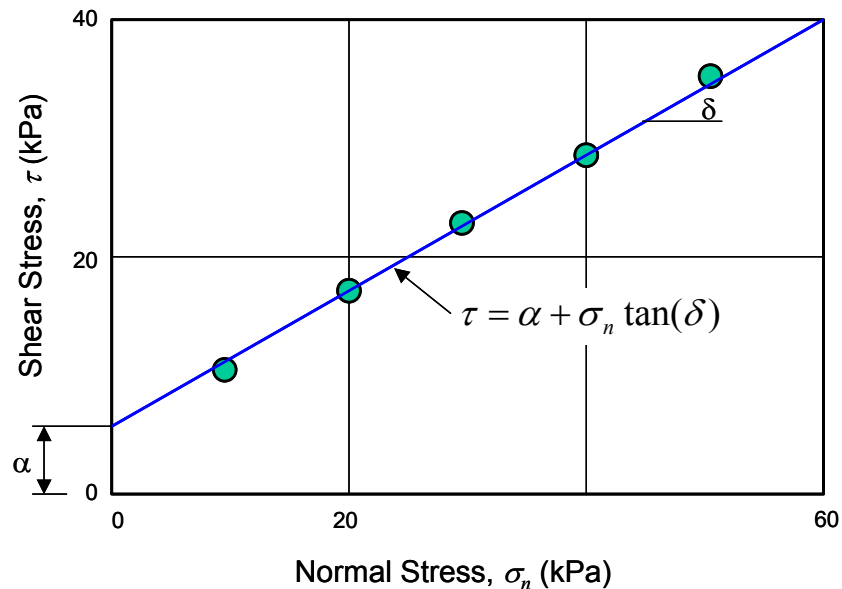
Figure 2.2 Typical plot of shear stress vs. normal stress obtained from direct shear testing of geomembrane-soil interface

The interface relationship between interface shearing resistance, τ and normal stress σ_n can be represented as a linear Mohr- Coulomb type failure envelope:

$$\tau = \alpha + \sigma_n \tan(\delta)$$
<div align="right">**[Eq. 2.1]**</div>

For interface shear testing, the above mentioned relationship is quite useful for most practical purposes and is most widely accepted failure criterion for the interface. The graph which it represents is known as the 'failure envelope' for the geomembrane-soil interface.

2.4   Peak and Residual Interface Shear Strength

2.4.1   Peak Interface Shear Strength

As explained earlier the peak interface shear strength is the maximum resistance offered by the interface that can be sustained on the surface of sliding. The angle of interface shearing resistance obtained by consideration of peak interface shear stresses is called the peak angle of interface shearing resistance.

2.4.2   Residual Interface Shear Strength

If shearing is continued after point 'B' as shown in Figure 2.2, the shear strength decreases rapidly from the peak value to eventually reach a steady state (ultimate) value (Point 'C' in Figure 2.2), which is maintained as the displacement increases. This shear strength which the interface ultimately reaches is known as the residual interface shear strength. The angle of interface shearing resistance obtained by consideration of residual interface shear stresses is called the residual angle of interface shearing resistance.

2.4.3   Use of Peak and Residual Shear Strength in Design

Gilbert and Byrne (1996) have mentioned that the peak interface strengths are mobilized at 1 to 15 mm of displacements and post peak strengths can be as small as 30 % of peak strength. According to Leschinsky (2001), the logic of using the residual values in design is quite compelling because progressive failure is likely in geosynthetic reinforced structures due to the following reasons:

- Strain levels developing in geosynthetics layers are non-uniform thus allowing non uniform deformations within the soil mass.

- Strains can develop to significant values in ductile geosynthetics thus potentially allowing for large plastic strains in soil to exceed local values required to mobilize soil residual strength.

- Geosynthetics are time-dependent materials and thus if a layer is overstressed relative to other layers, its creep strain rate will be larger than other layers allowing for non uniform mobilization of soil shear strength along the potential slip surfaces.

This means that while the soil is approaching its peak strength along portions of the potential slip surface, it would have exceeded its peak along other portions, potentially reaching its residual strength. If a ductile and time dependent reinforcement is used, such a situation is more likely to result. Hence, in such situations, it is recommended that residual values be used in design. Koerner (2003) summarized the following suggestions given by various researchers for use of peak or residual strength in design. These are listed from most conservative to least conservative approaches.

1. Use of residual strength for all conditions (Stark and Peoppel, 1994).

2. Use of residual strength of the interface having the lowest peak strength. This concept applies to multiple geosynthetic interfaces (after Koerner, 2003).

3. Use of peak strength at the base and residual strength throughout the steeper side slope. (Jones et al. 2000).

4. Use of peak strength at the top of slope and residual strength at the base of the slope (after Koerner, 2003).

5. Use of peak strengths for all non-seismic conditions (Koerner, 2003).

Koerner (2003) suggests that when using residual strength in design there is no likelihood at all of failure and so while such an approach is undoubtedly extremely conservative, it is unnecessarily so.

2.5   Standards for the Determination of Interface Shear Strength

Currently there are three standards in common use for interface shear testing procedures for geomembranes. Table 2.1 shows a detailed comparison of these three standards.

- ASTM D 5321-92 (American standard)
- BS 6906:1991 (British standard)
- GDA E 3-8 1998 (German recommendation for landfill design).

In North America, ASTM D 5321-92 is commonly used to determine interface shear resistance of geosynthetic and soils. Under ASTM D 5321 square or rectangular boxes are recommended and they should have a minimum dimension that is the greater of 300 mm (12 inches) or 15 times the

d_{85} of the coarser soil used in the test. This box allows the user to test larger gradation of soils such as gravels for leachate collection systems or similar applications. It also enables the user to evaluate the mode of shear failure over a larger specimen area. The minimum depth of the box containing soil is recommended to be 50 mm or six times the maximum particle of the coarser soil tested, whichever is greater. However it is also mentioned that containers smaller than those specified earlier can be used if it can be shown that data generated by smaller devices contain no bias when compared to the minimum size devices specified earlier.

Table 2.1 Comparison of British, North American and German standards for the determination of geomembrane-soil interface shear strength

Standard	BS6906:1991 (British standard)	ASTM D5321:2002 (North American standard)	GDA E3-8 1998 (German standard)
Test apparatus	Direct shear box about 300 mm square	Direct shear box minimum 300 mm square	Direct shear box minimum 300 mm square for geosynthetics without surface structure and 100 mm for fine grained soils
Number of tests conducted	9 tests in total (3 tests for each normal stress of 50, 100 and 200 kPa)	Minimum 3 tests at 3 different normal stresses (user defined)	3 tests with3 different normal stresses and 2 repeating tests with the mean valuewhih should match expected normal stress insitu.
Method of fixing geosynthetics	Clamped or glued to rigid substratum	Clamping outside shear area or gluing to a rigid substratum	Recommendation about support and fixation depends on individual test case
Shearing rate	Geosynthetic/geosynthetic and geosynthetic/non cohesive soil, 2 mm/min Geotextile/ soil, variable rate depending upon drainage	Geosynthetic/geosynthetic, 5 mm/min if no material specification Geosynthetic / soil slow enough to dissipate excess pore pressures If no excess pore pressures expected 1mm/min	Geosynthetic/geosynthetic and geosynthetic/non cohesive soil, 0.167 to 1 mm/min Geotextile/cohesive soil, 0.167 mm/min Geosynthetic liner /cohesive soil 0.005 mm/min
Location of materials in shear box	Geosynthetic/ geosynthetic, rigid substratum Geosynthetic/soil , either rigid substratum, soil in top or bottom box Depth of soil layer not specified	Geosynthetic/ geosynthetic, rigid substratum Geosynthetic/soil , geosynthetic supported by rigid substratum and soil in top or bottom box Depth of sand layer not specified	Geosynthetic/ geosynthetic, rigid substratum Geosynthetic/soil , geosynthetic supported by rigid substratum Soil either in top or bottom box Depth of soil layer not specified
Specific reporting requirements	All plots and calculations Describe failure mode	All plots and calculations	Detailed report about test equipment, procedures and observations during testing about measured data and further evaluation

Some researchers have used a 100 x 100 mm shear box for interface shear testing of smooth geomembranes and soils (Ling et al., 2001). The use of a 100 x 100 mm shear box can be justified because smooth geomembranes have a uniform surface structure as compared to other geosynthetic materials. Issues related to the effects of aperture and rib size, that are to be considered for geogrids, do not exist in a geomembrane. The geomembrane can be placed in various ways depending on how well it represents field conditions. This usually involves clamping the geosynthetic specimen from one or both ends or gluing it to a rigid surface.

2.6　Shear Strength Theory for Unsaturated Soils

2.6.1　Shear Strength of Unsaturated Soils

The shear strength theory of unsaturated soils is described here to provide an idea about how various factors contribute to shear strength under unsaturated condition. According to Fredlund and Rahardjo (1993) the shear strength of unsaturated soil can be formulated in terms of three independent stress state variables and any two of the three possible stress state variables can be used for the shear strength equation. The stress state variables $(\sigma - u_a)$ and $(u_a - u_w)$ have been shown to be the most advantageous combination for practice. Using these stress variables, the shear strength equation for unsaturated soil is written as follows:

$$\tau' = c' + (\sigma - u_a)\tan\phi' + (u_a - u_w)\tan\phi^b \qquad \text{[Eq. 2.2]}$$

where σ = total stress; c' = effective cohesion; u_a = pore air pressure (normally zero as was assumed in this study for the reasons discussed later); u_w = pore water pressure; ϕ' = the effective friction angle; ϕ^b is the parameter indicating increase in shear strength, $\Delta\tau$, per increment of suction, $\Delta\psi$.

The shear strength equation for saturated soil is a special case of the above equation. For an unsaturated soil, two stress state variables are used to describe its shear strength while only one stress state variable [i.e., effective normal stress $(\sigma - u_w)$] is required for a saturated soil.

The shear strength equation for an unsaturated soil exhibits a smooth transition to the shear strength equation for a saturated soil. As the soil approaches saturation, the pore water pressure, u_w approaches the pore-air pressure u_a and the matric suction goes to zero. The matric suction component vanishes and the shear strength equation for unsaturated soil reverts to equation for a saturated soil.

The relative magnitudes of $\tan\phi'$ and $\tan\phi^b$ in the equation for shear strength of an unsaturated soil can be described by parameter β (Bishop, 1959):

$$\beta = \frac{\tan\phi^b}{\tan\phi'}$$

[Eq. 2.3]

where β takes a value between 0 and 1 depending on the degree of saturation of the soil ($\beta = 1$ for fully saturated soil and $\beta = 0$ for dry soil).

2.6.2 Extended Mohr-Coulomb Failure Envelope for Unsaturated Soils

The Mohr's circle corresponding to a failure condition for unsaturated soils, can be plotted in a three dimensional manner as shown in Figure 2.3. The three dimensional plot has the shear stress τ, as the ordinate and the two stress state variables (u_a-u_w) and $(\sigma-u_w)$ as abscissas. The frontal plane represents saturated soil where matric suction is zero.
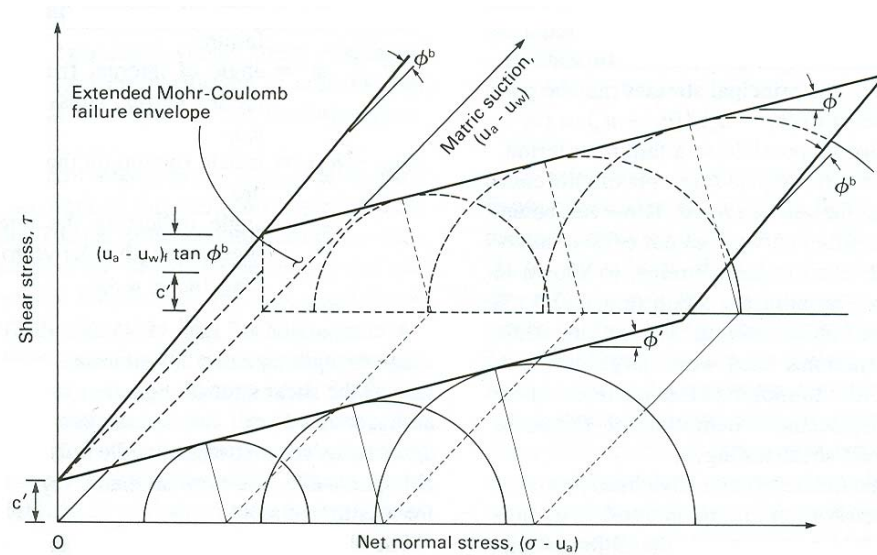
Figure 2.3 Extended Mohr-Coulomb failure envelope for unsaturated soils (Fredlund and Rahardjo, 1993)

The Mohr's stress circle for an unsaturated soil is plotted with respect to net normal stress axis $(\sigma-u_a)$, in the same manner as Mohr's stress circles are plotted for saturated soils with respect to effective stress axis $(\sigma-u_w)$. However, the location of Mohr's stress circle plot in the third

- 15 -

dimension is a function of matric suction. The surface tangent to the Mohr's stress circle at failure is referred to as the extended Mohr failure envelope for unsaturated soils (Fredlund and Rahardjo, 1993).

The strength of unsaturated soils is affected differently by changes in normal stress than by changes in matric suction. The increase in shear strength due to an increase in net normal stress is characterized by the friction angle ϕ' while the increase in shear strength caused by increase in matric suction is describe by angle ϕ^b. The value of ϕ^b is consistently equal to or less than ϕ' depending on the soil. Fredlund and Rahardjo (1993) have described various soils from different locations that have value of ϕ^b that is consistently equal to or less than ϕ'.

2.7   Factors/Mechanisms affecting Interface Shear Properties

The total shear resistance along a geomembrane soil interface may be a result of one or a combination of following mechanisms:

- Sliding
- Adhesion
- Rolling of soil particles
- Interlocking of soil particles and geomembrane surface
- Embedment of soil particles in geomembrane surface (plowing)
- Suction

The manner in which these mechanisms contribute to the interface shear strength of geomembrane-soil depends upon several factors described later. The identification of the mode of failure and understanding the relationship between test parameters selected and mode of failure is very important in predicting the behaviour of geomembrane soil interaction in field. Following are the factors that influence geomembrane soil interface shear behaviour.

2.7.1   *Normal Stress*

It has been observed that the strength envelope for many soils and geosynthetics is curved over a wide range of normal stresses (Figure 2.4). Even if the tests are conducted over a wide range of normal stress, the selection of design parameters is critical. For the data presented in Figure 2.4(a), the test results indicate a non linear response of shear stress versus normal stress.

Selection of different failure envelopes will result in different values of friction angles. For instance selection of no (1) provides a reasonable fit to the data at high pressures but severely overestimates the low-pressure response. Selection of No (2) provides a reasonable fit to the data at low pressures but severely overestimates high pressure response. For these data a bilinear envelope using No (1) and No (2) would reasonably approximate the actual laboratory response. If the designer dos not recognize the bilinear fit or the curved envelope, a best fit straight line through all data points may be justified. Hence data obtained for one specific application using a selected range of normal stresses can not be reliably used for a different application. For instance if data used for the design of a cap or landfill cover were used in design of base liner an unconservative design might result.

Dilation or contraction of soil particles takes place depending on the magnitude of normal stress. Koutsourais et al. (1991) reported that the dilation of soil under low normal stresses results in an increase in interface friction between the layers. Hence, geosynthetics that promote dilation at the interface exhibit greater interface friction under low normal stresses. Williams and Houlihan (1986) suggested that dilation is the primary component of interface friction and that highest interface friction angles are developed between layers where a significant amount of dilation occurs. Jones and Dixon (1998) mentioned that in general for an interface test, the test parameters define the failure envelope only for the range of normal stress tested and extrapolation of friction angle and adhesion outside the range may not be a good design practice. Furthermore the designer should recognize that the strength parameters 'a' and 'ϕ' are only mathematical expression of test results. These must not be viewed out of the context of the tested normal stress range.
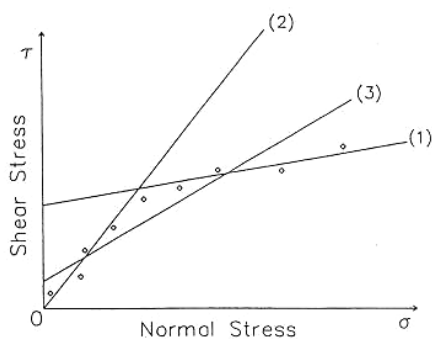
(a) Linear approximations   (b) p-order hyperbolic curve
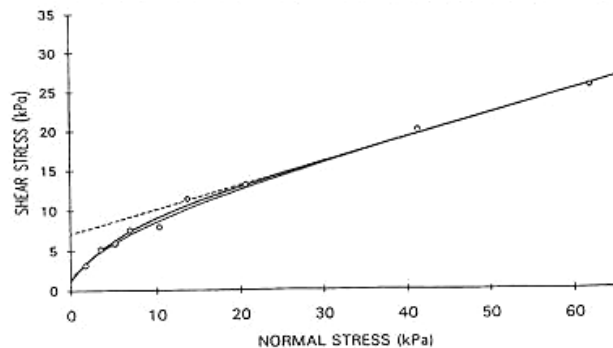
Figure 2.4 Non-Linear shear strength response and various fitting methods (after Giroud et al. 1992)

2.7.2 Soil Compaction Conditions

Soil compaction conditions involve the compaction moisture content and density. For a given compactive effort and dry density, clay tends to be more flocculated for compaction   when compacted dry of optimum moisture content as compared to compaction at higher moisture content on wet side (Lambe and Whitman, 1969). Increasing moisture content tends to increase interparticle repulsion permitting a more orderly arrangement of soil particles to be obtained. The permeability of cohesive soils that are used in landfills is controlled mainly by moisture content and dry unit weight at the time of compaction. According to Swan et al (1991), since permeability and shear strength of cohesive soils are affected by compaction conditions, it should be expected that the shear strength at the interface involving cohesive soils and geomembranes will also be affected by compaction conditions.

Seed and Boulanger (1991) conducted interface shear testing on various HDPE geomembrane- clay combinations. They found that as compacted friction angles for those interface combinations can change by a factor of two as a result of minor variations in density and water content. Ellithy and Gabr (2000) have observed that for as-compacted interfaces the increase in moisture content leads to a decrease in shear strength. Swan et al. (1991) conducted testing on soil and geomembranes by varying the water content and dry unit weight in each test. They found that the peak shear stresses increased with the increase in water content and increase in dry unit weight.

Mitchell et al. (1990) tested various interface combinations and found that presence of water affects the behaviour of interfaces considerably. They classified the interfaces as wet and dry. The wet interface consisted of soil compacted at optimum moisture content and then placed in water and allow to swelling for 24 hours prior to testing. The dry interfaces consisted of soil which was compacted at optimum moisture content and without soaking. They observed a considerable decrease in interface shear strength in the case of wet interfaces. Simpson (2000) suggests that no assurance can be made that the interface will remain dry, and therefore tests should be conducted in saturated conditions. Many researchers as mentioned above have reported a significant influence of compaction conditions on interface shear strength and hence the interface testing program should be selected such that it covers an appropriate range of compaction conditions in addition to all other important test variables.

2.7.3 Rate of Shear Displacement

There are different views regarding the selection of the appropriate rate of shear displacement and its effect on the interface shear strength. Bemben and Schulze (1993) stated that the effect of the displacement rate is significant. They found that high rates of displacement (60 mm/hr) together with flooded conditions produces large peak shear stresses for the glacial till and smooth HDPE interface. However they did not give any opinion regarding the effect of the displacement rate in the case of residual stress.

Fisherman and Pal (1994) tested the interface for smooth geomembrane and compacted clay (glacial till). They found that the interface shear behaviour within a range of rate of displacement of 0.3 mm/hr to 0.9 mm/hr does not change appreciably. However this was not the case for a textured geomembrane interface. Fisherman and Pal (1994) recommended that extremely low rates of shear displacement, in the order of 10^{-3} mm/hr, or the use of thin clay samples in contact with the smooth HDPE interface, should be employed to achieve drained conditions.

ASTM D 5321-92 specifies the rate of displacement for interface shear testing as 0.016 mm/hr (1mm/min.). This rate is intended for inter laboratory comparison purposes. However a displacement rate that best matches the anticipated field conditions should be selected. For interface shear testing when truly drained conditions are desired a considerably slower rate may be required. Bove (1990) stated that for applications where geomembranes are used, geomembranes may prevent soil drainage and hence the tests should be conducted in undrained conditions. For the reasons listed above, the interface shear testing involving a cohesive soil is generally performed under undrained conditions. Selecting the appropriate rate of displacement can make it possible to conduct the smooth HDPE/clay interface shear testing in either drained or undrained conditions. Due to this it is expected that variation in rate of displacement may produce different shearing response especially for smooth geomembrane-cohesive soil interfaces.

2.7.4 Consolidation

In many cases the critical interface is the one involving the soil (i.e. compacted clay). According to Gomez and Filz (1999), a significant increase in the interface strength may take place during the consolidation of clay layer in a composite liner. In the field, the consolidation of liner may take place under the imposed loads and this may substantially increase the interface shear

strength. Gomez and Filz (1999) further stated that during interface shear testing, the thixotropy of clay may induce a significant increase in the interface shear strength with time and this effect is more pronounced at higher compaction water contents. This thixotropic strength gain (comparative increase in the shear strength of clay geomembrane interface that is shared some time after compaction and application of normal load compared to the interface sheared immediately after compaction) may be important for interpretation of the results of testing programs in which interface shear tests are performed at different times after compaction of the clay specimens.

Swan (1999) reported that the effect of consolidation is more for the residual shear strength compared to the peak shear strength of the smooth geomembrane-clay interface. Fisherman and Pal (1994) stated that the shear displacement required to reach peak shear stresses is extremely small for clay-smooth HDPE interfaces and is of the order of 0.25 mm. Due to this reason, it is difficult to attain drained conditions during shear for interfaces involving clay having low coefficients of consolidation.

Conducting an interface direct shear test immediately after applying the normal stress (unconsolidated loading) would potentially simulate the relatively rapid placement of waste during landfilling operations. Allowing the clay to consolidate under the imposed normal load before conducting the interface test can model the long term response of the liner. It should be noted that it is not possible to guarantee and control whether the specimen is fully consolidated or not during interface shear testing.

2.7.5   Type of Geomembrane

The interface shear strength is obviously influenced by the type and essentially roughness of geomembranes with rough surfaced geomembranes having higher values of interface friction as compared to geomembranes having smooth surface. The overall stability of a given structure is governed by the strength of the weakest interface. In order to avoid the situation in which the geosmembrane interface represents a preferential failure surface, it would ideally be desirable that interface friction angle would be equal to or greater than the friction angle for soil itself. In order to approach such a condition, geomembrane manufacturers have developed textured geomembranes (geomembranes having sprayed or extruded textured surfaces) so that failure surface is moved slightly away from the polymer interface and passes through the soil. Dove et al. (1997) studied granular soil-geomembrane interface by quantifying the geomembrane

roughness in terms of R_S, a three dimensional surface roughness parameter defined as ratio of actual surface area to the nominal surface area. They defined a parameter called 'interface efficiency' as the ratio of peak interface friction angle to the peak soil friction angle. An 'interface efficiency' of 1 indicated interface strength being equal to the internal friction angle of the soil. They found that as the roughness of geomembrane is increased the strength increased up to a limiting value of roughness corresponding to roughness required to achieve full efficiency.

Textured geomembranes comes in various types such as textured–one-side and textured-both -sides. The frictional resistance for a textured geomembrane having textures on both sides is highest. While such textured products are useful in this regard, they have a number of disadvantages, particularly during construction and installation like difficulty in seaming the geomembranes particularly at a location different than edge of original roll, less puncture resistance etc. Further, in many cases the tensile strength and puncture resistance of a blown film geomembrane is 50% or less than that of a smooth geomembrane (Von Pein and Lewis 1991). This reduction is less compared to a geomembrane having texture only on one side. Because of this, smooth geomembranes continue to be more widely used.

There are also disadvantages in using textured geomembranes in construction due to the increased difficulty of working with textured products and the necessity to grind the textures when seaming is to be carried out at locations other than the edges of the original roll. All of these conditions continue to increase the installation cost of a textured geomembrane by $ 0.50 to $ 1.00 per m^2 compared with a smooth geomembrane.

2.7.6   *Effect of Hardness of Geosynthetic Polymer*

O'Rourke et al. (1990) conducted the interface shear tests on sand and geomembranes with the aim of investigating the effect of the hardness of the polymer on interface friction. They tested HDPE, polyvinyl chloride (PVC) geomembranes and pipes. From observation of the surfaces using Scanning Electron Microscope (SEM) before and after shearing, they found that hardness plays a very important role in development of interface shear strength. They concluded that the interface shear strength decreases as the hardness of the polymer increases.

The critical stress is the minimum amount of normal stress after which plowing occurs on the surface of geomembrane. The magnitude of critical stress is governed by the hardness of geomembrane and the nature of particles of the soil. The mechanism of particle movement at the interface is directly determined by the magnitude of normal stress relative to the critical stress,

which, in turn, is determined by the hardness of the surface. When the normal stress is less than the critical stress, sliding without damage to the surface is the primary mode of failure. When the stresses at the particle contacts are greater than the critical stress, particle motion along the surface involves both sliding and plowing. Plowing occurs when the normal stresses at the surface exceeds the critical stress. This forces the particles to penetrate the surface and remove material from the surface during translation. When plowing occurs in addition to sliding, an increased force is required to displace the soil relative to the surface, resulting in an increased interface friction. The amount of plowing or abrasive wear is a function of both surface hardness and shearing distance (Dove and Frost 1999).

2.7.7 *Effect of Shape of Soil Particles*

Vaid and Rinne (1995) conducted research on geomembrane and sand interfaces using a ring shear apparatus. They studied the influence of particle shape, confining pressure and relative displacement on the interfaces. They used smooth, textured HDPE and PVC geomembranes and did a quantitative assessment of surface texture using a profilometer. They found that the friction mobilized at sand-geomembrane interface is governed by the angularity of the sand and it is comparatively more for sand with higher particle angularity.

According to O'Rourke et al. (1990) the tendency of soil particles to induce wear on a surface is governed by the applied normal load and the physical and mechanical properties of the interface materials. Further angular particle exhibit large contact stresses resulting in greater interface friction angle. It seems obvious that the interface shear strength will be greater in the case of rough particles as compared to smooth ones. Zettler et al. (2000) mentioned that as particle angularity increases the interface shear strength along geomembrane interfaces also increases. This may be due to plowing of the particles in the surface of the geomembrane.

2.7.8 *Plasticity Index of Soil*

Ling et al. (2001) conducted some interface testing on PVC geomembranes using clays with different plasticity indices ranging from 35 to 100 %. They found that with increase in plasticity index up to a value of 70 %, the interface friction angle increases and beyond the plasticity index value of 70% the interface friction angle decreases. The soil surface may have a good interaction with smooth geomembrane depending upon the plasticity of soil and this may influence the shear behaviour of smooth geomembrane-soil interfaces.

2.7.9   Effect of Test Set-up

The test set up is also found to influence the results obtained by an interface shear test. Blumel and Stoewahse (1998) analyzed test results obtained using different types of shear devices including devices with a completely fixed upper box (with vertical and horizontal support) and devices with only a horizontally supported upper box. Figure 2.5 shows a direct shear test set up having horizontally supported upper box. In this type of test set up, tilting of the load plate or the tilting of the upper box may occur as shown in the Figure 2.5. The type of direct shear test set-up shown in Figure 2.6 has a completely fixed upper box. In this type of test set-up, the tilting of upper box may not take place but the tilting of loading plate may occur. Further vertical friction stresses can occur along the inner walls of the upper box which can lead to a reduction of the average vertical stress in friction interface.
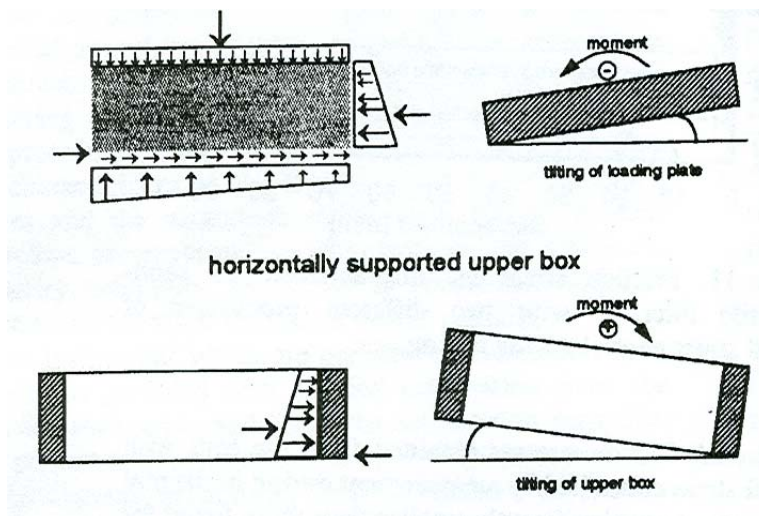
Figure 2.5 Interaction forces, stresses and deformations occurring in case of shear device with horizontally supported upper box. (Blumel and Stoewahse 1998)

Blumel and Stoewahse (1998) found, based on limited data for shear devices with horizontally supported upper box, that the friction stresses measured in tests with a fixed upper box are higher than those obtained from tests in devices with only horizontally supported upper box.

Another important aspect of test set up is the anchoring method of geomembrane. The geomembrane can be anchored to one side of box or it can be allowed to free float. Both of these methods are common. The free floating method, however, can introduce some non conservative

errors. As one box slides relative to geomembrane, portions of geomembrane can be compressed. Under these circumstances the stress state of the interface is unknown and the data is difficult to interpret. This stress state is rare in field, especially under slopes and this phenomenon can lead to serious scale effects in the laboratory (Smith and Criley, 1995). For interface shear tests involving smooth geomembranes, gluing of geomembrane to a rigid substratum is widely used practice (Ling et al., 2001, Mitchell et al., 1990, Gomez and Filz, 1999).
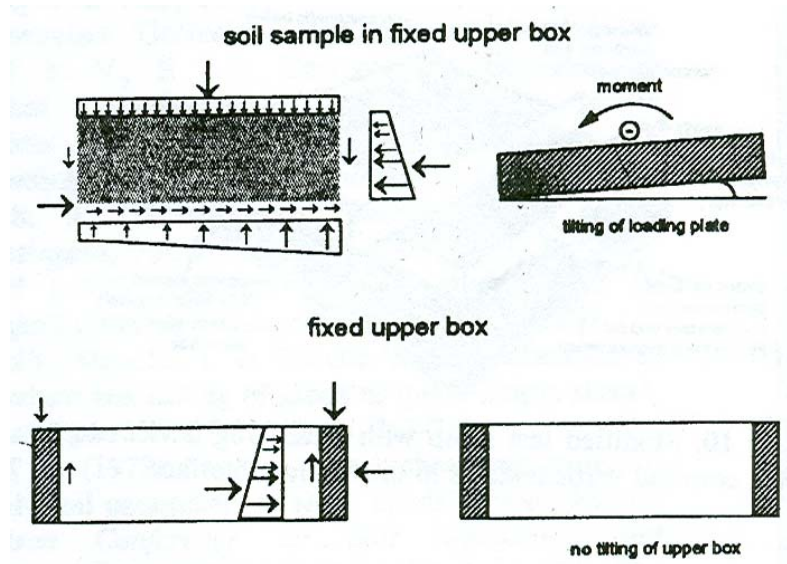
Figure 2.6 Interaction forces, stresses and deformations occurring in case of shear device with fixed upper box. (Blumel and Stoewahse 1998)

In general, the test equipment and set up affect the characteristic of stress versus displacement curves, and the magnitude of peak stresses. Hence it is recommended that the test set up and equipment should be in accordance with the expected situations at the site as well as possible. The method of load application and its effect should always be considered when carrying out interface shear tests.

2.8   Pore-water Pressure Aspects of Interface Shear Testing

Jones and Dixon (1998) mentioned that the testing of interface is complicated due to the presence of pore pressures at the interface during shearing. These pore pressures may be positive or

negative (suction) and they can increase or decrease effective stress at interface thus making the assessment of interface shear strength more difficult.

According to Fisherman and Pal (1994), the failure plane must pass through the soil material at or near the interface. They mentioned that the effective stress in the soil depends on the drainage conditions. During the drained test, the pore water pressure remain close to zero during the shear and deformations are compressive similar to those for the clay alone. During undrained shear testing of a textured geomembrane and clay a dilative response is observed. Due to lack of drainage and the tendency for dilation, a reduction in pore pressure occurs near the interface. This results in a tendency to increase the effective confining pressure which in turn results in increase in interface shear strength.

According to Bemben and Schulze (1995), initial suction can develop with in a wet clay specimen (at low water contents) either at the end of setup (set up includes fabrication actions, consolidation and shearing actions) or at the end of consolidation and can be maintained during shearing. The creation of suction (negative pore pressures) is accompanied by the formation of menisci at the air boundary surface of soil specimen due to absence of free water at the interface. The form of this suction is same as self created capillary state in a fine grained soil located above water table. Bemben and Schulze (1995) further predicted that for the tests that are conducted under unsaturated conditions, absence of free water at the boundaries promotes initial suction prior to and during shearing. They warned that initial capillary suction may affect the values of failure stresses obtained by such tests. Further if proper judgement is not used, interpretation of test results may lead to unconservative design.

The effect of this suction can be offset by using a sufficiently slow rate of displacement. Bemben and Schulze (1995) did not measure this suction and suggested that suction effects can be offset by making sure that the test is conducted under flooded boundary conditions and with a high degree of saturation. They further suggest that ASTM D5321-92 as it applies to fine grained soil/geomembrane testing is not adequate as it does not addresses the existence and effects of initial suction and suction observed during sliding on test results.

It is noteworthy that no attempt was made to measure the pore pressures that may be developed during interface shear testing. The pore pressure controls the magnitude of effective normal stress and they may play an important role in mobilization of interface shear strength.

2.9   Summary

A significant amount of research work has been carried out on direct shear testing of soil-geomembrane interfaces during past 15 years. The interface shear strength of geomembrane and soils is controlled by the factors discussed above. The interface friction angle is more sensitive to some of these factors compared to others. Many researchers have conducted the interface shear testing under as compacted (unsaturated) conditions. However they have used principles of saturated soil mechanics to interpret the results of these tests. Most of the researchers have emphasized the importance of conducting the interface shear testing to represent the field conditions as close as possible. However a detailed review of published literature on geomembrane-soil interface shear testing has revealed that there has been no previous attempt to measure pore water pressure at or near the geomembrane-soil interface. It is therefore not surprising to see that interface shear test results are interpreted in terms of total stress space instead of effective stress space.

With this in mind the thesis attempts to find the role of pore pressures developed on interface shear strength of smooth geomembrane and soils. Further a comparison of the results interpreted in terms of total stress space and effective stress space and using unsaturated soil mechanics principles is also made. Because the interface involves geomembrane and this might introduce many complications in application of soil mechanics principles. Hence the possibility of additional mechanisms that may control the interface shear behaviour of geomembrane-soil interfaces is also taken into consideration.

Chapter 3   Materials and Laboratory Testing Program

3.1   Introduction

Chapter 3 presents the details about the materials that were used for this study. It also describes the testing program carried out. The testing program includes the tests carried out on soil, soil geomembrane interface including the tests conducted with and without pore pressure measurements. The tests conducted without pore pressure measurements were used for determining the effects of various factors on shear behaviour of geomembrane-soil interface. A portion of chapter 3 is devoted to the equipments used in the testing program and the modification of these equipments to suit the testing requirements. The experimental set up is also described.

3.2   Scope of the Testing Program

In the present study the interface shear testing was carried out for various interfaces shown in table. The tests were conducted with and without measurement of pore pressures. The tests with pore pressure measurement were conducted using a modified direct shear box with a miniature pore pressure transducer (called as PPT hereafter) installed adjacent to the surface of the geomembrane. The working principle of the PPT and its usage is described later in this chapter. The interface shear tests were carried on smooth geomembrane and various types of soils. The soils used in the testing program included sand bentonite mixture having 3 % and 6 % bentonite (in combination with Ottawa sand), sand and artificial sandy silt mixture (described in detail later in this chapter). Tests were conducted without pore pressure measurements. This was to determine the effects of various parameters on interface shear behaviour. Total of 8 tests were conducted on silty sand interface with pore pressure measurement and a number of tests were conducted on sand bentonite mixture- geomembrane interface. In addition to this dry and saturated tests on each type of soil were also carried out.

3.3   Materials Used

3.3.1   Sand-Bentonite Mixture

A sand bentonite mixture was used having 3 % and 6 % bentonite in combination with Ottawa sand. The grain size distribution for these materials is as shown in the Figure 3.1.
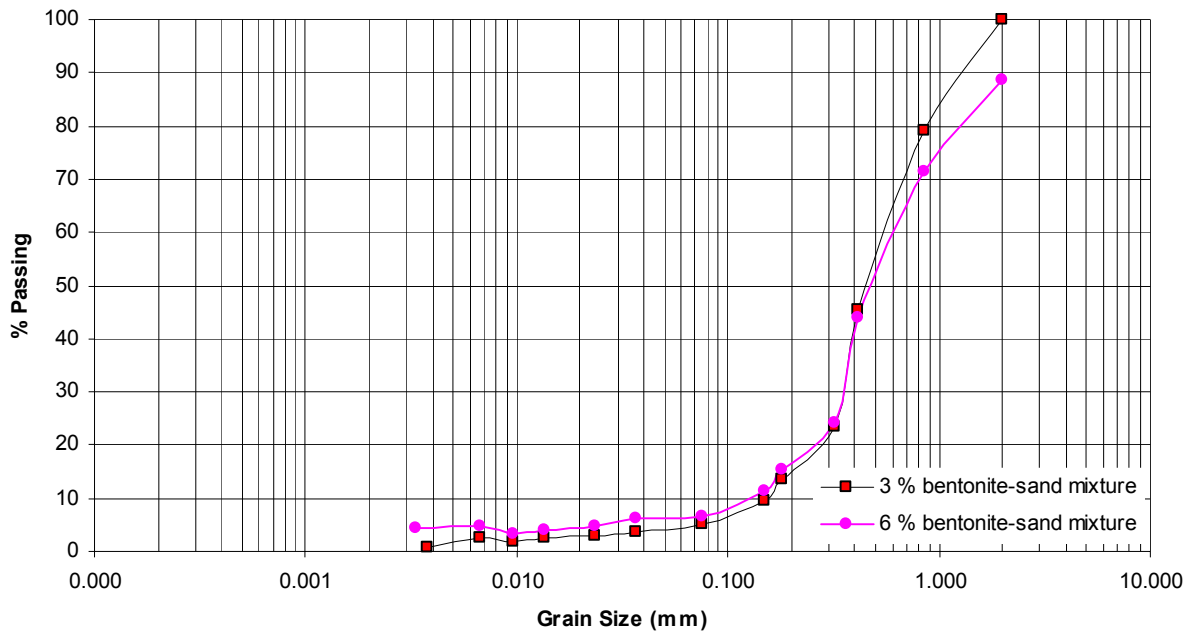
Figure 3.1 Grain size distribution for 3% sand bentonite mixture and 6% sand bentonite mixture

3.3.2   Artifical Silty Sand Mixture

A common requirement for the soil component of liner is that it should have a hydraulic conductivity of 1×10^{-7} cm/sec. or less. According to Ellithy and Gabr (2000), this requirement is usually met by soils that have at least 20 % fines (fine silt and clay sized particles). It is well known that the variation of properties in natural soils is very large and thus artificial soils were used in this study. In order to effectively vary suction by varying the moisture content during compaction, it was necessary to select a soil for which the suction-moisture content relationship (i.e. the Soil Water Characteristic Curve or SWCC) exhibits a gradual increase in suction with a decrease in moisture content, thus avoiding any sharp changes across the range of suctions of interest (0 to 50 kPa). Therefore, the grain-size distribution of the soil was adjusted using the procedure suggested by Fredlund et al. (2002) until a soil that exhibited the SWCC described above was obtained.

The grain-size distribution of the selected soil is shown in Figure 3.2. The final silty sand mixture is a mixture of seven different soils. All soils were taken in appropriate proportions and mixed thoroughly in order to get a uniform soil mass of 10 kg. Table 3.1 shows the percentage of each soil used in the final soil mixture. It can be seen from Figure 3.2 that the soil contained approximately 65% sand-sized particles and approximately 35% silt-sized particles.

Table 3.1 Percentage of various soils used to make the silty sand mixture

No.	SOIL	% by weight
1	Ottawa Sand	10
2	Natural Sand	15
3	Silica Sand	14
4	Marshal Blender	14
5	98102 Binder	17
6	Silt	20
7	Indian Head Till	10
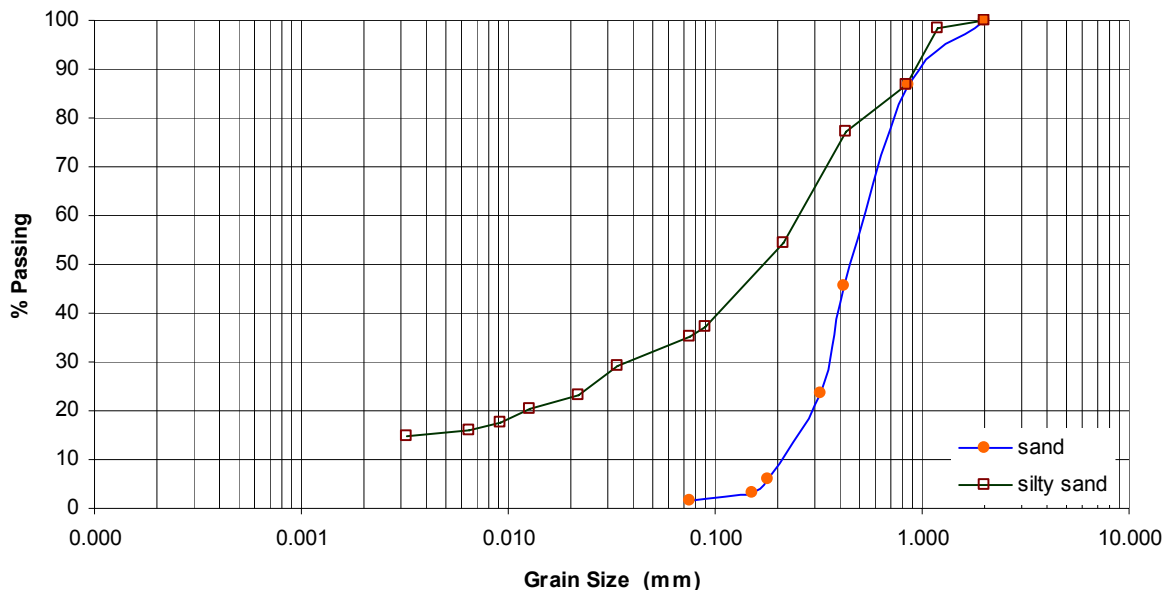
Figure 3.2 Grain size distribution curve for the silty sand mixture and sand

Based on the grain size distribution, the proposed soil it is classified as silty sand. The index properties of the silty sand are as shown in the Table 3.2. The maximum dry density for the silty sand mixture was found to be 2022 kg/m^3 at optimum moisture content of 11 % (using Standard Proctor test in accordance with ASTM D698-00ae1, 2000).

Table 3.2 Grain size distribution curve for the silty sand mixture and sand

Liquid limit (LL)	16.54 %
Plastic limit (PL)	12.04 %
Plasticity index (PI)	4.5 %

3.3.3 Geomembrane

The geomembrane used in the present study was a 60 mil (1.5 mm thick) non-textured, high-density polyethylene (HDPE) geomembrane manufactured by GSE Inc., Houston TX, USA.

3.4 Measurement of Soil Suction

One of the purposes of this study was to investigate the role of soil suction on interface shear behaviour. There are various soil suction measurement devices, which have been broadly categorized into two methods: direct and indirect. Some examples of the direct method of measuring soil suction are tensiometer and the null type pressure plate. Examples of indirect measurement devices are the filter paper technique and the thermal conductivity sensor (Fredlund and Rahardjo, 1993). Two of the most common devices for direct measurement of soil suction are tensiometers and miniature pore pressure transducers (PPT). The direct measurement of soil suction is usually preferred as measured pore water pressures are more rapidly reflected (Meilani et al., 2002). The response time for a brand new tensiometer under favourable soil conditions can be about 30 minutes (Taber, 2003). Further it was not practical to employ filter paper technique for measuring suction changes inside a direct shear box closer to the interface.

3.4.1 Tensiometers

It is possible to measure suction near the interface using a tensiometer. However, the use of a tensiometer has several drawbacks. The tensiometer holds a large amount of water that needs to be exchanged between soil and tensiometer in order to reach equilibrium and several hours may

be required for stable pore pressure measurements. The amount of water exchanged between the soil and the tensiometer can affect soil sample moisture content in the vicinity of the porous cup of the tensiometer. Preliminary trials were made using a tensiometer and this equipment was not found to yield a sufficiently rapid response.

3.4.2   Miniature Pore-pressure Transducer (PPT)

Miniature PPTs are commonly used in geotechnical applications for the measurement of positive pore pressure and soil suction. Figure 3.3 shows a longitudinal cross section of the miniature PPT (Type PDCR81 manufactured by Druck Corporation, USA). It consists of a 0.09 mm thick single crystal silicon diaphragm that has a fully active strain gauge bridge diffused into its surface. A high air-entry porous stone is placed at the tip of the transducer just overlying the diaphragm. One side of diaphragm is exposed to atmosphere via the transducer cabling while the other side is exposed to the pore water via the porous stone at the tip of transducer. The space between the porous stone and the diaphragm forms a water compartment. The deformation of the diaphragm causes a change in voltage measured across the strain gauge that is equated to pressure.

Miniature PPTs are frequently used in various geotechnical applications particularly in centrifuge modelling for measuring the positive pore pressures in saturated soils (e.g. Sharma and Bolton, 1996). They are also used in triaxial testing of unsaturated soils to measure matric suction along the height of soil specimen (Meilani et al. 2002). They have also been successfully used to measure matric suction in silts (Murleetharan and Granger, 1999).
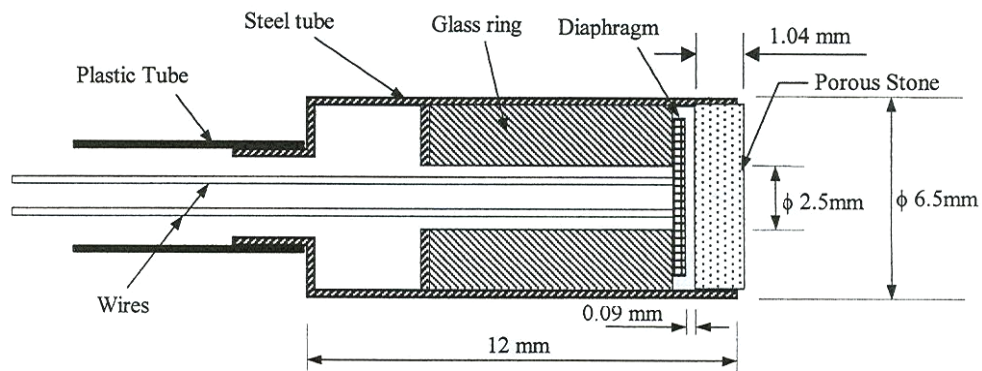
Figure 3.3 Miniature Pore Pressure Transducer PDCR 81 (Murleetharan and Granger 1999).

The small size of the PPT is ideal for this application. It has a quick response time since a very small amount of fluid is required to be exchanged between the water compartment of PPT and the surrounding soil. Considering the disadvantages associated with tensiometers, it was decided to use a miniature pore pressure transducer to measure soil suction close to the geomembrane soil interface.

3.4.3   *Working Principle of Suction Measurement using a PPT*

The principle of making suction measurements using a PPT is based on the equilibrium between the pore pressure in the soil and the pore water pressure in the water compartment of the PPT. In a saturated soil specimen, the positive pressure causes the flow of water from the soil into the water compartment of the PPT, which in turn causes the diaphragm to deform (Figure 3.4). In an unsaturated soil specimen, before the equilibrium is attained, negative pressure causes the water from water compartment in the PPT to flow into the soil (Figure 3.4).
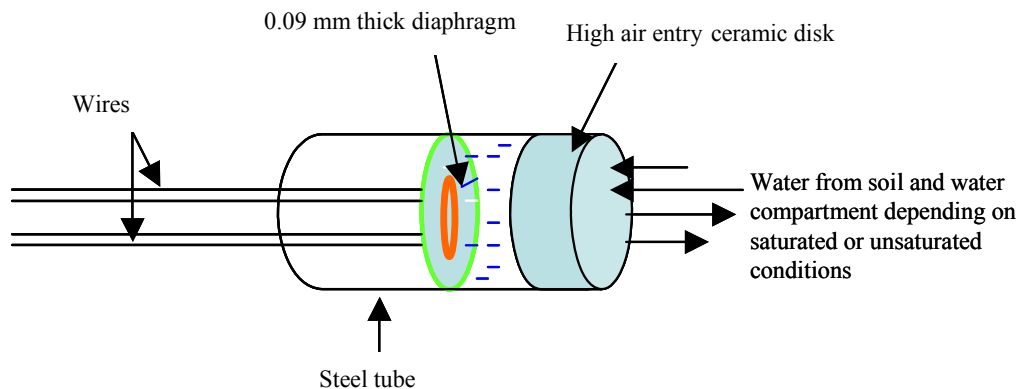
Figure 3.4 Use of PPT in Saturated/Unsaturated soil

The PPT must be saturated and calibrated prior to use to measure soil suction. It is critical to keep the water compartment of the PPT completely filled and the ceramic disc fully saturated for accurate measurements. The method of saturation and calibration of the PPT is described in later sections. One of the main limitations of a miniature PPT used is that it can only be used for fairly low suction ranges (typically < 50 kPa).   It loses accuracy and response time as pore-water pressure approaches –100 kPa because of the cavitation of pore water.

3.5   Details of Testing Program

3.5.1   Direct Shear Box

The interface shear tests were conducted at the Geotechnical Engineering Laboratory of the University of Saskatchewan using a conventional direct shear apparatus (Clockhouse Engineering Ltd. England, Type-K12). A square base direct shear box (100 mm x 100 mm) split horizontally at mid-height was used. The total height of the box was 79 mm. Normal stress is applied by placing dead weights on a hanger. Vertical and horizontal displacements are monitored using two Linear Variable Differential Transformers (LVDTs). The rate of shear displacement can be accurately controlled between 0.32 and 48.5 mm per hour. The direct shear box is capable of a maximum shear displacement of 14 mm.

Although ASTM D5321-02 (ASTM, 2002) recommends a shear box having base dimensions of 300 mm x 300 mm, the use of the box described above can be justified based on the fact that only a non-textured, smooth, geomembrane was used in the present study. Non-textured geomembrane has a homogenous surface structure compared to other geosynthetic materials such as geogrids or geonets. Therefore, it is reasonable to assume that the scale effect of using a smaller direct shear box is likely to be negligible as the effects of aperture rib and size do not apply to smooth geomembranes. Further a 100 mm X 100 mm box is adequate for testing fine grained soils in contact with non textured geomembranes (Ellithy and Gabr, 2000, Fisherman and Pal, 1994). Most importantly, the purpose of the study was to investigate the pore pressures that are developed at the interface rather than to carry out "standard" testing.

Prior to its use in interface shear testing, the direct shear box was calibrated to measure the friction between the upper and the lower boxes. Such calibration was necessary because of the low values of shear stress expected for the geomembrane–soil interface. The shear stress value corresponding to the friction between the upper and the lower boxes was subtracted from the measured interface shear stress values to obtain the correct interface shear stress values.

3.5.2   Modifications to the Direct Shear Box

The direct shear apparatus was modified in order to make it suitable for geomembrane-soil interface shear testing as well as to include a miniature pore pressure transducer for the measurement of pore-water pressures in close proximity to the geomembrane-soil interface during testing. A schematic cross-section of the modified direct shear box is shown in Figure 3.5.
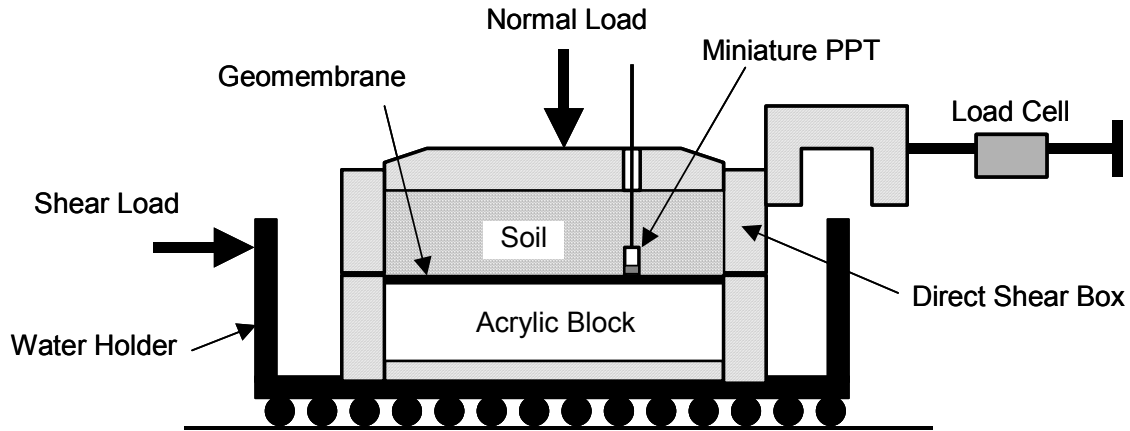
Figure 3.5 Set-up for the interface shear testing with PPT in place

An acrylic (Plexiglas®) block was used to hold the upper surface of the geomembrane at the elevation of the shearing surface. The geomembrane specimens were cut to 100 mm x 100 mm and glued to the top of the acrylic block. The height of the acrylic block-geomembrane assembly was 38 mm.

Various methods have been suggested for keeping geosynthetics in place during shearing including clamping (Fox et al., 1997) and gluing (Ling et al., 2001). Clamping was avoided as clamping may increase the likelihood of a progressive failure and thus reduce the measured peak interface shear strength (Fox et al., 1997). In the present study, for simplicity and in order to minimize the potential for any movement of the geomembrane during shearing, the geomembrane specimen was glued to the acrylic block. Contact cement (LePage Prestite®) was used and based on the recommendations of Stark and Poeppel (1994), the acrylic block with glued geomembrane was kept under compressive stress for 24 hours to ensure proper bonding. Application of compressive stress for 24 hours also helps to reduce elongation of the geomembrane during shearing and encourages a sliding type of failure (Bove, 1990). The acrylic block-geomembrane assembly was stored away from sunlight and dust prior to testing.

The acrylic block-geomembrane assembly was mounted in the lower half of the shear box and oriented so that the shear displacement was applied along the roll direction. The soil to be used in the testing was placed at the desired moisture content into the upper half of the shear box immediately over the geomembrane surface. A 40 mm x 40 mm square tamper was used to compact the soil to the desired density. Samples were examined for the presence of surface

irregularities and those samples that exhibited visible defects or irregular surface features were discarded.

Again, it should be noted that, while the approach taken in this study may not perfectly replicate the stress conditions in the field, the purpose of the study was to investigate the role of soil suction rather than to carry out "standard" testing. Figure 3.6 shows step by step illustration of the interface direct shear test setup.

(A)

(B)

(C)

(D)
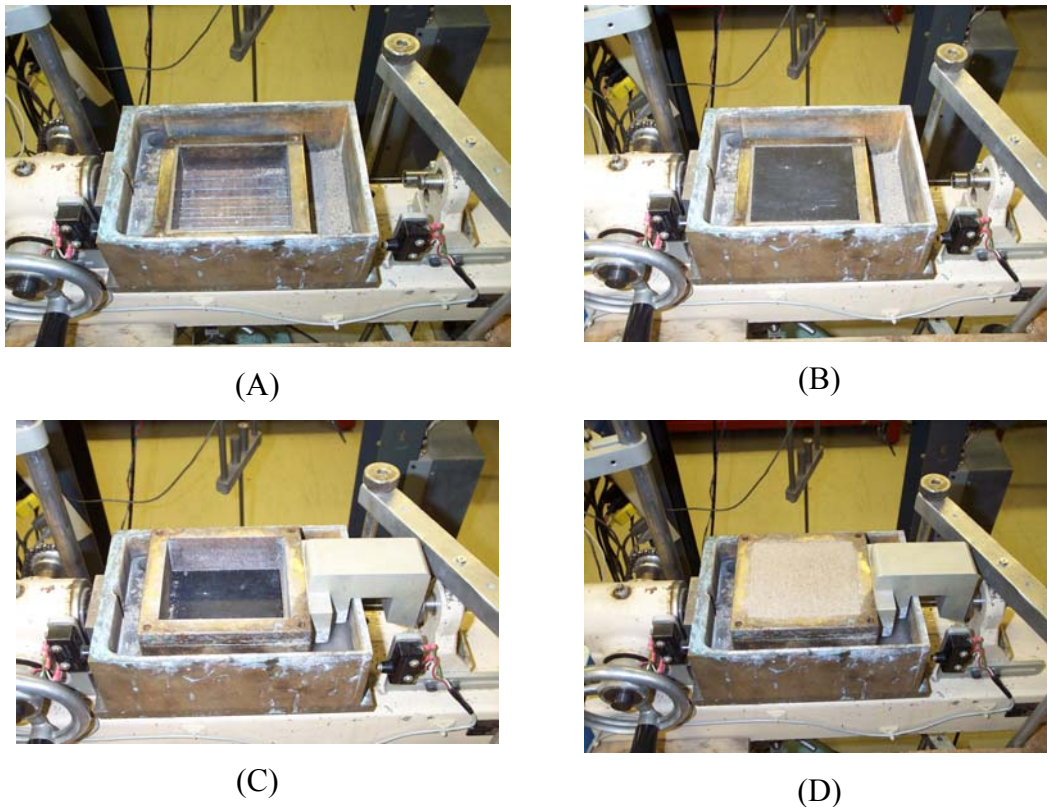
Figure 3.6 Step-by-step illustration of the interface shear test set-up: (A) Empty lower box in place; (B) Lower box with geomembrane glued on a plexiglass block; (C) Upper box in placed properly over the lower box; (D) Upper box with soil compacted on surface of geomembrane

3.5.3   *Placement of PPT in the Direct Shear Box*

In order to accurately measure the pore pressure at the interface, the transducer should be kept inside the direct shear box as close to the interface as possible. For this purpose, a new load plate was fabricated that was similar to the load plate of the direct shear box. A 6 mm diameter hole was drilled through the load plate as close as possible to the centre, to facilitate insertion of the transducer (Figure 3.7).
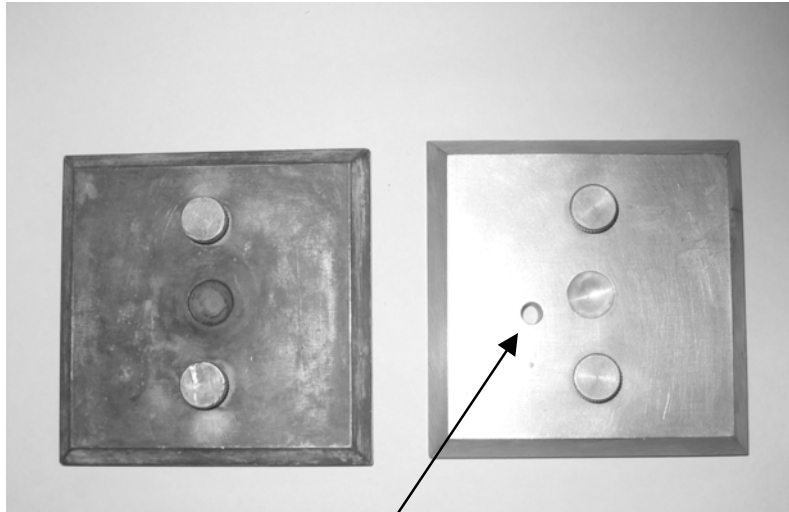
6 mm diameter Hole for inserting PPT inside
direct shear box

Figure 3.7 Modifications done to the load plate for the insertion of PPT

Once the soil was compacted to the desired density, a hole was made through the soil to the surface of geomembrane (with a small layer of soil left just above the surface of geomembrane) and the miniature PPT was inserted through this hole. The hole was backfilled with soil and recompacted once the PPT was installed at the interface as shown earlier in Figure 3.5. The data obtained from PPT was recorded by a data acquisition system. The values were recorded at 10 seconds interval. The PPT was found to be quite sensitive to the changes in pore pressure.

3.5.4   Saturation of the PPT

The PPT tip was saturated using a procedure suggested by Take and Bolton (2003). The PPT is saturated in a small steel pressure cell. The pressure cell is connected to a vacuum pump and filled with deionised, de-aired water up to 75% of its volume. The PPT is air-dried and inserted into the cell, sealed and a vacuum of 90 kPa is applied. The transducer takes about 30 minutes to be in equilibrium with the vacuum. Once the transducer is in equilibrium with the cell, the cell is rotated through 90º slowly introducing water to the porous stone while still under vacuum. The transducer was kept in this position for about 2 hours at 90 kPa vacuum (Figure 3.8).
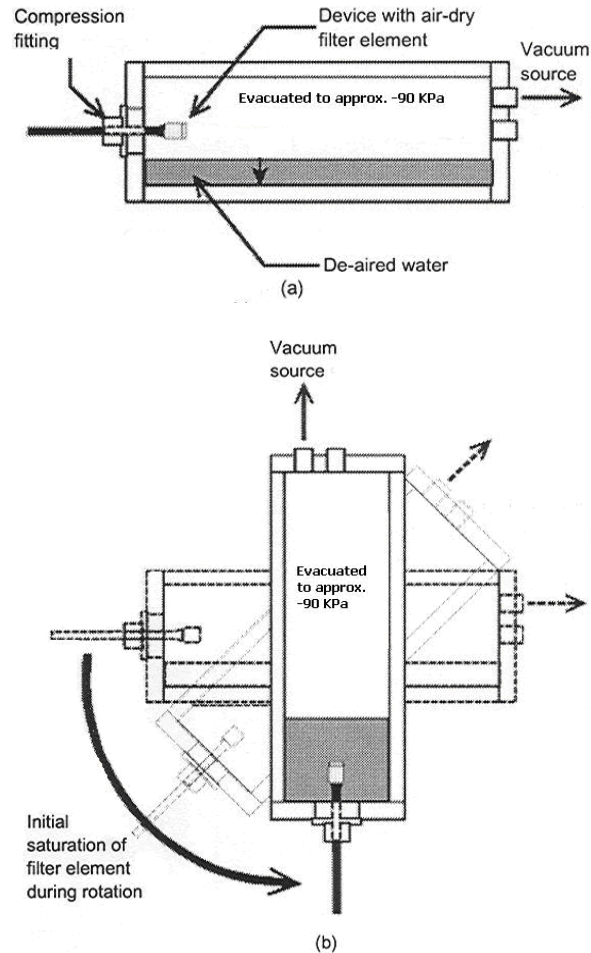
Figure 3.8 Saturation of the PPT. (a) de-airing of water and evacuation of chamber; (b) saturation (After Take and Bolton, 2003)

3.5.5 Calibration of the PPT

The PPT was calibrated prior to its use using the same pressure cell in which the PPT was saturated. The pressure was applied with 10 kPa increments and the corresponding voltage change was noted. Both positive and negative pressures were applied. The calibration curve was found to be linear and repeatable, confirming that the PPT was in a good working condition.

3.5.6 Establishing Equilibrium Time of the PPT

Equilibrium is considered when the saturated PPT placed inside soil gives a fairly constant reading that is equal to the pore pressure of the soil. The response of the miniature PPT was tested for soil at various water contents and densities. This included the time for which it stays at

equilibrium, once it is kept in soil or at the interface. It was found that the PPT had a different equilibrium time when placed in soil samples of different moisture contents. The time required to reach equilibrium was a function of volume and velocity of flow. In general, with less moisture content, the time to equilibrium was also less. This may be because at higher water contents there is decrease in pressure gradient across the porous tip and a corresponding decrease in flow volume. This results in corresponding increase in time to reach equilibrium. For water contents of 6 % and 13 %, the time at equilibrium was found to be 440 minutes and 1400 minutes, respectively.

3.6   Testing Procedure

Direct shear testing was carried out on the various soils used (soils only) as well as on the several soil/geomembrane interface combinations. Each test series was performed under 4 normal stresses of 5, 12, 20 and 30 kPa. This range of normal stresses is representative of the range of normal stresses commonly encountered in landfill cover systems, lagoon liners and other common applications.

3.6.1   Selection of Geomembrane Specimen

It was very important to carefully select the geomembrane specimen to be as uniform as possible and representative of the geomembrane material to be tested. This reduces the potential for biased test results caused by significant differences in the properties of the specimens. The general condition of the geomembrane specimen should be carefully noted and recorded before and after direct shear testing (Bove, 1990). The following items, as suggested by Bove (1990), were checked and recorded for geomembrane specimen before and after the test:

- Inspection of geomembrane surface for abrasion and any pattern of abrasion
- Sign of elongation or other damage
- Development of wrinkles
- Embedment of soil particles
- Differential movement between geomembrane and contact surface
- Excessive deformation at edges

The geomembrane specimen was stored away from sunlight and was protected from dust. Each geomembrane specimen was sheared in the roll direction. This takes into account the variation in the friction values associated with manufacturing.

3.6.2   Interface Shear Testing under Saturated Conditions

For testing under saturated conditions, the soil at given moisture content was compacted over the geomembrane specimen to a specified density. A 4 cm X 4 cm square tamper was used to compact the soil. Water was then slowly poured into the water holder surrounding the direct shear box. This was considered an effective procedure for saturating the soil. After this, the PPT was installed (as described in section) and shearing was started once the equilibrium between the miniature PPT and the surrounding soil was established. The equilibrium was considered to be established when the PPT started reading same value of suction over a long period of time.

3.6.3   Interface Shear Testing under Unsaturated Conditions

For testing under unsaturated conditions, the soil was compacted over the geomembrane specimen using same method to achieve the specified density and moisture content. For each of these tests, the PPT was installed (as described in section) immediately after compaction of the soil. Shearing was started only after establishing equilibrium between the miniature PPT and the surrounding soil.

3.6.4   Tests conducted without pore pressure measurement

In addition to all the above-mentioned tests, some additional tests were conducted in which the miniature PPT was not installed. The purpose of conducting these tests was to examine the effect of including the miniature PPT on the interface shear strength. It was observed that the set up for pore pressure measurement had negligible effect on the performance of the interface shear tests.

3.7   Soil-Water Characteristic Curve (SWCC)

The soil-water characteristic curve defines the relationship between the amount of water in the soil and soil suction (Fredlund and Rahardjo, 1993). The amount of water can be gravimetric water content, w, volumetric water content, θ or degree of saturations, S. The relationship encompasses both desorption or drying and absorption or wetting process. Volumetric water

content, θ, can be defined as the ratio of volume of water to the total volume of soil. The relationship between volumetric water content and gravimetric water content can be written as

$$\theta = w.\rho_d \qquad \qquad \text{[Eq. 3.1]}$$

where, ρ_d is the dry density of the soil.

The SWCC may also be defined as storage function. That is, the SWCC gives an indication of the water holding capacity of the soil structure over a range of suctions. The water content defines the volume of water contained in the pores of the soil. Figure 3.9 shows a typical SWCC for a silty soil along with some of its key characteristics. The main curve shown is a desorption curve. The adsorption curve differs from the desorption curve as a result of hysteresis. The end point of adsorption curve differs from the starting point of desorption curve because of the air entrapment in the soil. Both curves have almost similar form.
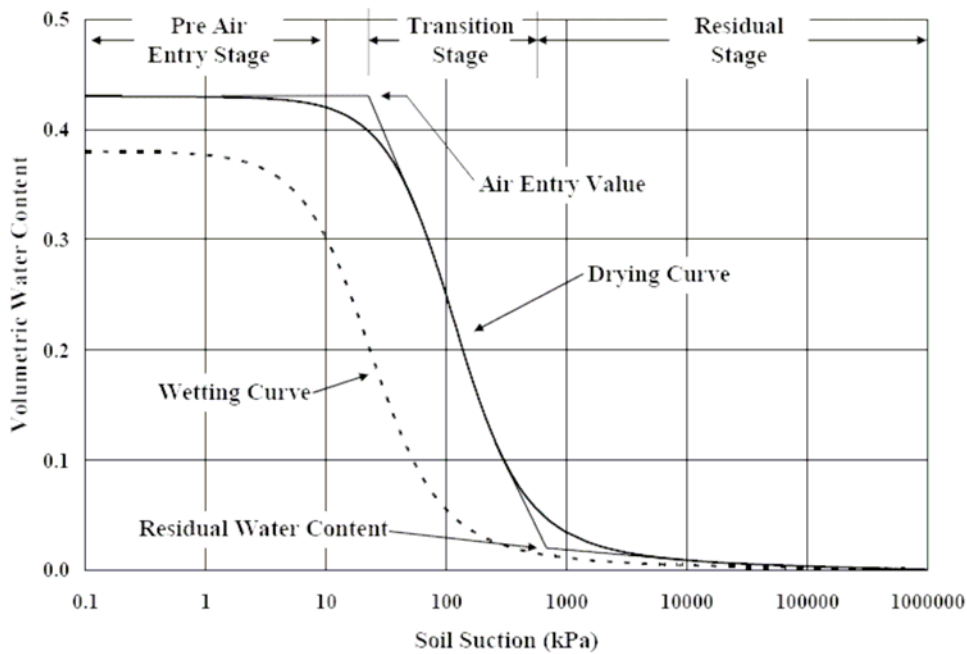
Figure 3.9 Typical SWCC for a silty soil (Fredlund and Rahardjo, 1993)

The saturated water content is the water content at which all the voids in soil are filled with water. The saturated water content and the air entry value, or bubbling pressure, for the soil generally increases with plasticity of the soil. Other factors such as stress history also affect the shape of soil-water characteristic curve of the soil. The soil-water characteristic curve can be

- 40 -

divided into three stages as shown in figure 3.9. The first point of importance on soil-water characteristic curve is air entry value. During the pre air entry stage, the material des not drain and water content remains constant. The soil starts to desaturate in the transition stage. The water content reduces significantly with increase in suction in this stage. The air entry value of the soil is the matric suction at which air starts to enter the largest pores in the soil. The amount of water at soil particle or aggregate contact reduces as desaturation continues. Eventually a large increase in suction leads to a relatively small change in water content 9or degree of saturation). This stage is referred to residual stage of unsaturation. The water content in soil at the commencement of this stage is generally referred to as residual water content. The amount of water present in soil is very small in this stage.

3.7.1 Obtaining the SWCC from the grain size distribution of the soil

Fredlund et al. (2002) presented a procedure for estimating the SWCC from information on the grain size distribution and the volume-mass properties of a soil. In this method they considered grain-size distribution curve as incremental particle sizes from the smallest to the largest. The grain size distribution curve is a continuous curve representing the mass of particles of various sizes present in soil. The SWCC is primarily a representation of the pore sizes present in soil. The basis of the SWCC estimation from the grain size distribution of the soil involves translation of particle size distribution into pore size distribution.

This method does not address the effect of stress history, fabric, confinement and hysteresis. This method can be reliably used to predict SWCC for sands and silts. It is difficult to predict SWCC for clays, tills and loams using this method (Fredlund et al., 2002). The details of the grain size distribution model are described in a paper by Fredlund et al., 2000. Fredlund and Xing (1994) gave an empirical equation to represent SWCC. This equation is used as the basis for the estimation of SWCC. The Fredlund and Xing equation has the following form,

$$w_w = w_s \left[1 - \frac{\ln\left(1 + \frac{\psi}{h_r}\right)}{\ln\left(1 + \frac{10^6}{h_r}\right)} \right] \left[\frac{1}{\left\{ \ln\left[\exp(1) + \left(\frac{\psi}{a_f}\right)^{n_f} \right] \right\}^{m_f}} \right]$$

[Eq. 3.2]

where

w_s - Saturated gravimetric water content

w_w - gravimetric water content

a_f - a fitting parameter corresponding to the soil suction at the inflection point and is related to air entry value of the soil

n_f - a fitting parameter related to rate of desaturation of the soil

m_f - a fitting soil parameter related to the curvature of the function in high suction range.

ψ – matric suction (kPa)

h_r - a constant parameter used to represent the soil suction at the residual water content and is selected to be 3000 kPa generally.

The Fredlund and Xing equation gives relationship between water content and suction due to its ability to fit entire range of soil suctions. However for low suctions the method is not as good as Van Genuchten method.

An estimation of each parameter of Fredlund-Xing equation is required for each interval of particle sizes. Further it is assumed that smooth transition (on logarithmic scale) exists for the representation of SWCC when moving from coarse sized particles to fine sized particles. The Fredlund-Xing equation was used in this study for the computer program used to obtain SWCC as described later.

3.7.2   *Determination of SWCC for Soil using VADOSE/W*

The software VADOSE/W (Geo-Slope International 2004) is equipped with an automated option for estimating the SWCC on the basis of grain size distribution. The software can determine the SWCC by using any one of the different equations like Fredlund and Xing Equation (Fredlund and Xing, 1994), Van Genuchten Equation (Van Genuchten, 1980), Arya and Paris Equation (Aryan ad Paris, 1981) etc. depending upon the preference of the user. For determining the SWCC for a soil, the grain size distribution of the soil is provided as input for the grain size distribution function for that soil. In addition to this, values of parameters like coefficient of volume compressibility, a_f, m_f and n_f along with water content at saturation are to be used for estimation of SWCC. It then readily gives the SWCC for that soil.

3.7.3 Determination of SWCC using Tempe Cell

Tempe cells (modified pressure plate cell) can be used effectively to measure the SWCC for a soil at the particular density (Figure 3.10). The apparatus is designed to apply the matric suction to a soil specimen. The apparatus is based on axis translation technique such that matric suction greater than 100 kPa can be applied to the soil sample without causing cavitation of the water in the apparatus. A single soil specimen can be used to obtain the numerous points on the SWCC. This is due to the fact that the soil specimen is not required to be removed at each suction value.

The major drawback of a Tempe cell is that air bubbles may form in the water filled grooves below the air entry stone. The air is produced by air diffusing through the high air entry stone. These air bubbles will displace water from system causing an inaccurate assessment of water lost from soil from one suction stage to another. To overcome this water below the porous stone is flushed at regular intervals to remove any excess air bubbles. The results obtained by pressure Tempe cell are quite reliable. The SWCC obtained by Tempe cell was used for comparison with SWCCs obtained using other methods.
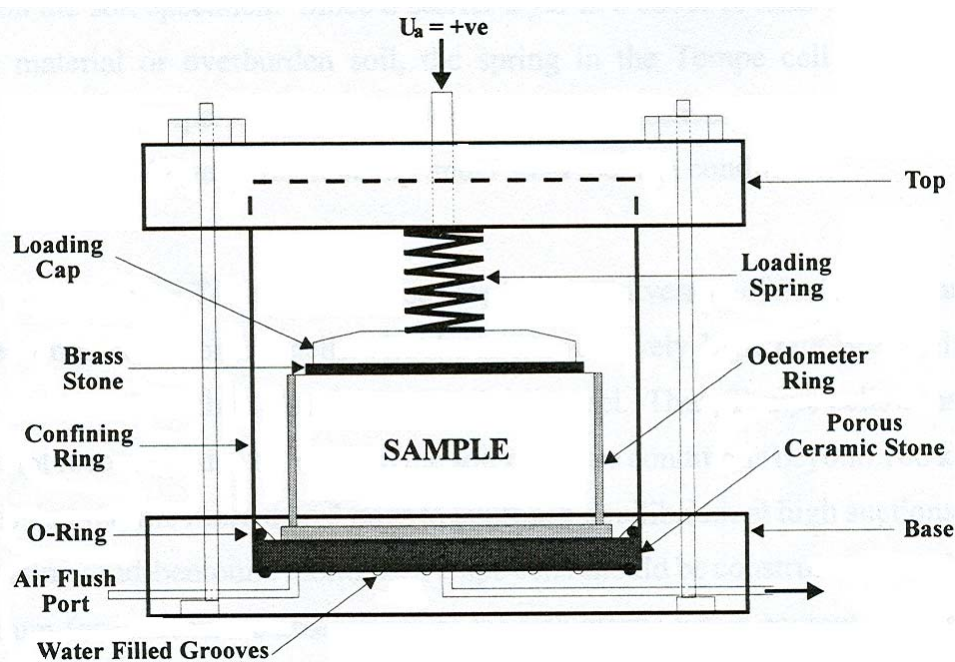
Figure 3.10 Tempe Cell and its components (Stoicescue 1997)

The procedure for a Tempe cell set-up (Stoicescue, 1997) is as follows:

1. The air entry stone was saturated in de-aired water for 24 hours prior to setup of the Tempe cell apparatus for use in measuring SWCC of soil.

2. The saturated air entry stone was positioned into the apparatus with O-rings in place to prevent leakage around the corner

3. The mass of Tempe cell apparatus including O-rings, stones, loading cap springs, screws and tubing was recorded prior t inserting the soil specimen into the apparatus. The area below the air entry stone including the connecting tubing was completely filled with de-aired, distilled water prior to weighing.

4. The soil specimen was prepared in consolidation ring at desired density and water content (bulk density of 2132 kg/m^3, dry density of 1920 kg/m^3 and w/c = 11%).

5. This specimen was saturated and weighed. It was then placed in the middle of the air entry stone as shown in Figure 3.10.

6. The top stone, loading cap and spring were placed on top of the soil specimen.

7. The top of cell was gently placed onto the loading spring.

8. To ensure that soil specimen was under 0 kPa suction, the port on top of apparatus was opened to atmospheric pressure. The mass of discharge into the vial was recorded over time. The condition of equilibrium or 0 kPa was assumed when there was zero discharge into the vial.

9. Any air bubbles accumulated in the tubing or below the air-entry stone were flushed using de-aired, distilled water.

10. After 0 kPa conditions were achieved, mass of apparatus + soil+ specimen ring was measured and recorded. Based on this mass of soil specimen at 0 kPa could be calculated.

11. Based on above recordings, the saturated volumetric water content of the specimen at 0 kPa was obtained.

3.7.4   *Comparison of SWCCs for Silty Sand Obtained using Different Methods*

The SWCC as estimated with VADOSE/ W using Fredlund and Xing Equation (Fredlund and Xing, 1994) and Tempe cell for the sandy silt is shown in Figure 3.11. For the silty sand sample tested the SWCCs were also measured using tensiometer and miniature PPT. However using miniature PPT and tensiometer the suctions could not be accurately measured beyond 30 kPa. As

can be seen from Figure 3.13, the SWCC obtained using various methods matched well between 0.2 to 30 kPa. The exception to this was SWCC using tensiometer which was matched well upto 25 kPa and SWCC obtained using PPT were matched upto 30 kPa only. The point on SWCCs (obtained using tensiometer and PPT) that fall below the range of all other SWCCs indicates this deviation due to limitations of tensiometer and PPT. This was probably due the fact that PPT and tensiometer were capable of measuring suction values accurately up to 25 to 30 kPa only. Figure 3.13 also shows the SWCC obtained for sand using Fredlund and Xing equation (Fredlund and Xing, 1994).
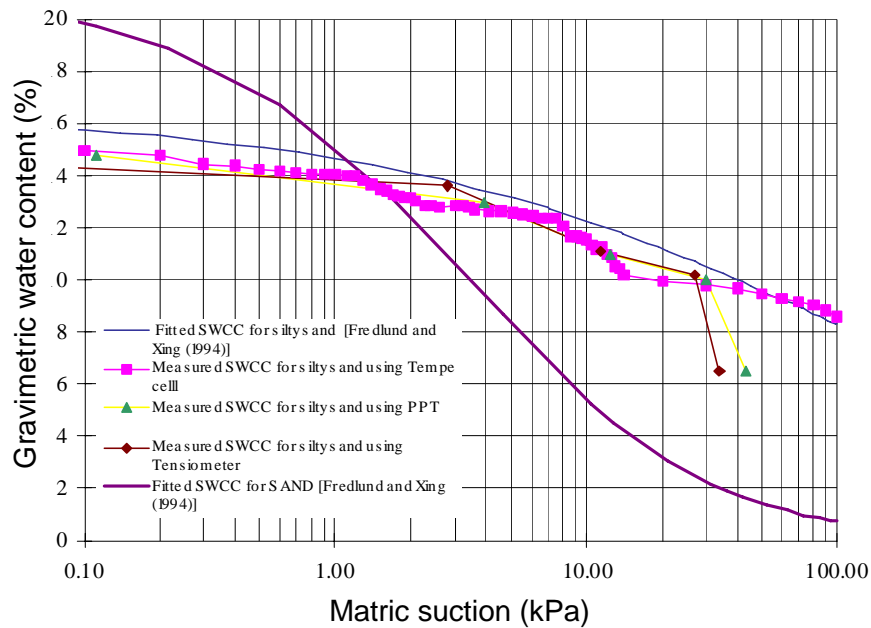
Figure 3.11 SWCC for the silty sand mixture using different methods

3.8 Summary

The experimental set up was planned according to the requirements of the study to be undertaken. The equipment used was properly calibrated. The details of testing under saturated as well as unsaturated conditions were discussed. The procedure followed to carry out the interface shear testing with and without pore pressure measurement was also outlined. Chapter 4 presents the details of the test results obtained. In addition to this the soil-water characteristic curve that was obtained using various methods is also explained.

Chapter 4   Presentation of Results

4.1   Introduction

Chapter 4 presents the results of the test program carried out in Chapter 3. The data obtained for the various tests is presented. This includes data obtained for tests conducted to determine the effect of various test parameters on interface shear behaviour (these tests were conducted without pore pressure measurement) as well as data for all other tests conducted with pore pressure measurement.

4.2   Effect of Various Test Parameters on Interface Shear Behaviour

It is a beneficial to have some basic knowledge of the effect of various test parameters on the interface shear test. Keeping this in mind and to determine the significance of the various parameters, interface shear testing was carried out on several sand bentonite mixtures, under varying test conditions. These conditions included rate of displacement, water content and density. Following this, some observations were made regarding the effect of various parameters on the interface shear strength. The sand bentonite mixture was compacted on top of the geomembrane using varying density, water content and bentonite content for the sand bentonite mixture. The rate of displacement was also varied in some of the tests.

4.2.1   Effect of Placement Density

The density of compacted soil can play an important role in interface friction behaviour of sand/bentonite and geomembrane. Figure 4.1 shows the variation of friction angle with density of the compacted sand/bentonite mixture. Over the range of densities tested the friction angle was found to increase with increase in density of compacted soil bentonite provided all other testing conditions remained same. Interface friction angle was found to vary between 15 ° to 19 °. It can also be seen that the variation of interface friction angle with bulk density is linear when the interface is sheared very slowly (i.e. drained response). For faster rates this variation becomes non-linear, especially at higher placement densities.
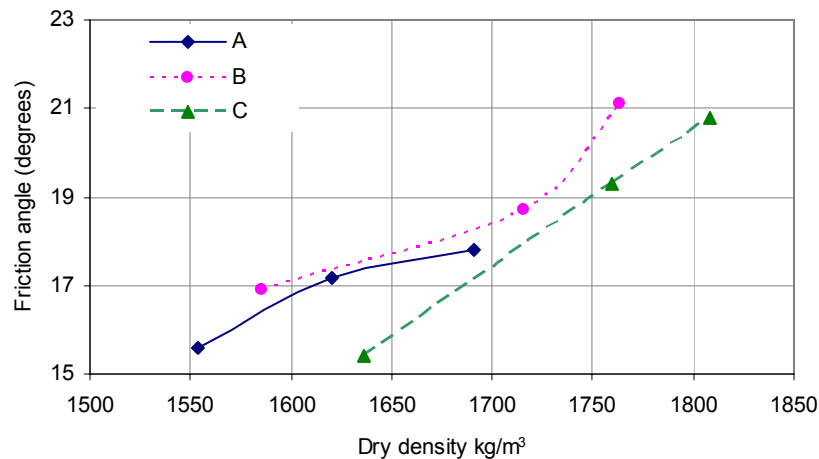
A - 3% sand bentonite, w/c = 12.6%, displacement rate = 12 mm/h

B - 6% sand bentonite, w/c = 11%, displacement rate = 42.5 mm/h

C - 3% sand bentonite, w/c = 8.2%, displacement rate = 2.5 mm/h

Figure 4.1 Effect of density on sand bentonite mixture and geomembrane interface

It should be noted that to achieve a higher density greater compactive effort is needed. This results in more number of soil particle contacts with the geomembrane which in turn results in higher friction coefficients. The tests are conducted at relatively low normal stresses. At those stresses there is a possibility of dilation of the compacted soil. Te amount of dilation is more at higher densities of the compacted soil. This dilation may also have contributed to the higher friction resistance of the interfaces at higher densities. In general for the three sets of test combinations, the friction angle increased with increase in density of compacted soil.

4.2.2   Effect of the Rate of Displacement

The interface shear tests that are carried out at a slower displacement rate run for a longer time than the tests carried out at a faster displacement rate. According to Gomez and Filz (1999), after the compaction the clay structure tends to accommodate the lower energy level. During this process, a more flocculated soil structure and lower (more negative) pore pressures are generated with curing time after compaction. For a test with slow rate of displacement, the soil sample gets more curing time after compaction due to longer duration of the test. Hence the results for a slower test may be different than those results obtained for a faster test with similar testing conditions.

Figure 4.2 shows the variation of the friction angle with the rate of displacement. For the range of the different rates of displacement tested, the friction angle was found to increase with the increase in rate of displacement. It should be noted that all of these tests were conducted under unsaturated conditions and suctions were present at the interface due to absence of free water at the boundaries. Therefore, it is likely that at slow shearing rates the test conditions were drained and there was ample time available for suctions to dissipate. At higher displacement the suction was not getting dissipated which may have contributed to increase in friction angle.
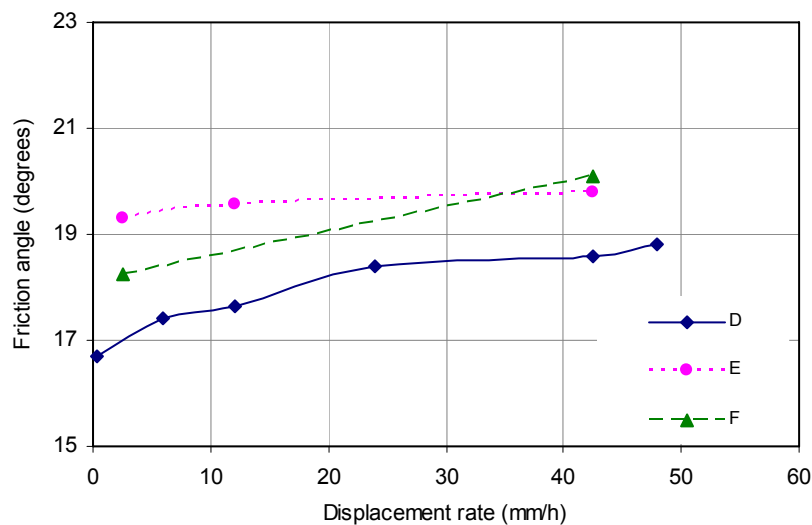
D - 3% sand bentonite, dry density = 1685 kg/m^3, w/c = 13%
E - 3% sand bentonite, dry density = 1760 kg/m^3, w/c = 8.2%
F - 6% sand bentonite, dry density = 1799 kg/m^3, w/c = 8.8%

Figure 4.2 Effect of rate of displacement on sand bentonite mixture and geomembrane interface

At intermediate shearing rates, the suctions were changing with time and so was the interface shear strength. Selecting a shearing rate faster than 24 mm/h did not seem to affect the interface friction angle. It is likely that at shearing rates faster than 24 mm/h, pore pressures do not get dissipated, resulting in constant interface shear strength. For test combination A and for the rate of displacement range 0.3 to 24 mm/h the effect was pronounced however it was comparatively less beyond that rate of displacement which included the range 24 to 48 mm/h.

Interface friction angle was found to vary between 16 ° to 19 ° for the test combination D. For other two test combinations, the friction angle varied from 18 ° to 21 ° for the rate of

displacement range 3 to 42.5 mm/h. In general interface friction angle increased with increase in rate of displacement.

4.2.3 *Effect of Placement Water Content*

As described in chapter 2, the water content can have a considerable effect on the interface shear behaviour of soil-geomembrane interface. In this study, the water content was varied by keeping the other parameters like density, rate of displacement constant. The density used in this particular analysis was bulk density which is different from the analysis carried out to determine the effect of rate of displacement and the dry density. This made it difficult to analyse the isolated effect of water content on interface shear behaviour. The results reported for this particular analysis are based on bulk density of the compacted soil.

Figure 4.3 shows the variation of interface friction angle with the water content of the sand bentonite mixture. Based on the range of water content combinations tested and by keeping all other test parameters same, it can be seen that the friction angle decreases significantly with increases in water content from 6 to 8 %. The change in friction angle is comparatively less when the water content was increased from 8 % to 13 %. The friction angle varied from 17 ° to 22 °.
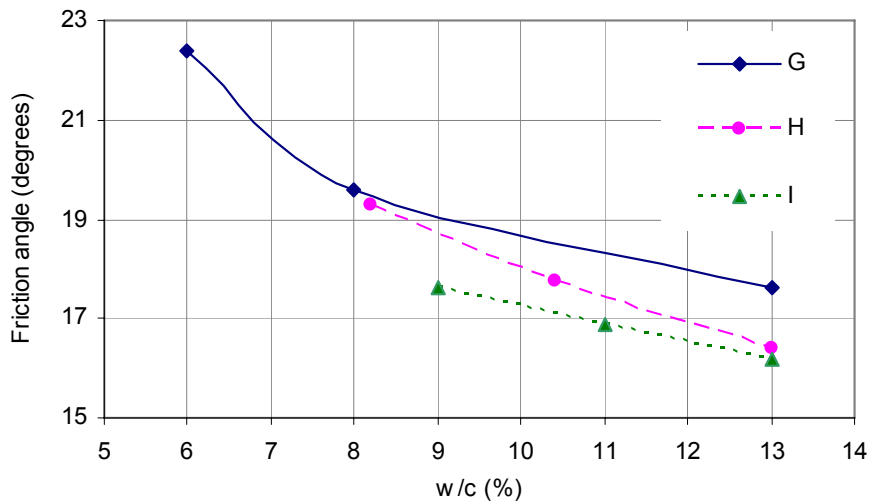
A - 3% sand bentonite, bulk density = 1904 kg/m^3, displacement rate = 12 mm/h

B - 3% sand bentonite, bulk density = 1904 kg/m^3, displacement rate = 2.5 mm/h

C - 6% sand bentonite, bulk density = 1760 kg/m^3, displacement rate = 42.5 mm/h

Figure 4.3 Effect of water content on sand bentonite mixture and geomembrane interface

Based on the three set of test combinations A, B and C, it can be concluded that the friction angle decreases with increases in water content of the compacted soil, provided all other conditions remain same. This was because at higher moisture contents there is more water at the interface which provides a lubricated geomembrane surface for the soil particles to slide on.

It should be noted that the density used in this particular case was bulk density and hence it is quite difficult to quantify the effect of water content based on the bulk density of compacted sand bentonite mixture. However based on the published literature on interface shear testing of smooth geomembrane and soils it is predicted that the friction angle will decrease with increase in water content of soil bentonite mixture if same dry density were used for the all of the tests included in Figure 4.3.

4.2.4 *Importance of Various Test Parameters for Interface Shear Testing*

It can be seen from Figure 4.1, Figure 4.2 and Figure 4.3, rate of displacement has comparatively less influence on interface shear behaviour of geomembrane soil interface. For those tests where use of PPT is made to measure suction at the interface, it is very crucial to control the duration of test in order to ensure that the PPT is able to respond to the suctions effectively. This is because the PPT may not stay saturated for longer durations (beyond 7 hours) in soils with low water contents. If a very slow rate of displacement is used, this may result in a test with very long duration for which the PPT may not stay saturated. Further if a fast rate of displacement is used, it was predicted that the PPT may not be able to effectively record the changes in suction during shearing (as PPT may not have a sufficiently rapid response time). Meilani et al., (2002) reported a response time of less than 3 seconds for a sudden application of pressure of 500 kPa. However to be on conservative side it was decided not use a faster rate of displacement. Because of this reason, most of the tests were conducted at a rate of displacement of 12 mm/h and 3 mm/h.

4.3   Interface Shear Tests under Saturated and Bone Dry Conditions

4.3.1 *Silty Sand Mixture under Saturated Conditions (No Geomembrane Present)*

Direct shear testing was conducted on silty sand mixture and sand (without geomembrane) under saturated conditions. These tests were conducted to establish whether inclusion of the miniature PPT had any influence on the results of direct shear test. The silty sand was compacted at bulk density of 2132 kg/m^3 (w/c = 11%) and sand was compacted at the density of 1733 kg/m^3. For

the tests involving saturated silty sand mixture as well as saturated uniform sand, the pore-water pressure was found to be almost equal to zero during the shearing process as indicated by the miniature PPT readings. The results of the direct shear tests done using saturated soils are presented in Table 4.1. The PPT has a relatively small area compared to the area of the direct shear box and hence presence of PPT caused minimal interference. For both the silty sand mixture and the sand, tests carried out without the miniature PPT gave exactly the same results as those tests that had the miniature PPT installed. Therefore it can be inferred that the presence of the miniature PPT inside the direct shear box does not affect the test results.

Table 4.1 Results of direct shear testing on sand and silty sand (no geomembrane) under saturated conditions

Test no	soil type	Φ'_p (degrees)	c'_p (kPa)	Φ'_r (degrees)	c'_r (kPa)
1	Sand no GM	35.4	0	29.5	0
15	Silty sand no GM	32.2	0	28.6	0

4.3.2 Sand and Sand-Geomembrane Interfaces under Bone Dry Conditions

Direct shear testing was carried out on sand and sand/geomembrane interface under dry conditions. The purpose of doing these tests was to compare the results obtained under saturated and dry conditions.

The values of friction angles for sand under saturated as well as dry conditions were found to be the same. The results and comparisons are shown in Figure 4.4. A trial test was conducted by using the PPT to measure pore pressures. However when the saturated PPT was inserted inside the shear box through the compacted dry sand, the porous stone tip of the PPT desaturated rapidly and the water from water compartment inside the PPT was quickly lost to the surrounding sand. As mentioned in section 3.4.1 it is critical to keep the water compartment of the PPT completely filled and the ceramic stone tip fully saturated for accurate measurements. In this test the PPT did not stay saturated and was not able to measure pore pressure effectively. Based on this it was decided not use the PPT under dry conditions.

Peak failure envelopes for sand

shear stress (kPa) — 25, 20, 15, 10, 5, 0
normal stress (kPa) — 0, 10, 20, 30, 40

▲ sat. sand (TS)
△ sat. sand (ES)
● dry sand (TS)

Dry Sand Interface

Φ'_{Gp} = 22.7°	a'_p = 0.8 kPa	Φ'_{Gr} = 17.1°	a'_r = 2 kPa

Sat Sand TS space	Sat Sand ES space	Dry Sand **TS** space
Φ'_p = 35.4 °	Φ'_p= 35 °	Φ'_p = 35.7°
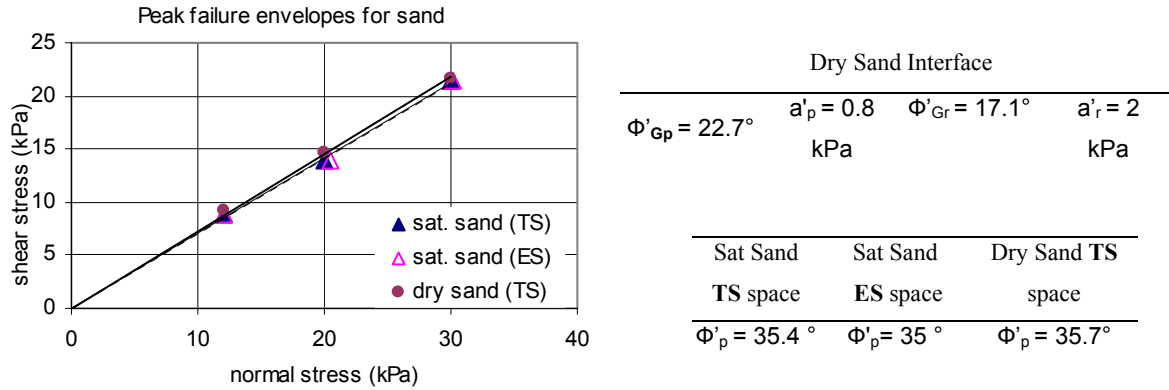
Figure 4.4 Failure envelopes for saturated and dry sand (without Geomembrane)

4.3.3 *Saturated Silty Sand-Geomembrane and Sand-Geomembrane Interfaces*

Interface direct shear testing was conducted on the silty sand mixture and sand (both with geomembrane) under saturated conditions. The major purpose of carrying out these tests was to obtain the values of values of effective friction angle (ϕ') and effective adhesion (a'). These values were to be used for analysis of the interface shear test results using unsaturated soil mechanics principles. This is discussed in detail later.

(A) Saturated Interface direct shear test on sand-geomembrane interface

The sand was compacted at the density of 1733 kg/m^3 on the surface of geomembrane (similar to the procedure discussed in Chapter 3). The results of this test are shown in Table 4.2.

Table 4.2 Results of interface direct shear testing on sand under saturated conditions

Test no	soil type	Φ'_{Gp} (degrees)	a'_p (kPa)	Φ'_{Gr} (degrees)	a'_r (kPa)
3	Sand interface	21.0	2.5	18.4	2.8

(B) Saturated Interface direct shear test on sand-geomembrane interface

The silty sand was compacted at bulk density of 2132 kg/m^3 (w/c = 10%). As mentioned before, saturated conditions were obtained by soaking the compacted soil for 24 hours prior to interface

shear testing. The results for this test (and similar test for which the PPT was used) are reported in terms of the regular plots of shear stress versus displacement. In addition to this the suction was plotted as ordinate with time as abscissa (Figure 4.5). The displacement axis and time axis are plotted to the same scale in that the increment in displacement axis corresponded to the increment in time required for the same displacement. This test was conducted at a rate of displacement of 3 mm/hr and it takes 20 minutes for a displacement of 1mm. Consequently in presenting the test results for this test, the increment on displacement axis is 1mm and the increment on the time axis is 20 minutes which is also the time taken for a displacement of 1 mm considering the rate of displacement of 3mm/h. This method helps with easy comparison of data and is followed for reporting the results for all tests with pore pressure measurement.

As seen from Figure 4.5, pore-water pressures are close to zero for the entire test except at the beginning of shearing when up to 2 kPa of pore-water pressure could be measured. The increase in pore-water pressure could be caused by contraction of soil pores in the vicinity of the PPT. After some shear displacement, pore-water pressure values are generally stable and very close to zero. The presence of free water at geomembrane-soil interface appears encourage dissipation of pore pressures. Hence pore-water pressures dissipate almost as quickly as they are generated.

Figure 4.5 Typical interface shear test results for saturated silty sand-geomembrane interface: (a) Plots of time versus pore pressure for the interface test; (b) Plots of Displacement versus shear stress for the interface shear test [Test specifications: 10% moisture content; bulk density of silty sand 2132 kg/m³].

Figure 4.6 shows typical interface shear strength envelopes for geomembrane-soil interface under saturated conditions. These envelopes were obtained by fitting linear regression lines through each set of interface shear stress vs. normal stress data. For all regression lines, R^2 was between 0.98 and 1.00. For each regression line, the following Mohr-Coulomb type equation was used to obtain values of interface friction angle (ϕ_G) and adhesion (a)

$$\tau = a + \sigma_n \tan(\phi_G)$$ **[Eq. 4.1]**

where τ is the interface shear strength and σ_n is the total normal stress. Eq. 4.1 can be written in terms of effective normal stress as:

$$\tau = a + \sigma'_n \tan(\phi_G')$$ **[Eq. 4.2]**

where σ'_n is the effective normal stress,' a' is the adhesion and ϕ_G' is the interface friction angle in terms of effective stress. Table 4.3 gives a summary of results for all the interface shear tests conducted under saturated conditions. Effective normal stress values for the interface shear strength envelopes were obtained by using Terzaghi's effective stress equation:

$$\sigma'_n = \sigma_n - u_w$$ **[Eq. 4.3]**

where u_w is the pore-water pressure. Since pore-water pressures during shearing are close to zero, both the total stress (TS) and effective stress (ES) envelopes give nearly identical values of both interface friction angle as well as adhesion. Values of peak interface shear strength parameters were found to be only marginally higher than those of residual shear strength parameters. It is likely that true residual state was not reached in any of these tests and the end-of-the-test shear stress values are used to obtain residual shear strength parameters given in Table 4.3. Esterhuizen et al. (2001) point out that shear strains of the order of 50 % may be needed for a geomembrane-soil interface to reach residual conditions. It was not possible to apply such large shear strains using the modified direct shear apparatus used in the present study.
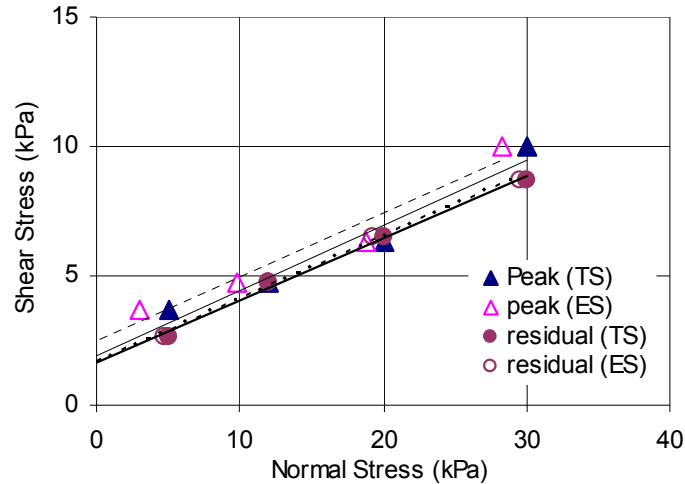
Figure 4.6 Interface shear strength envelopes under saturated condition [silty sand mixture, bulk density of soil = 2132 kg/m3, w = 10 %, rate of shearing = 3 mm/h].

Table 4.3 Results of interface direct shear testing on silty sand under saturated conditions

Test no	soil type	Φ'_{Gp} (degrees)	a'_p (kPa)	Φ'_{Gr} (degrees)	a'_r (kPa)
6	Silty sand interface	14.1	2.0	13.4	1.6

4.4   Interface Shear Tests under Unsaturated Conditions

A number of tests were conducted on silty sand with measurement of pore pressures throughout the course of test. The procedure for conducting these tests was as mentioned in Chapter 3. Rate of displacement used for these tests was 12 mm/h and 3 mm/h for faster and slower test respectively.

4.4.1   Tests at 8% Water Content

Figure 4.7 shows the results for sandy silt/geomembrane interface at 8% water content. This can be considered as a typical test results for geomembrane-soil interface under unsaturated conditions. The test results are reported in similar manner as explained for the saturated test (silty sand-geomembrane interface under saturated conditions) with pore pressure measurement. The zero on the time axis presents the start of the shearing process. The suction at this stage can be considered as the suction of the as compacted soil.
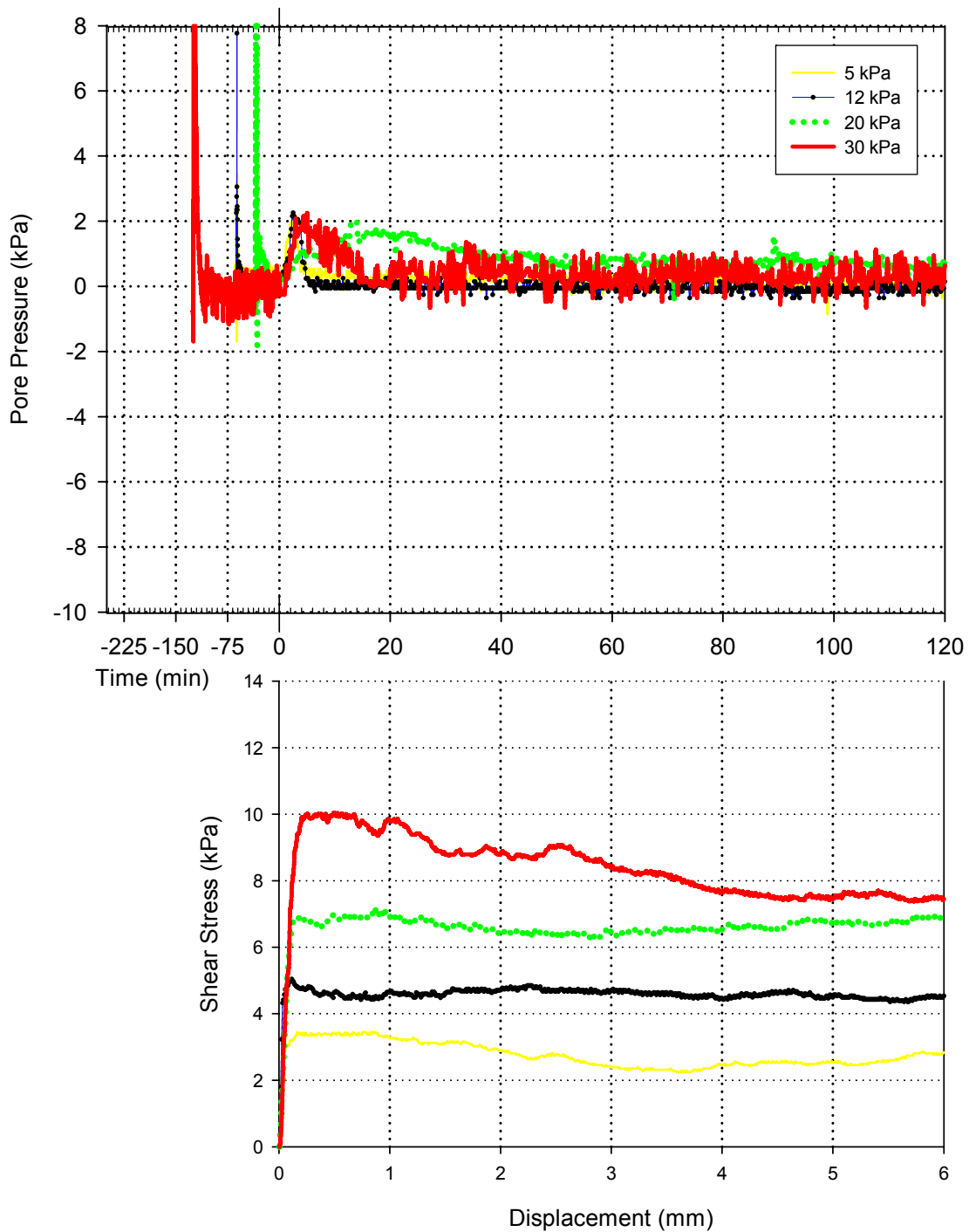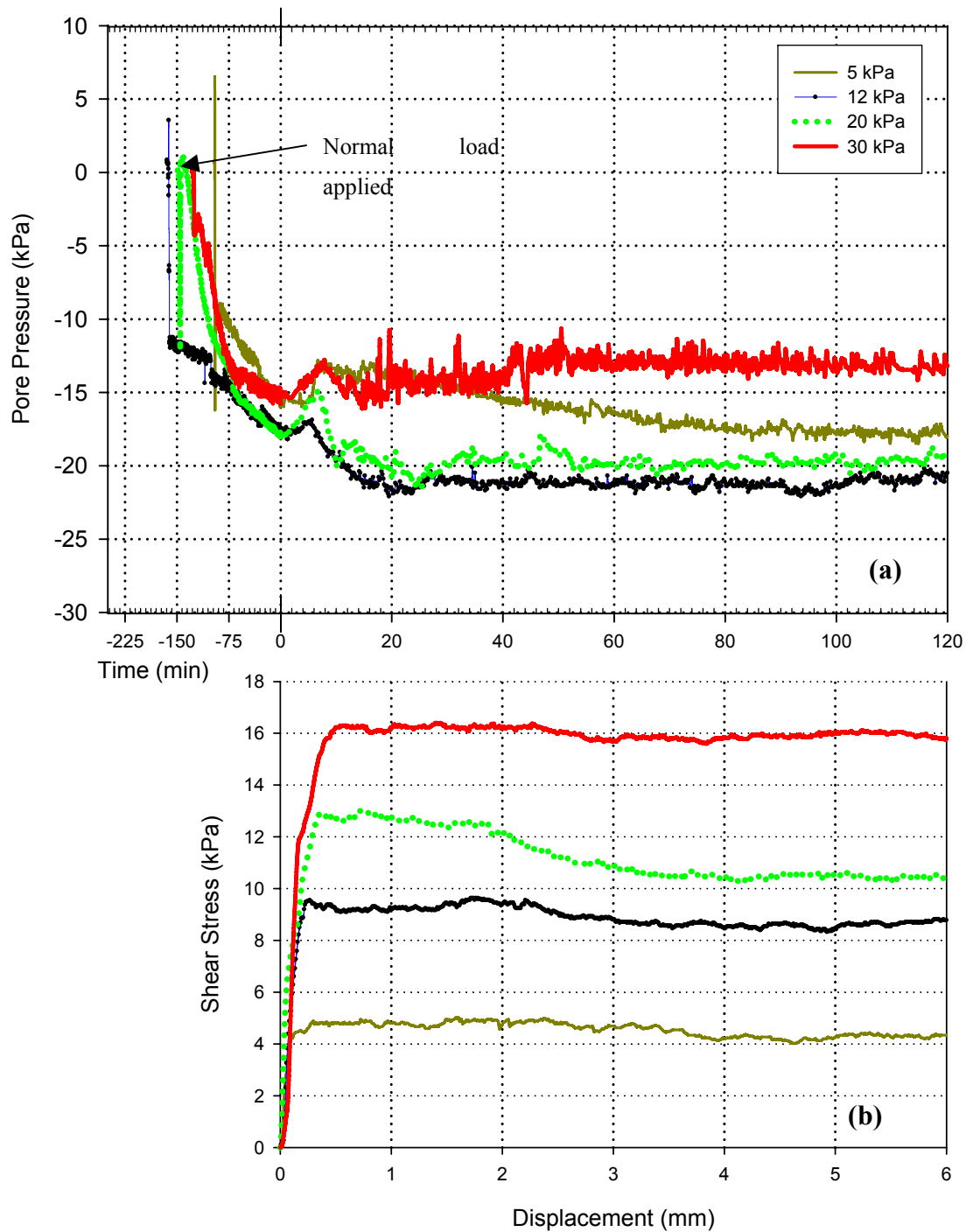
Figure 4.7 Typical interface shear test results for unsaturated sandy silt interface :(a) Plots of time versus pore pressure for the interface test; (b) Plots of Displacement versus shear stress for the interface shear test [Test specifications: 8% moisture content; bulk density of soil 2132 kg/m3.]

The suction is different for each of the normal stresses applied. It should be noted that change in matric suction takes place when normal stress is applied to the soil. It can be assumed that volume change takes place due o increase in normal stress. It is further assumed that this volume change is due to compression of air in the voids and dissolution of air in the water.

It can be seen from Figure 4.7 that the peak shear strength is reached at very small displacement. Throughout the course of shearing, negative pore pressures were recorded by the PPT installed in close proximity of the geomembrane soil interface. In this test, at the instant when shearing process began, the magnitude of soil suction present at the interface was not lower for lower normal stresses. Once the shearing was started the pore pressures decreased for some displacement. After this pore pressures were kept oscillating near a fairly constant reading. During the shearing process, changes in soil suction were observed. These can be attributed to lack of free water at the interface.

Figure 4.8 shows typical interface shear strength envelopes for geomembrane-soil interface tests conducted under unsaturated conditions. These envelopes were obtained by fitting linear regression lines through each set of interface shear stress vs. normal stress data. For all regression lines, R^2 was between 0.95 and 1.00. For each regression line, values of interface friction angle and adhesion were obtained using equation (4.1) or (4.2). It can be seen that for the failure envelopes using total stress space, peak and residual shear stresses plot on straight lines with slopes of 23.3 ^{0} and 21.8 ^{0} and y-intercepts ("adhesion") of 3.1 kPa and 3.1 kPa, respectively in terms of total stress space. The pore pressure, u_w was negative. Therefore, equation (3) gave effective normal stresses that were greater than total normal stresses. The failure envelopes obtained in effective stress space gives negative adhesions and steep slopes. Table 4.4 shows the results obtained from various combinations of interface shear test on soil / geomembrane interface under unsaturated conditions. Detailed analysis of these results is shown in later sections.
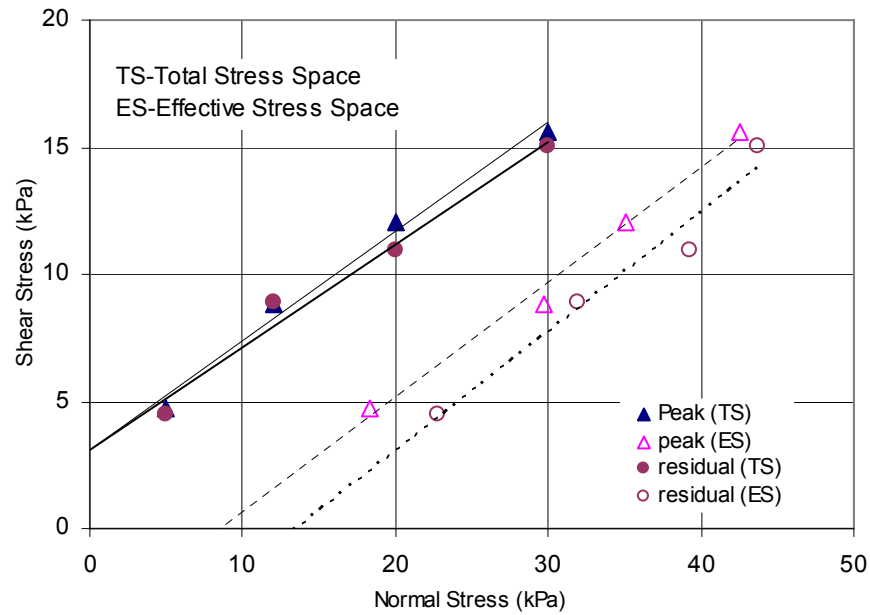
Figure 4.8 Interface shear strength envelopes under unsaturated condition [silty sand mixture, w = 8 %, rate of shearing = 3 mm/h].

Table 4.4 Summary of results for various interface tests under unsaturated conditions

Test no	soil type	Bulk Density (kg/m³)	w/c %	speed mm/h	Φ_{Gp} (deg)	a_p (kPa)	Φ''_{Gp} (deg)	a''_p (kPa)	Φ_{Gr} (deg)	a_r (kPa)	Φ''_{Gr} (deg)	a''_r (kPa)
4	6 % s/b	1904	8	12	21.1	2.4	21.5	-5.6	16.6	3.6	17.6	-4
5	6 % s/b	1904	8	3	19.8	2.8	21.7	-5.6	19.2	2.3	21.3	-7.2
8	Silty sand	2132	13	12	21.2	1.9	23	-0.3	21.3	1.4	21.8	-0.58
9	Silty sand	2132	8.9	12	23.7	1.8	30	-12.1	20	2.3	17.2	-3.6
10	Silty sand	2132	10	3	21.4	2.4	23.6	-3.1	20.3	1.8	22.2	-3.9
11	Silty sand	2132	10	12	22.4	3.0	25.1	-2.4	20.9	2.3	25.9	-6.0
12	Silty sand	2132	13	3	20.6	1.7	23.7	-0.1	20	1.1	21.2	-0.4
13	Silty sand	2132	8.9	3	23.2	3.1	24.3	-3.8	21.9	3.1	25.2	-6.3

It can be seen from Figure 4.8 and Table 4.4 that negative values of adhesion were obtained for both the peak and the residual interface shear strength envelopes plotted in terms of effective stress (ES). In this test the peak and residual failure envelopes in terms of effective normal stresses do not make sense, as can seen from Figure 4.8. They have negative y-intercepts and steep slopes. This is not surprising given that equation (4.3) is applicable only for saturated soils. It is more appropriate to examine the results in the light of unsaturated soil mechanics concepts.

Analysis using unsaturated soil mechanics principles

Based on the shear strength equation for an unsaturated soil (Fredlund and Rahardjo, 1993), an equation for the unsaturated interface shear strength can be written as:

$$\tau = a' + (\sigma_n - u_a)\tan\phi_G' + (u_a - u_w)\tan\phi_G{}^b \qquad \textbf{[Eq. 4.4]}$$

where u_a is the pore-air pressure, and $\phi_G{}^b$ is a parameter relating the change in interface shear strength with the change in matric suction. The values of adhesion 'a'' and interface friction angle ϕ_G' in Eq. 4.4 should be obtained using saturated interface shear tests (i.e. zero matric suction at the interface). In the present study, the PPT was vented to the atmosphere at the back. herefore, u_a can be assumed to be zero. Eliminating u_a from equation (4), we obtain:

$$\tau = a' + \sigma_n\tan\phi_G' - u_w\tan\phi_G{}^b \qquad \textbf{[Eq. 4.5]}$$

Eq. 4.5 can be rearranged as

$$\tau = a' + (\sigma_n - \beta \cdot u_w)\tan\phi_G' \qquad \textbf{[Eq. 4.6]}$$

where $\beta = (\tan\phi_G{}^b / \tan\phi_G')$.

Using Eq. 4.6, values of interface shear strength were calculated for unsaturated interface shear tests involving the silty sand mixture. For each suite of interface shear tests (5 kPa, 12 kPa, 20 kPa and 30 kPa normal stress), it was decided to choose the same β (obtained by trial and error) value for all normal stress values.

Figure 4.9 shows failure envelopes obtained for this interface shear test using concepts of total stress space, effective stress space and unsaturated soil mechanics principles (as explained above). Figure 4.9(a) and (b) shows the failure envelopes in total stress space and effective stress space same as those shown in Figure 4.8. It should be noted that failure envelope in effective

stress space is obtained using a β value of 1. However it can be seen that when β value of 1 is used the failure envelopes do not make sense and are steep with negative adhesion values. Further when β values of 0.44 and 0.35 are used, the failure envelopes pass through origin and show a slope of 23.7 ^{0} and 23.3 ^{0} for peak and residual respectively as shown in Figure 4.9(c). Based on this it can be predicted that magnitude of shear strength parameters is influenced by β value.

Figure 4.9 Typical failure envelopes for unsaturated sandy silt interface: (a) Failure envelopes in total stress space; (b) Failure envelopes in effective stress space calculate by assuming β = 1; (c) Failure envelopes in effective stress space calculate by assuming β values of 0.44 and 0.35. [Test specifications: 8% moisture content; bulk density of soil 2132 kg/m3]

4.4.2   Tests at 10 % Water Content

Similar to the results reported for previous test, the results for sandy silt/geomembrane interface test at 10 % water content are shown in Figure 4.10. The variation in the soil suction for this test was quite similar to variation in the soil suction for the previous test. Beyond the peak shear stress, the soil suction increased continuously for tests with lower normal stress, reaching a steady value at large shear displacements (residual condition). For the tests with higher normal stress (e.g. 30 kPa), the soil suction decreased to a steady value at large shear displacements. It is likely that the tendency of the soil particles to dilate is suppressed at higher normal stress, resulting in lower soil suction values. The failure envelopes for this test in terms of total and effective normal stress are shown in Figure 4.11.

Figure 4.11(a) shows the variation of peak and residual shear stresses with total normal stress acting on the soil-geomembrane interface. The peak and the residual shear stresses plot on straight lines with slopes of 22.4° and 20.9° and y-intercepts ("adhesion") of 3.0 kPa and 2.3 kPa, respectively. Figure 4.11(b) shows the variation of peak and residual shear stresses with effective normal stress at the interface, calculated by assuming $\beta = 1$. Again it is clear from Figure 4.11(b) that both the peak and the residual failure envelopes in terms of effective stress do not make sense. Their slopes are too steep and their y-intercepts are negative.

If, however, β values of 0.59 and 0.49 are used for the peak and residual conditions, respectively, both the failure envelopes pass through the origin and show slopes of 24° and 22.1° (for peak and residual, respectively) as shown in Figure 4.11(c).
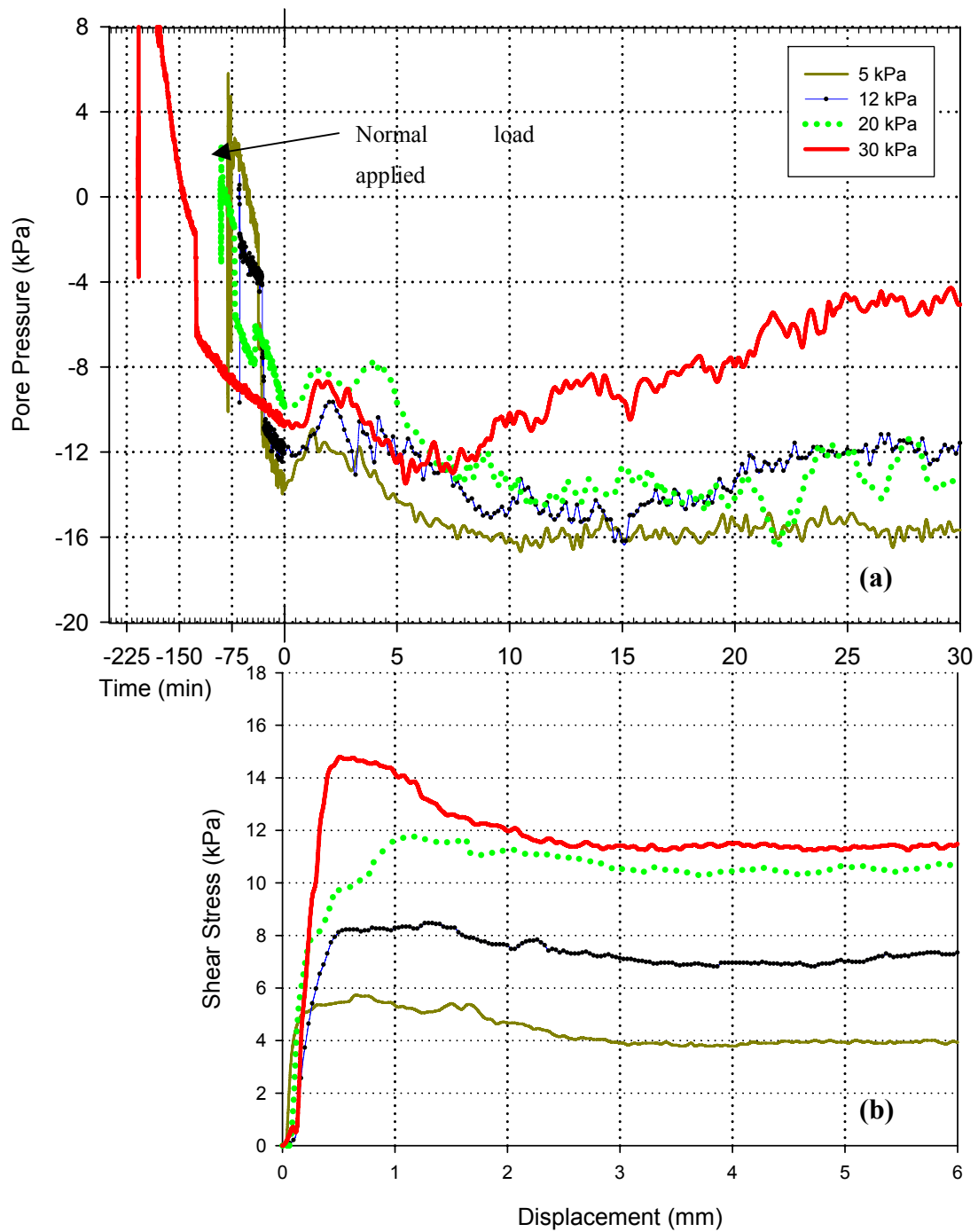
Figure 4.10 Typical interface shear test results for unsaturated sandy silt interface: (a) Plots of time versus pore pressure for the interface test; (b) Plots of Displacement versus shear stress for the interface shear test
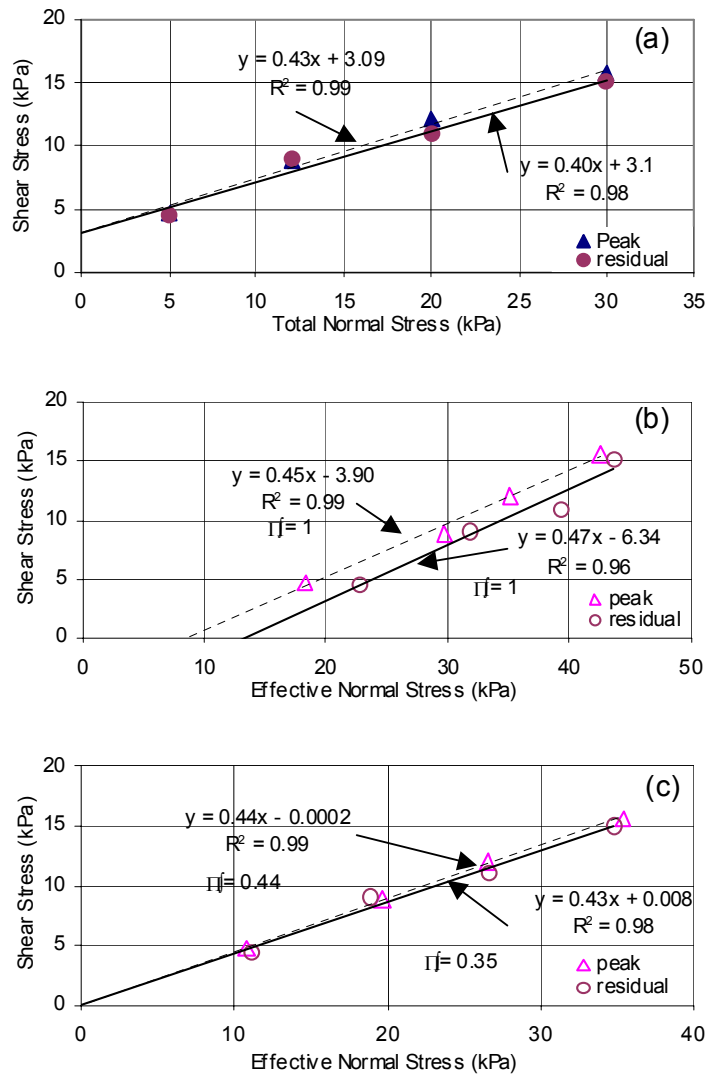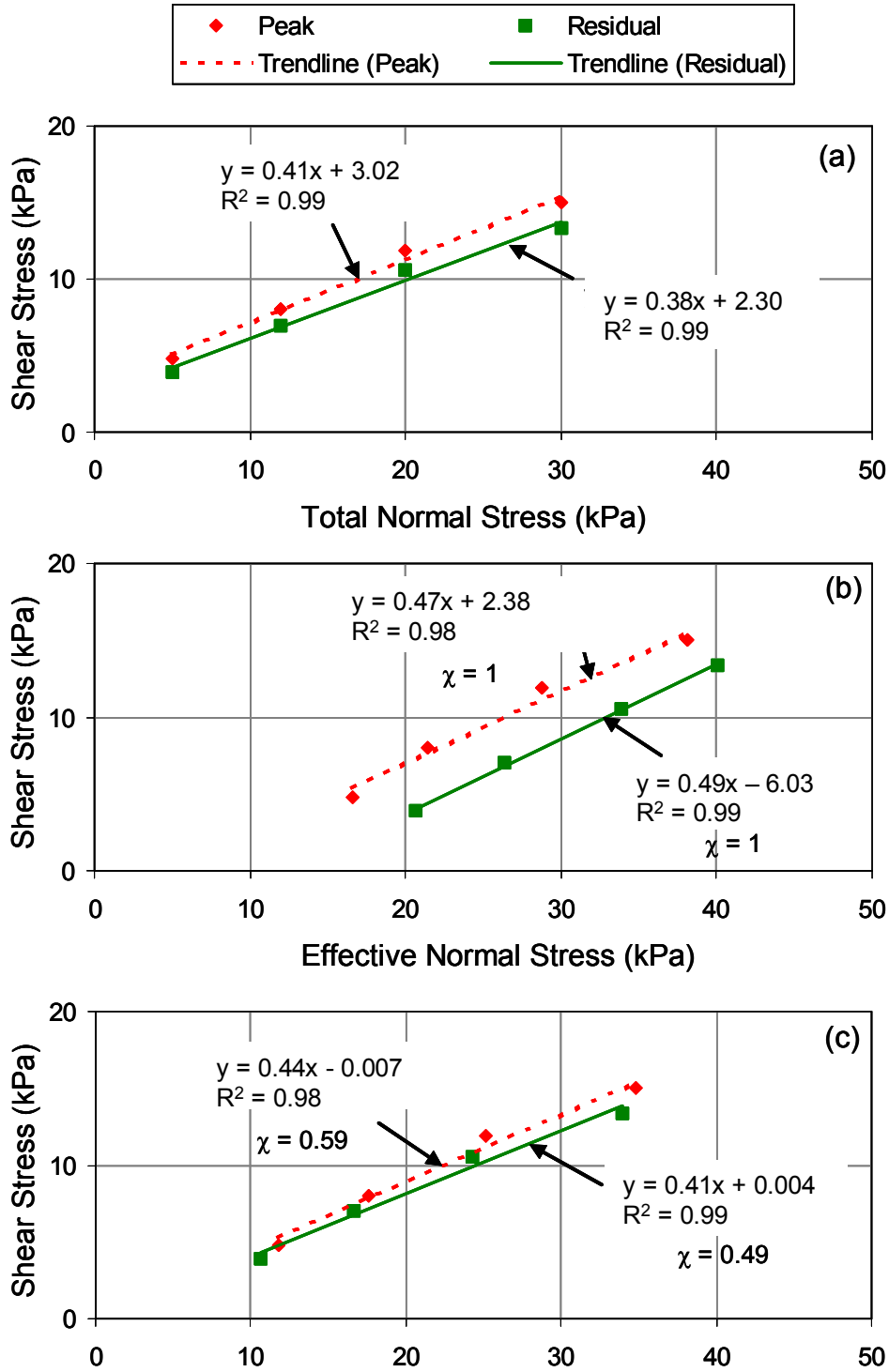
Figure 4.11 Typical failure envelopes for unsaturated sandy silt interface: (a) Failure envelopes in total stress space; (b) Failure envelopes in effective stress space calculate by assuming β = 1; (c) Failure envelopes in effective stress space calculate by assuming β values of 0.49 and 0.59. [Test specifications: 10% moisture content; bulk density of soil 2132 kg/m3]

4.4.3   Testing at 13 % Water Content

Similar to previous tests, Figure 4.12 shows a typical variation of pore pressure with time before and during the shearing process with silty sand at 13 % water content. Also included in this figure is the variation of shear stress with shear displacement. It can be seen from the Figure 4.12 that, prior to beginning of shear, the soil suction kept increasing (more negative). This can be due to continuous loss of moisture (evaporation) from soil into the atmospheric air. As soon as the shearing was started the magnitude of soil suction present at the interface was generally lower for higher normal stress values. This can be attributed to greater compression of void spaces at high normal stresses, resulting in slight increase in the degree of saturation of the soil. Because air is continuously diffusing through the porous tip of the transducer, the transducer response does not stay at a constant value but oscillates slightly around it.

During the shearing process, changes in soil suction were observed. Throughout the course of shearing, the soil suction showed a decreasing trend that is less negative (except for 30 kPa normal stress after some time). This may be attributed to compression of soil particles in response to application of shear stress. The suction kept changing between 0 and 6 kPa for most of the duration of the test.

From the results presented in Figure 4.12, variations of shear stress with total as well as effective normal stress can be obtained as shown in Figure 4.13. The peak and the residual shear stresses plot on straight lines with slopes of 20.8° and 19.8° and y-intercepts ("adhesion") of 1.7 kPa and 1.1kPa, respectively.
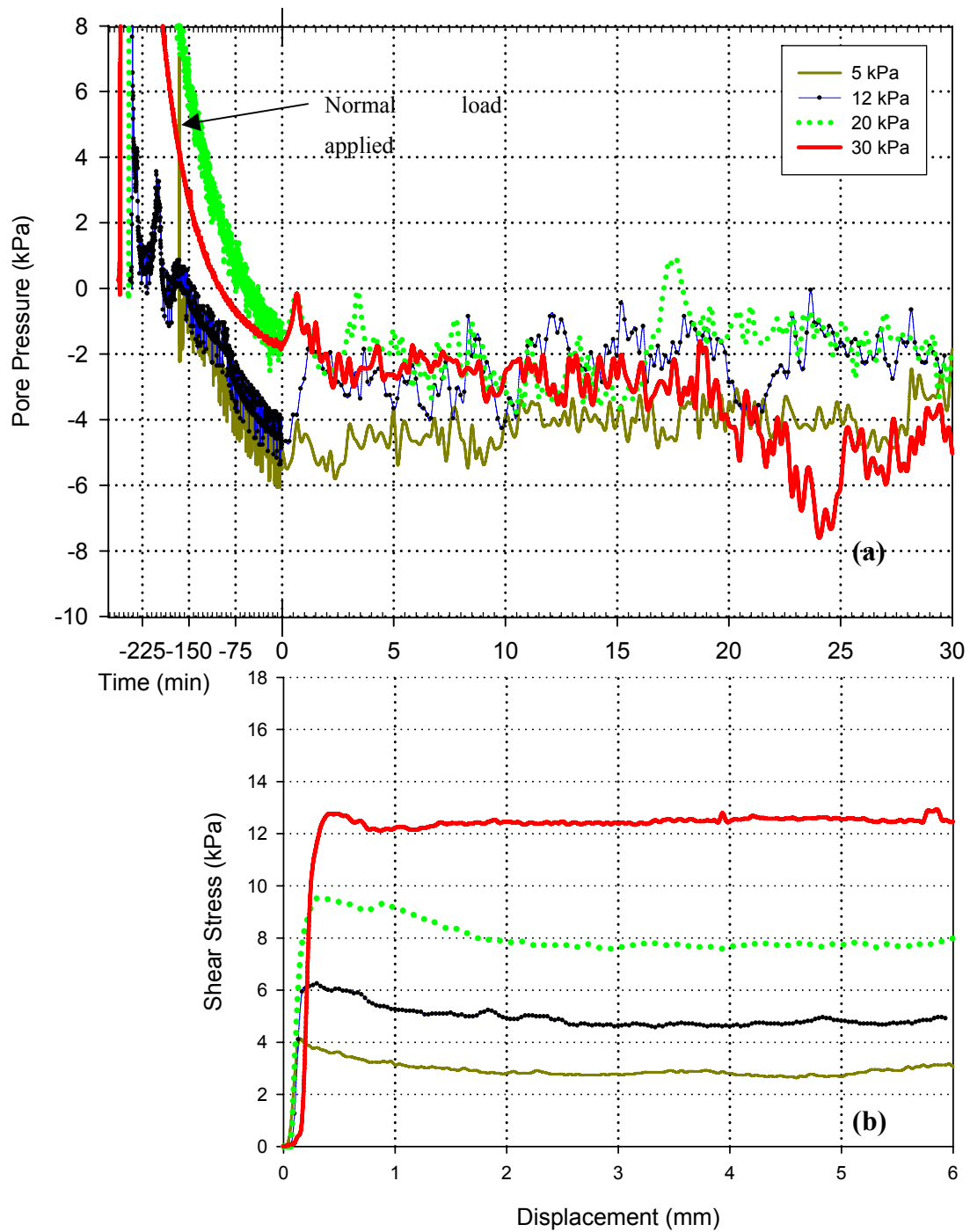
Figure 4.12 Typical interface shear test results for unsaturated sandy silt interface: (a) Plots of time versus pore pressure for the interface test; (b) Plots of Displacement versus shear stress for the interface shear test [Test specifications: 13% moisture content; bulk density of soil 2132 kg/m3.]
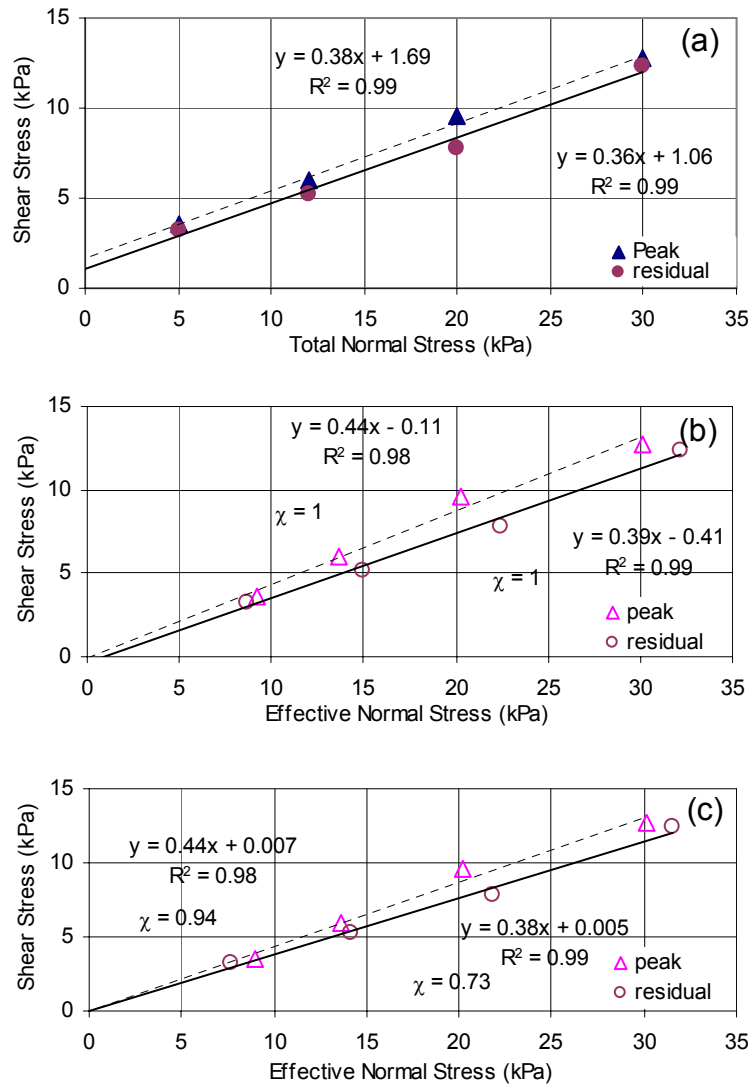
Figure 4.13 Typical failure envelopes for unsaturated sandy silt interface: (a) Failure envelopes in total stress space; (b) Failure envelopes in effective stress space calculate by assuming β = 1; (c) Failure envelopes in effective stress space calculate by assuming β values of 0.94 and 0.73. [Test specifications: 13% moisture content; bulk density of soil 2132 kg/m3]

Figure 4.13(b) shows the variation of peak and residual shear stresses with effective normal stress at the interface, calculated by assuming $\beta = 1$. Although straight-line relationships could be observed for both the peak and the residual shear stresses, both the peak and the residual failure envelopes have negative y-intercepts. . If, however, β values of 0.94 and 0.73 are used for the

peak and residual cases, respectively, both the failure envelopes pass through the origin and show slopes of 23.7° and 20.8° (for peak and residual, respectively) as shown in Figure 4.13(c).

A summary of this analysis for peak and residual failure envelopes is shown in Table 4.5 and Table 4.6, respectively. Based on the data for all tests it seems that the magnitude of effective normal stress (and therefore shear strength parameters) is influenced by β values.

Table 4.5 Analysis of the test results using different values of β (peak failure envelopes)

Test specification	Type of Normal stress	β-value	R^2	slope (degrees)	y-intercept (kPa)	Degree of saturation S	S^2
Silty sand interface with 8 % w/c	Total σ_n	--	0.987	23.3	3.08		
	Effective σ_n	1	0.988	24.2	-3.89	0.56	0.32
	Effective σ_n	0.45	0.998	23.7	-0.0002		
Silty sand interface with 10 % w/c	Total σ_n	--	0.990	20.4	3.0		
	Effective σ_n	1	0.978	24.7	-2.38	0.69	0.47
	Effective σ_n	0.59	0.984	24	-0.006		
Silty sand interface with 13 % w/c	Total σ_n	--	0.995	20.8	1.7		
	Effective σ_n	1	0.981	23.7	-0.11	0.87	0.76
	Effective σ_n	0.94	0.983	23.2	0.0069		
Silty sand interface with 15 % w/c	Total σ_n	--	--	--	--		
	Effective σ_n	1	0.981	14	2	1	1
	Effective σ_n	--	--	--	--		

Table 4.6 Analysis of the test results using different values of β (residual failure envelopes)

Test specification	Type of Normal stress	β-value	R^2	slope (degrees)	y-intercept (kPa)	Degree of saturation S	S^2
Silty sand interface with 8 % w/c	Total σ_n	--	0.98	21.8	3.1		
	Effective σ_n	1	0.96	25.1	-6.3	0.56	0.32
	Effective σ_n	0.35	0.98	23.3	0.008		
Silty sand interface with 10 % w/c	Total σ_n	--	0.99	20.9	2.3		
	Effective σ_n	1	0.99	26.1	-6.0	0.69	0.47
	Effective σ_n	0.49	0.98	22.1	0.004		
Silty sand interface with 13 % w/c	Total σ_n	--	0.99	19.8	1.1		
	Effective σ_n	1	0.99	21.3	-0.4	0.87	0.76
	Effective σ_n	0.73	0.99	20.8	0.004		
Silty sand interface with 15 % w/c	Total σ_n	--	--	--	--		
	Effective σ_n	1	0.981	13.4	1.6	1	1
	Effective σ_n	--	--	--	--		

4.5 Relationship between degree of saturation and parameter 'β' for silty sand and geomembrane interface shear tests

According to Fredlund and Rahardjo (1993) at saturation, the value of angle ϕ_G^b is same as value of angle ϕ_G'. Due to this the value of β is 1 at saturation and it decreases with decrease in water content. Fredlund et al, (1996) described a parameter 'k' whose value ranges from 1.0 to 3.0. They predicted values of shear strength function based on value of parameter 'k'. They observed that value of 'k' affects the rate at which angle varies with the variation in matric suction. According to Fredlund et al, (1996) it can be considered that $\beta \propto S^k$, where S is the degree of saturation. If $k=2$ we get, $\beta \propto S^2$. Based on this it was decided to observe the variation of parameter β with degree of saturation. Figure 4.14 shows variation of β with square of the degree of saturation 'S'.
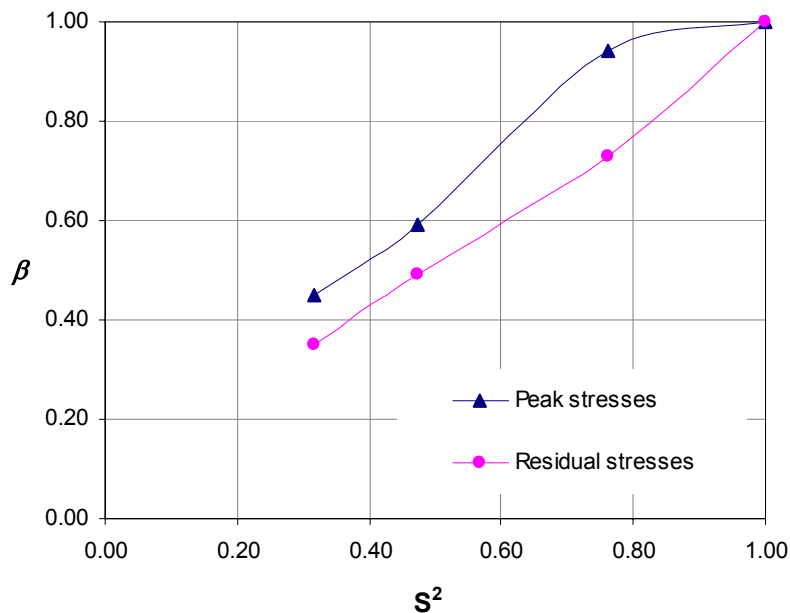
Figure 4.14 Variation of the values of β (values needed to achieve a perfect matching between measured and calculated shear stresses) with degree of saturation.

For the limited amount of tests carried out in this study, it was observed that the value of parameter β decreased with decrease in degree of saturation. The value of angle ϕ_G^b decreases

compared to the friction angle ϕ_G' as the soil desaturates. Beyond residual degree of saturation the increase in suction produces a very little increase in shear strength. Thus the value of angle ϕ_G^b is fairly constant beyond residual water content. Thus it can be assumed that the value of parameter β will be fairly constant beyond a residual degree of saturation. Fredlund and Rahardjo (1993) pointed out that relationship of β in equation 4.7 is only applicable to evaluation of shear strength of soil. From practical engineering standpoint, it would appear to be better to use the (σ-u_a) and (u_a-u_w) stress state variables in an independent manner for designating the shear strength of unsaturated soil.

4.6   Shear Strength and Matric Suction

For the range of suctions studied, the shear strength was found to increase with an increase in suction. This behaviour was similar to observations made by Fredlund et al, (1996) which was true particularly at low normal stresses. According to Vanapalli et al, (1996) rate at which shear strength changes in unsaturated soil is related to area of water (water menisci are in contact with soil or aggregate). At saturation stage there is no reduction in area of water. Under this condition single stress state variable (σ -u_w) describes behaviour of soil. When the soil desaturates, the water content reduces significantly with increase in suction. The amount of water at the soil particle or aggregate contacts reduces as desaturation continues.

There is linear increase in shear strength with increase in matric suction of soil up to air entry value. The rate of desaturation with respect to matric suction is greatest between air entry value and suction corresponding to residual water content conditions. There is a non linear increase in shear strength in this region. The non linearity of shear strength envelope with matric suction is result of diminishing contribution of matric suction to shear strength as the water content of soil approaches residual water content. In present study the soil used is silty sand and it desaturates faster compared to clay and hence the shear strength will decrease at matric suctions higher than the residual matric suctions. This is due to the fact that at residual suctions, very little water is left in the soil pores and hence large increase in suction will not result in large increase in shear strength. Hence for the present set of tests it is predicted that there will be very little increase in shear strength at higher matric suctions.

Gan and Fredlund, (1996) mentioned that the shear strength is function of two area variables, A_0 and A_u, where A_0 is total area contribution from soil and water in saturated soil and A_u is total area contribution from soil and water in unsaturated soil. Low normal stresses were used in this study and it is possible that dilation of soil may have taken place. On one hand dilation increases shear strength due to interlocking effects and on the other hand dilation during shear tends to decrease the contribution of matric suction to shear strength because of disruption of water phase. Hence it is predicted that in present study, dilation of soil particularly for tests conducted at low water contents (high dry densities) may have contributed to increase in shear strength.

4.7 Summary

This chapter presented the results for the test conducted as discussed in Chapter 3. it was observed that the results obtained in terms of effective stress did not make sense. Due to this unsaturated soil mechanics principles were used to analyse these results. Further the role of degree of saturation was also addressed. Finally the effect of matric suction on shear strength was discussed.

Chapter 5   Analysis of Results

5.1   Introduction

This chapter presents a detailed analysis of the test results. As mentioned in Chapter 1, the study of interfaces is complicated due to presence of geomembrane (a polymer material other than soil) hence there is need to study the interface shear behaviour from Tribology (the science of the mechanisms of friction, and wear of interacting surfaces, geomembrane in this case) point of view. This chapter investigates the possibility of other controlling mechanisms for the interface shear behaviour of smooth geomembrane and soil and studies the interface from Tribology point of view.

5.2   Detailed Analysis of Test Results

As noted in Chapter 4, the interface shear strength is influenced by value of parameter β. Because of this it was decided to calculate interface shear strength values using equation 4.6 and different values of β. The value of β was adjusted so that the root mean square error between measured and calculated interface shear strength was minimum. Spreadsheets were used to do this analysis and to obtain the optimum value of β. For a given test, same value of β was used for all normal stresses.

Figure 5.1 shows the variation in measured and calculated shear stress values for the silty sand–geomembrane interface shear test at 8 % water content. Different values of β are chosen by trial and error and corresponding root mean square (RMS) error is obtained between calculated and measured shear stress and the value corresponding to smallest RMS error was selected to calculate the interface shear strength. In this particular example smallest value of RMS error which is 1.84 is obtained for a β value of 1.11.

Using the same approach as discussed above, values of β were obtained for all the tests. The resulting β values ranged from 0.4 to 2.1 for the various test series. Figure 5.2 shows a plot of measured versus calculated shear stresses for various tests using the values of β selected as described earlier.
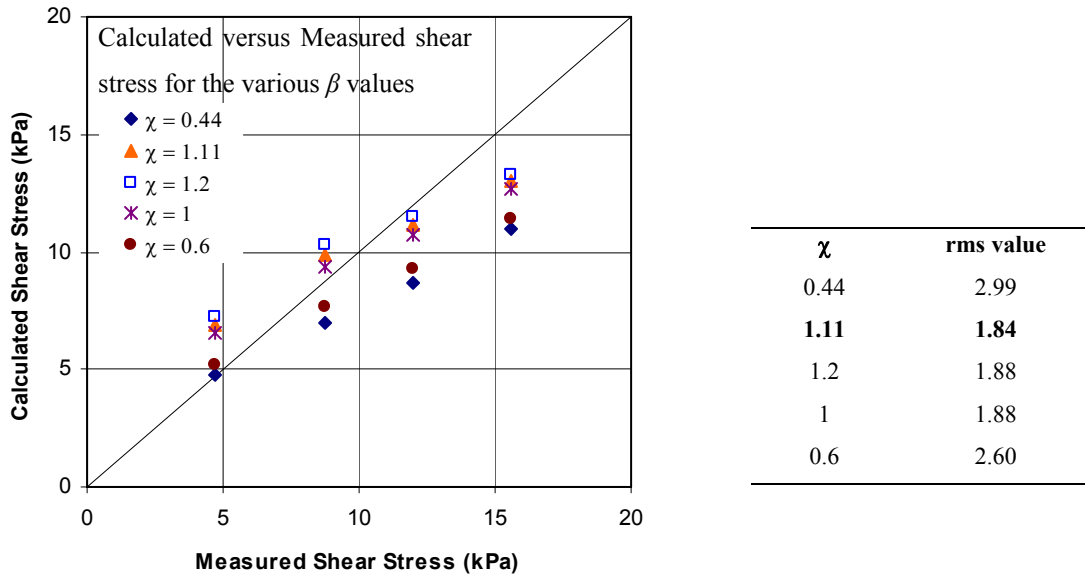
Figure 5.1 Measured versus calculated shear stress for unsaturated sandy silt interface [Test specifications: 8% moisture content; bulk density of soil 2132 kg/m3].
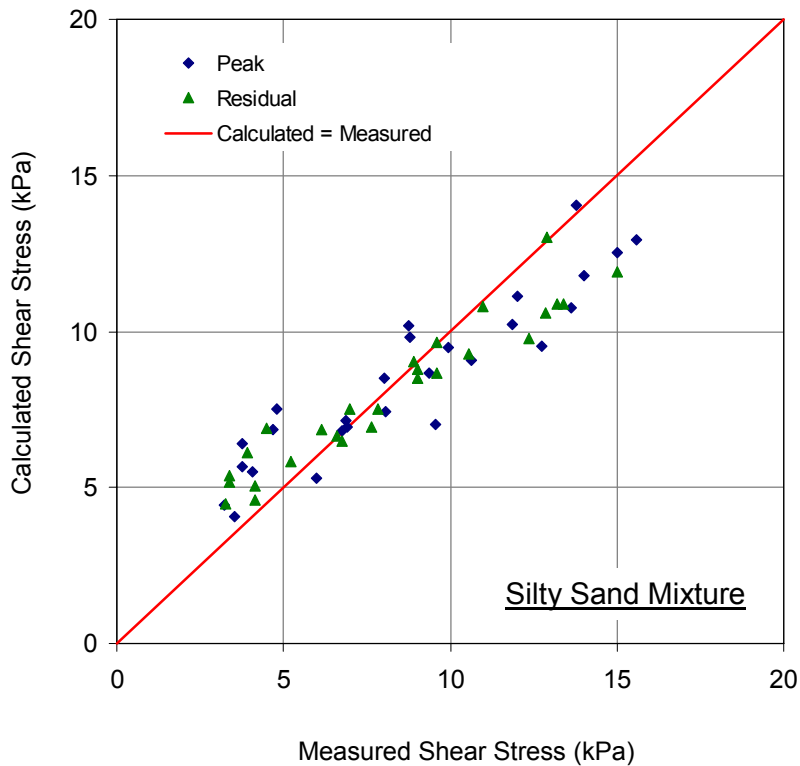
Figure 5.2 Measured vs. Calculated Shear Stresses [All tests using Silty Sand Mixture].

It is evident from Figure 5.2 that despite adjusting the β value (even to greater than 1) to obtain a calculated shear stress value close to the measured shear stress value, equation 4.6 can not adequately predict the measured shear stresses. At low normal stress ($\leq$ 12 kPa), Equation 4.6 overestimates the shear stress relative to the measured values whereas the reverse is true for high normal stresses ($\geq$ 20 kPa). Clearly, a constant β value for the entire range of normal stresses is not appropriate.

At low normal stresses, the soil exhibited slightly larger suction in most of the tests. Therefore, β values are likely to be lower at low normal stress. As the normal stress increases, soil suction decreases somewhat, likely reflecting some compression of the soil or accumulation of moisture at the interface; the effect is essentially to move the material upwards along the SWCC. It is therefore reasonable that β values should increase with increasing normal stress. If lower β values are used for low normal stresses and higher β values for the higher normal stresses, it is possible to achieve a perfect match between calculated and measured shear stress; i.e. calculating β for each stress increment (individual test) rather than minimising RMS error for an entire series of tests. This approach was taken and the results obtained are presented in Figure 5.3.
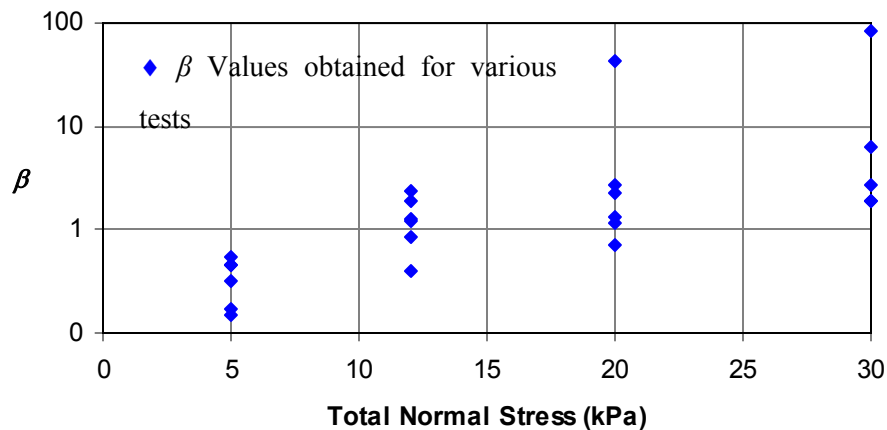
Figure 5.3 Values of β needed to achieve perfect matching between measured and calculated shear stresses [All tests using Silty Sand Mixture].

This procedure, however, results in unrealistically high β values greater than 2 at normal stresses ≥ 20 kPa as shown in Figure 5.3. For example, a β value between 2 and 90 was needed for tests conducted at 30 kPa normal stress. It is therefore inferred that the shear strength model represented by equation 4.6 is appropriate only for low normal stresses. Fredlund and Rahardjo (1993) mentioned that β relationship (in equation 4.7) is only applicable to evaluation of shear strength of soil. From practical engineering standpoint, it would appear to be better to use the (σ-u_a) and (u_a-u_w) stress state variables in an independent manner for designating the shear strength of unsaturated soil. At high normal stresses, it is likely that a different mechanism of failure occurs. The possibility of a different failure mechanism is investigated in next section.

5.3   Possibility of a Different Failure Mechanism

As mentioned in earlier section, it is difficult to analyse the test results using unsaturated soil mechanics principles. It is suspected that at high normal stresses, the shear failure may not take place at the soil-geomembrane interface but within the geomembrane itself. For a sandy soil, it is easy to imagine soil particles embedding themselves in the geomembrane when a normal stress is applied at the interface. If such embedding occurred, the particles would have to "plough" through the geomembrane material during the shearing process. Zettler et al. (2000) reported the occurrence of such a failure mechanism at the soil-geomembrane interface. Deatherage et al, (1987) has also mentioned that at high normal stresses there is increase in particle embedment in geomembrane surface resulting in higher friction angle values. Indeed, if "ploughing" is the dominant mechanism at the soil-geomembrane interface, soil suction would have little if any role in the interpretation of test results. This is described in detail in later sections of this chapter.

5.3.1   *Profile of a Typical Soil Particle in case of Soil Only and Soil-Geomembrane Interface*

Figure 5.4 shows the typical profile of soil particles in case of normal soil and in contact with the surface of geomembrane. In case of normal soil the particle 'c' is surrounded by other soil particles and typical elements of a soil matrix like water air, capillaries, etc. the same type of forces act on this particle in all directions. However, in case of the soil particle in contact with a geomembrane the particle is in contact with geomembrane on one side. Due to this the manner in which different forces act on this soil particle is non-uniform. In general, the profile of a soil particle in normal condition and in case of interface that is in contact with a geomembrane is

quite different (Figure 5.4) and hence the analysis gets more complex. Further the failure is combinations of plowing of soil particles into geomembrane surface, sliding, clay particle reorientation and other different mechanisms. It is quite difficult to account for all of those mechanisms using the principles of unsaturated soil mechanics.

(a)   (b)
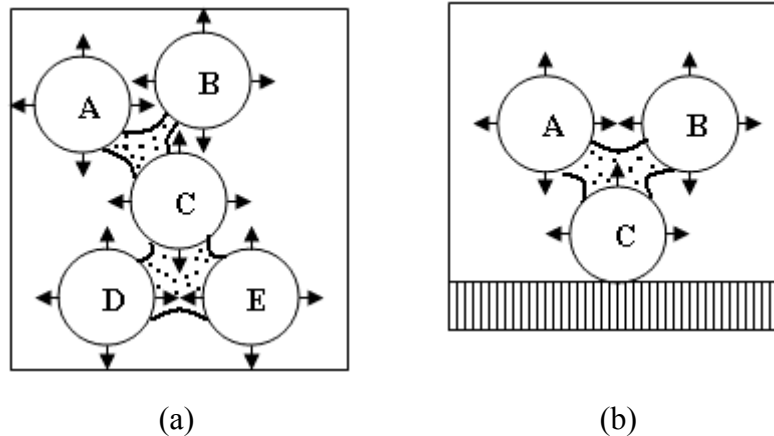
Figure 5.4 Profile of a typical soil particle in case of (a) soil only and (b) soil-geomembrane interface

5.3.2 *Necessity for Surface Roughness Measurement*

Williams and Houlihan (1987) studied the various soil geomembrane interface properties using a modified direct shear apparatus. They found that the magnitude of interface friction depends upon the surface roughness, tensile strength and modulus of geomembrane; the type composition, particle size and water content of the soil. The surface topography of geomembrane affects the interface shear strength and hence a change in surface topography will directly influence the shear strength of the interface. Dove and Frost (1996) mentioned that the surface topography of a geomembrane is potentially damaged by the plowing of soil particles, and this may result in surface wear.

The value of friction angle for silty sand as obtained from the direct shear test was about 31^0. Based on those values, it can be seen that the value of efficiency of the interface (ratio of friction angle of interface to the friction angle of soil only without geomembrane) was less than 1. This indicated that the failure was not taking place inside the soil but was occurring at the geomembrane surface. A relative movement (slip) between the soil and the geomembrane likely occurred at the surface of geomembrane. Such movement of soil particles at the geomembrane would result in some damage to the surface of geomembrane. Because of this it was decided to

study the extent of damage to the geomembrane samples after the failure. For this additional interface shear tests were carried out. For these particular tests surface roughness measurements of geomembrane samples was done before and after the interface shear test. Surface roughness measurements were carried out in machine direction and cross machine direction of the geomembrane.

5.3.3   Method for Geomembrane Surface Roughness Measurement

Development of a viable profiling method and a quantitative roughness measure are necessary first steps toward using surface characteristics for describing and predicting interface behaviour, and designing interfaces for specific purposes (Dove and Frost, 1996). It is also reported that non-textured geomembranes have a significant surface topography when observed to a correct scale. The surface roughness measurement in this study was conducted using a surface profilometer. The parameter 'R_a' (unit microns) was used to report the surface roughness. Surface roughness measurements were carried out on the geomembrane samples before and after the interface shear testing. The change in surface roughness ΔR (in %), was calculated as

$$\Delta R = \frac{[R_a]_{after} - [R_a]_{before}}{[R_a]_{before}} \times 100$$

[Eq. 5.1]

5.3.4   Details of Geomembrane Surface Topography Changes

As mentioned by Dove and Frost (2000) the surface roughness change in case of geomembrane is primarily a function of sliding and plowing of the soil particles. Further the tendency of soil particles to induce wear on geomembrane surface depends upon applied normal load and properties of the interface materials which may include the shape of particles and hardness of the geomembrane into consideration. If the geomembrane is hard by nature the particle will take more energy to plow into the surface of geomembrane and vice versa. However most of the soil particles encountered are harder than the relatively soft non-textured HDPE geomembrane.

Figure 5.5 shows the variation in ΔR with normal stress for various geomembrane-soil interfaces. It can be seen that surface roughness increases significantly with increase in magnitude of normal stress applied. The rate of increase of surface roughness is higher for higher normal stresses. For interface shear testing using dry sand, this increase is more than 30 % at 30

kPa normal stress. It is likely that at low normal stresses, the soil particles "slide and scratch" the geomembrane surface during shear whereas at high normal stresses, these particles embed themselves within the geomembrane surface and "plow" it during shear. The change in surface roughness is less at higher water content as compared to the lower water content. The effect of water content on change in surface roughness is described later in this section. The result of surface roughness tests shows that the failure of geomembrane is taking place.
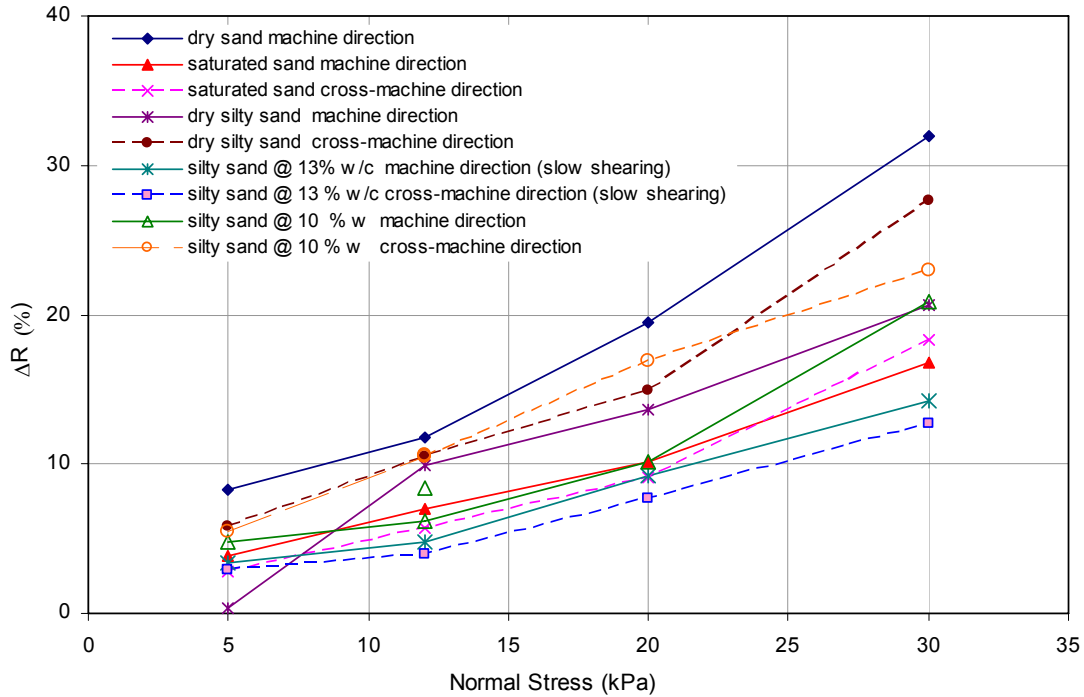
Figure 5.5 Change in surface roughness of geomembrane at various normal stress values

The depth of the trenches being plowed by soil particles depends on the shape and the angularity of soil particles, the density of soil and the normal stress at the points of contact between soil particles and the geomembrane surface. At higher normal stresses, the depth of embedment of soil particles is greater, resulting in deeper trenches being plowed during shear. The deeper the trench, the greater is the change in surface roughness of the geomembrane surface and vice versa. Also, plowing of deeper trenches would require higher shear stresses at the interface. This could be the reason for high interface shear strengths at high normal stresses.

Less work is needed to be done by the particles due to larger contact stresses at higher normal stresses. The geomembrane was glued to the plexiglass block and hence the work

required by the soil particles might be less compared with the anchored geomembrane. In case of anchored geomembrane the geomembrane has scope for movement relative to the plowing soil particles. For a fixed geomembrane, as was in this study there is neligible movement of geomembrane with respect to the plowing particles. After shearing the surface of geomembrane was no longer smooth. The surface of geomembrane was found to be visibly damaged at the end of test. Sliding and plowing was found to be the primary mechanism for geomembrane failure as mentioned by Dove and Frost, (1999).

5.3.5 *Effect of Water Content on Geomembrane Surface Roughness Change*

Figure 5.6 shows the variation of ΔR with water content. It can be observed that in general the change in surface roughness decreases with increase in water content. At lower water content the change in surface roughness is comparatively more than change in surface roughness in case of saturated interfaces or at high water contents.
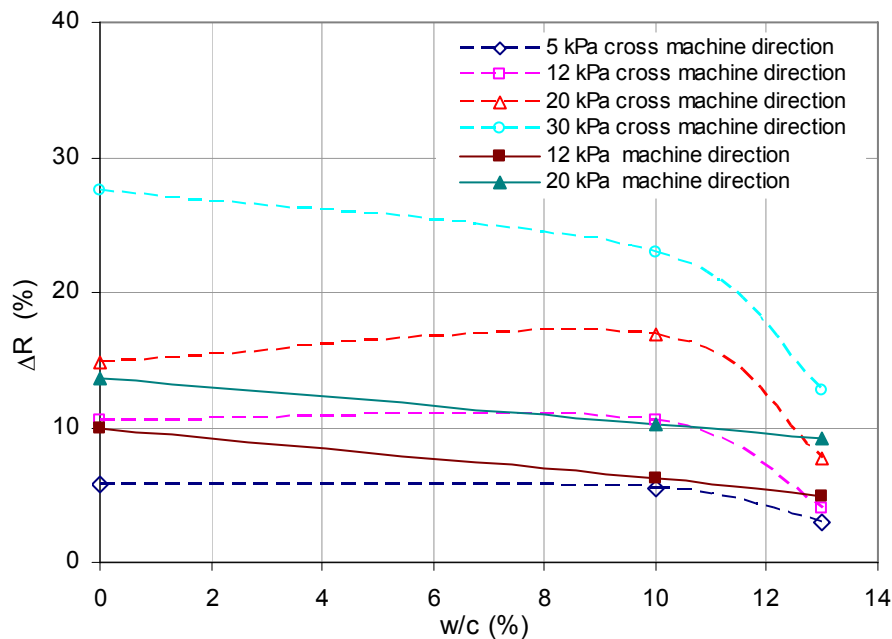
Figure 5.6 Variation of change in surface roughness of geomembrane with water content (For Silty sand interfaces at various water contents)

The placement water content, *w*, also appears to affect the change in surface roughness of the geomembrane as shown in Figure 5.6. At lower values of *w*, there is greater suction within the soil, resulting in higher effective normal stresses at the geomembrane-soil interface. This, in turn, results in deeper embedment of soil particles and plowing of deeper trenches, thereby increasing the surface roughness considerably. At higher values of *w*, nearly saturated conditions prevail at the geomembrane-soil interface, resulting in lower effective normal stresses, lower depth of embedment of soil particles, and therefore, lower change in surface roughness and lower mobilized interface shear strength.

For the saturated interfaces the presence of water film on surface of geomembrane prevents the plowing of soil particles slightly by providing a more smooth and lubricated geomembrane surface in addition to this it prevents the direct contact of soil particles with surface of geomembrane. This results in decrease in change in surface roughness with increase in moisture content of the compacted soil. This behaviour was observed for most of the tests (Figure 5.6). For the test conducted at 12 kPa, value of ΔR under dry conditions is comparatively less. This may be due to possible error in surface roughness measurement.

5.4 Summary

A detailed analysis of all the test results was done in this chapter. The limitations of the unsaturated soil mechanics principles at higher normal stresses were discussed. Further the interface shear behaviour of geomembrane-soil interfaces was analysed from the point-of-view of tribology. Chapter 6 presents the conclusions that can be drawn based on this study and various recommendations that can be made to the industry and designers based on this study.

Chapter 6   Conclusions and Recommendations

6.1   Summary

The objectives of this study are mentioned in section. The study was done in order to evaluate the effect of the suctions on interface shear behaviour and investigation of possible other mechanisms that may play an important role in the shear strength of smooth geomembrane-soil interface. To achieve these objectives, the study was divided into four parts.

- Development of an apparatus/method to evaluate the effect of soil suction on interface shear behaviour.
- Analysis of the test results in terms of total stress space and effective stress space.
- Analysis of test results using principles of unsaturated soil mechanics and the feasibility of applying these principles for analysis.
- Study of interface shear behaviour from the point of view of tribology.

In Chapter 2 a comprehensive literature review was presented along with some fundamental principles related to shear strength of unsaturated soil mechanics. Chapter 3 provided the details of the test set up and the materials used. Chapter 4 presented the results obtained from the various tests carried out. A detailed analysis of the test results was carried out in Chapter 5. Role of other possible mechanisms contributing to interface shear behaviour of geomembrane-soils was also discussed in Chapter 5.

6.2   Conclusions

6.2.1   Development of Interface Shear Testing Method

A method has been developed to evaluate the effect of soil suction on the soil-geomembrane interface shear strength parameters particularly under unsaturated conditions. The method utilizes a miniature pore pressure transducer installed at the soil-geomembrane interface to record soil suction during shearing process, thus making it possible to analyze the test results in terms of

effective stresses. The method is simple, economical and requires only a few simple modifications to a standard direct shear box. The method was tested using different soils (sand, sand/bentonite mixture and silty sand mixture) and it was found to give reliable results at low soil suction values.

6.2.2 Effects of Various Parameters on Interface Shear Behaviour

For the various sand bentonite mixture- geomembrane interface combinations tested it was observed that the interface friction behaviour is governed by the dry density of the compacted soil bentonite mixture and to a lesser extent by the rate of displacement. For the range of densities tested it was observed that the interface friction angle increases with increase in density of the soil. Over the range of rates of displacement used, it was found that the interface friction angle increases slightly with increases in the rate of displacement, although this effect was less prominent than the effect of density. The interface friction angle was found to be relatively more sensitive to the compaction water content as compared to density of compacted soil or the rate of displacement. It was difficult to isolate the effect of compaction water content as the tests carried out for this particular set of data were done using bulk density of compacted soil. However based on the published literature and some of the tests it is predicted that interface friction angle decreases with increase in moisture content of the compacted soil.

6.2.3 Analysis of Test Results in terms of Total and Effective Stresses

It was found that plotting the interface shear strength values against applied total normal stress values gives interface shear strength envelopes that are consistent with those published in literature. However, a similar plotting in terms of effective normal stress values as obtained from applied total normal stress and measured pore-water pressure values, proved to be difficult. For failure envelopes in effective stress space negative adhesions and steep slopes were obtained.

6.2.4 Analysis of Test Results using Unsaturated Soil Mechanics Principles

At low normal effective stresses, it was possible to predict interface shear strength values using unsaturated soil mechanics concepts and matric suctions measured in the vicinity of geomembrane soil interface during the shearing process. At high normal stresses, the use of unsaturated soil mechanics concept resulted in calculated shear strength values that were significantly lower than the measured values. Based on interface shear tests carried out, it was

found that at low normal stresses the soil suction affects the mobilization of shear stresses at the soil-geomembrane interface; however it is not straightforward to incorporate measured soil suction values in the interpretation of interface shear test results. Due to complex nature of the interfaces involving smooth geomembranes and soils under unsaturated conditions and the various factors involved , principles of unsaturated soil mechanics an not be easily applied in analyzing this type of interfaces.

6.2.5 The β Parameter

For the limited amount of tests carried out in this study, it was observed that the value of parameter β is proportional to the degree of saturation. It was 1 for the saturated interface conditions and it decreased with decrease in degree of saturation. For a series of tests carried out at near-constant moisture content and bulk density, it was found that in order to match the observed shear stress values, a constant value of parameter β (i.e. constant value of ϕ^b) is not satisfactory; the apparent variation of β with total normal stress must be taken into account. It would not, therefore, be typically possible to establish the magnitude of effective normal stress at the interface and test results could only be interpreted in terms of total normal stress. At normal stress greater than 20 kPa, test results could not be interpreted using the shear strength equation for unsaturated soils. Application of the equation to calculate shear strength at the interface resulted in unusually high values of β.

6.2.6 Other Possible Mechanisms

An examination of the change in surface roughness of the geomembrane surface confirmed that the failure mechanism changed from a sliding mechanism (sliding of soil mass on geomembrane surface) to plowing mechanism (formation of trenches along the shearing direction) at high normal stresses. Soil particles were getting embedded into geomembrane surface. As a result, additional shear strength was getting mobilized at the interface over and above the one mobilized by standard frictional sliding. Sliding and plowing was found to be the dominant mechanism for the failure of the geomembrane surface.

6.2.7 Factors Controlling the Changes in Surface Roughness of Geomembrane

The magnitude of the failure of the geomembrane is controlled by the size and shape of particle, normal stress. The effect of other parameters like density and rate of displacement could not be

determined due to limited amount of testing carried out. However it is speculated that at for same conditions the magnitude of surface roughness failure is greater at higher densities due to the fact that large number of particles are in contact with geomembrane at higher normal stresses. The normal load does have a significant impact on the surface damage of the geomembrane. This is because at higher normal stresses particle can easily plow into the geomembrane surface. Less work is needed for plowing, to be done by the particles due to larger contact stresses at higher normal stresses. The water content also influences the failure of geomembrane surfaces. At higher water content the film of water provides a lubricated surface for the soil particles to slide easily. Further presence of water helps in providing smooth and lubricated surface of the geomembrane which results in somehow reduced plowing.

6.3   Limitations

1. The pore pressures were measured close to the centre of soil specimen. Due to this the pore pressure profile at edge of soil specimen was not known. There is possibility of large pore pressure accumulation at the edge of soil specimen compared to the centre of soil specimen and pore pressure may be different at the edge of soil specimen than at the centre of soil specimen.

2. The shearing takes place over a predetermined shear plane. This forced plane may not necessarily the weakest one especially in actual field conditions.

3. The testing was carried out at relatively low normal stresses and hence the results can not be generalised for the high normal stresses.

4. The PPT has to be saturated in order to measure the pore pressures effectively and hence the PPT can not be used at very low water contents.

5. The stone at the tip of PPT tends to get desaturated with time and depending on surrounding soil conditions and hence prior testing should be conducted in similar environments in order to determine the response of the PPT for a particular set of conditions.

6. The PPT can not be used for very long durations and hence slow rates (resulting in longer run time for a test) of displacement can not be used in the interface shear testing.

7. The repeatability in this type of testing using a PPT to measure the pore pressures is less compared to traditional interface shear testing (except in case of saturated interfaces). This is because the way PPT responds depends on several factors which are difficult to control.

6.4   Recommendations

6.4.1   Recommendations for Low Normal Stress Applications

Based on limited tests carried out it was observed that suction contributes to shearing resistance especially at low normal stresses. For low normal stress applications such as landfill covers, if a high friction coefficient is required for a smooth geomembrane it is recommended that soils with angular particles should be used. This is due to the fact that less work is needed by the angular particles to plow geomembrane surface and plowing can be possible at relatively low normal stresses which also helps to achieve additional interface shear strength.

6.4.2   Recommendations for High Normal Stress Applications

At higher normal stresses soil particles gets embedded into surface of geomembrane and plow trenches along the geomembrane surface. Hence at higher normal stresses additional shear strength gets mobilized at the interface over and above the one mobilized by standard frictional sliding. Hence use of classic sliding failure mechanism for geomembrane soil interface at high normal stress may be conservative.

The shear mechanisms and resulting friction coefficients of smooth geomembrane-soil interfaces depend considerably upon combination of normal load and material characteristics. At very high normal stress applications such as reservoirs, landfills of high capacity landfills and with use of coarse and angular material, it is strongly recommended that thick geomembranes should be used to reduce the influence of damage due to particle plowing or indentation on the system. This will also help in taking the advantage of additional interface shear strength available de to the effect of plowing.

6.4.3   Other Recommendations

Based on the findings of this work, it is suggested that a smooth geomembrane should be designed (may be using a special composite material) having a special surface and thickness which will encourage plowing of soil particles resulting in increased interface friction angle.

Most of the geosynthetic engineers are geotechnical engineers and hence they obviously make use of geotechnical principles in design with geosynthetics. However it is suggested that proper design values that are supported by testing carried out at site specific conditions should always

used and caution should be exerted when using the principles of soil mechanics in designing with geomembranes.

6.5   Suggestions for Future Research

Further research is needed in this area to better understand what happens at the interface and how this is influenced by various factors. In addition to laboratory data it will be useful to obtain relevant field data involving pore pressure distribution etc.

Future research should focus on how various parameters can influence the surface topography of geomembrane, the extent of this influence, and how these factors influence the behaviour of the interface in actual field.

It is also recommended that PPT should be installed at edges of specimen in addition to the one at the centre of specimen. This will give a better idea about the pore pressure profile. The efficiency of PPT can be improved with development of new techniques and this should be taken into account and best methods should be adopted to keep the PPT saturated for longer time and capable of measuring suction of higher magnitudes. Different methods should be tried to make the use of PPT as efficient as possible.

Hardness of geomembranes play an important role in geomembrane surface topography changes and hence research should also involve the characterization of hardness of the geomembrane in relation to interface friction behaviour.

References

Arya, L.M. and Paris, J.F. 1981. A physico-empirical model to predict the soil moisture characteristic from particle-size distribution and bulk density data. Soil Science Society of America Journal, 45: pp 1023-1030.

ASTM 2000. D698-00ae1: Standard Test Methods for Laboratory Compaction Characteristics of Soil Using Standard Effort (12,400 ft-lbf/ft^3 (600 kN-m/m^3)). American Society for Testing of Materials, West Conshohocken, PA, USA.

ASTM 2002. D5321-02: Standard Test Method for Determining the Coefficient of Soil and Geosynthetic or Geosynthetic and Geosynthetic Friction by the Direct Shear Method. American Society for Testing of Materials, West Conshohocken, PA, USA.

Bachus, R.C., Soderman, K.L., and Swan, R.H., 1993. Factors which affect the soil/geosynthetic and geosynthetic/geosynthetic interface shear strength for materials used in landfill lining systems. Proceedings of the 1993 Annual Meeting of the South Florida Section of ASCE, Naples, 1993, pp. 28-38.

Bemben, S.M. and Schulze, D.A. 1993. The influences of selected testing procedure on soil/geomembrane shear strength measurements, Proceedings of Geosynthetics '93 conference, Vancouver, Canada, pp. 1043-1056.

Bemben, S.M. and Schulze, D.A. 1995. The influence of selected testing procedures on soil/geomembrane shear strength measurements. *In* Proceedings of the Geosynthetics'95 Conference, Nashville, USA. pp. 1043-1056.

Bishop, A.W. 1959. The principle of effective stress. Lecture delivered in Oslo, Norway in 1955; published in Teknisk Ukeblad, **106** (39): pp. 859-863.

Blumel, W. and Stoewahse, C. 1998. Geosynthetics interface friction testing in Germany- effect of test setups, Proceedings of 6th international conference on geosynthetics, Atlanta , Georgia, USA

Bove., J.A. 1990. Direct shear friction testing for geosynthetics in waste containment. Geosynthetic testing for waste containment applications. American Society for Testing of Materials Special Technical Publication No. 1081. *Edited by* R. M. Koerner. American Society for Testing of Materials, West Conshohocken, PA, USA pp. 241-256.

Byrne, R.J., Kendall, J., and Brown, S., 1992. Causes and mechanism of failure, Kettleman Hills landfill B-19, unit IA, Stability and performance of slopes and embankments-II, Seed R.B. and Boulanger, R.W., editors, Geotechnical special publication no. 31, ASCE, 1992, Proceedings of speciality conference held in Berkeley, CA, USA, Vol. 2 pp. 1188-1215.

Deatherage, J. David, J. R. and Hansen, L. A. 1987. Shear Testing Of Geomembrane Soil Interfaces. Geotech Asp of Heap Leach. Design. Society of Mining Engineers1987, pp. 45-50

Dove J. E., Frost J. D., Han J. and Bachus R. C. 1997. The influence of geomembrane surface roughness on interface strength. Proceeding of Geosynthetics '97, Long Beach, CA. North American Geosynthetics society.

Dove J.E. and Frost, J.D. 1999. Peak friction behaviour of geomembrane particle interfaces. ASCE Journal of Geotechnical and Geoenvironmental Engineering. **125** (7): pp 544-555

Ellithy, G.S. and Gabr, M.A. 2000. Compaction moisture effect on geomembrane/clay interface shear strength. Geotechnical Special Publication, n 103, 2000, pp 39-53

Esterhuizen, J.J.B., Filz, G.M., Duncan, J.M., 2001. Constitutive behavior of geosynthetic interfaces. ASCE Journal of Geotechnical and geoenvironmental Engineering, **127**(10): pp. 834-840.

Evans, W.D., Stark, T.D., Wilson, V.L. and Gonda, J.M. 1998, Design consideration of geosynthetic clay liners. Proceedings of 20th International Madison Waste Conference, University of Wisconsin, Madison, pp.203-28.

Fishman, K.L. and Pal, S. 1994. Further study of geomembrane / cohesive soil interface shears behaviour'. Geotextiles and Geomembranes, **13** (9): pp. 571-590

Fox, P.J., Rowland, M.G., Scheithe, J.R., Davis, K.L., Supple, M.R. and Crow, C. 1997. Design and evaluation of a large direct shear machine for geosynthetic clay liners. American Society for Testing of Materials Geotechnical Testing Journal, **20** (3): pp. 279–288.

Fredlund, D.G. & Xing, A. 1994. Equations for the soil-water characteristic curve. Canadian Geotechnical Journal, **31**: pp. 521-532.

Fredlund, D.G. and Rahardjo, H. 1993. Soil Mechanics for Unsaturated Soils. John Wiley and Sons, New York.

Fredlund, D.G., Xing. A., Fredlund, M.D. and Barbour, S.L. 1995. The relationship of the unsaturated soil shear strength to the soil-water characteristic curve. Canadian Geotechnical Journal. **33**(3)**:** pp 440-448.

Fredlund, M.D., Wilson, G.W. & Fredlund, D.G. 2002. Use of grain size distribution for estimation of the soil-water characteristic curve. Canadian Geotechnical Journal, **39**: pp.1103-1117.

Gan, J. and Fredlund, D.g., 1996. Shear strength characteristics of two saprolitic soils. Canadian Geotechnical Journal, **33**: pp.595-609.

Gilbert, R. B. and Bryne, R. J. 1996. Strain-softening behavior of waste containment system interfaces.'' Geosynthetics International., **3**(2):pp. 181–203.

Giroud, J.P. Darrasse, J. and Bachus, R.C. 1989. Hyperbolic expression for Soil-Geosynthetic or Geosynthetic-Geosynthetic interface shear strength. Geotextiles and Geomembranes. **12** (3): pp 35-46.

Gomez J.E. and Filz, G.M. 1999, Effects of consolidation on strength of the interface between a clay liner and smooth geomembrane. Proceedings of Geosynthetics '99 conference, Boston, USA, pp. 681-696.

Goodhue, M.J., Edil, T.B. and Benson, C.H. 2001. Interaction of foundry sands with geosynthetics'. ASCE Journal of Geotechnical and Geoenvironmental Engineering. **127**(4):pp. 353-362.

Jones, D.R.V. & Dixon, N. 1998. The stability of geosynthetic landfill lining systems. *In* Geotechnical engineering of landfills. *Edited by* N. Dixon, E.J. Murray and D.R.V. Jones. Thomas Telford, London, UK. pp. 99-117.

Koerner, 2003. A recommendation to use peak shear strengths for geosynthetic interface design. Geosynthetics Fabrics Report, April, 2003.

Koerner, R. M. and Soong, T.Y. 2000, Stability assessment of ten large landfill failures. Advances in Systems using Geosynthetics, Geotechnical Special Publication, No. 103, ASCE, 2000: pp. 1-38.

Koerner, R.M. 1998. Designing with Geosynthetics. Prentice-Hall Inc., Englewood Cliffs, N.J.

Koutsourais, M.M., Sprague, C.J. and Pucetas, R.C. 1991, Interfacial friction study of cap and liner components for landfill design. Geotextiles and Geomembranes, **10**, pp 531-548.

Lambe, T.W. and Whitman, R.V., 1969. Soil Mechanics. John Wiley and Sons.

Ling, H.I., Pamuk, A., Dechasakulsom, M., Mohri, Y. and Burke, C. 2001. Interaction between PVC geomembranes and compacted clays. American Society of Civil Engineers Journal of Geotechnical and Geoenvironmental Engineering, **127** (11): pp. 950-954.

Meilani. I., Rahardjo. H., Leong, E.C. & Fredlund D.G. 2002. Mini suction probe for matric suction measurement. Canadian Geotechnical Journal, **39**: pp. 1427-1432.

Mitchell, J.K., Seed, R.B. & Seed, H.B. 1990. Kettleman Hills waste landfill slope failure – I: Liner-system properties. American Society of Civil Engineers Journal of Geotechnical Engineering, **116** (4): pp. 647-668.

Muraleetharan, K.K. & Granger, K.K. 1999. The use of miniature pore pressure transducers in measuring matric suction in unsaturated soils. American Society for Testing of Materials Geotechnical Testing Journal, **22** (3): pp. 226-234.

O'Rourke T. D., Druschel S. J. and Netravalli A. N. 1990 Shear strength characteristics of sand-polymer interfaces. ASCE Journal of Geotechnical Engineering. **116** (3):pp. 451- 469

Rowe, R.K., Ho, S.K. and Fisher, D.G. 1985. Determination of soil-geotextile interface strength properties. Proceedings of the 2nd Canadian symposium on Geotextiles and Geomembranes, Edmonton. BiTech Publishers Limited, Vancouver, Canada.

Seed, R.B. & Boulanger, R.W. 1991. Smooth HDPE-clay liner interface shear strengths: Compaction effects. American Society of Civil Engineers Journal of Geotechnical Engineering, **117** (4): pp. 686-693.

Seed, R.B., Mitchell J.K. & Seed, H.B. 1990. Kettleman Hills waste landfill slope failure – II: Stability analysis. American Society of Civil Engineers Journal of Geotechnical Engineering, **116** (4): pp. 669-689.

Sharma, J.S. and Bolton, M.D. 1996. Centrifuge modelling of reinforced embankments on soft clay reinforced by geogrids. Geotextiles and Geomembranes, **14**: pp. 1-17.

Simpson, B. E. 2000. Five factors influencing the clay/geomembrane interface. Geotechnical Special Publication, n 46/2, pp 995-1004.

Smith, M.E. and Criley, K. 1995. Interface shear strength is not for the uninitiated. Geotehnical Fabrics Report, April, 995.

Stark, T. D. and Poeppel, A. R. 1994. Landfill liner interface strengths from torsional-ring-shear tests'. American Society of Civil Engineers Journal of Geotechnical Engineering, **120** (3): pp. 597-617.

Stark, T.D., Eid, H.T., Evans, W.D., and Sherry, P. (2000). "Municipal Solid Waste Slope Failure II: Stability Analyses," ASCE Journal of Geotechnical and geoenvironmental Engineering, **126** (5): pp. 408-419.

Stark, Timothy D., Poeppel, A.R. 1994. Landfill liner interface strengths from torsional-ring shear tests. American Society of Civil Engineers Journal of Geotechnical Engineering, **120** (3): pp. 597-617.

Stoewahse, C., Dixon, N., Jones, D. R., Blumel, W. and Kamugisha, P., 2002. Geosynthetic interface shear behaviour: part 1 Test Methods. Ground Engineeering, February 2002. pp 35-41.

Stoicescue, J.T. 1997. Properties of unsaturated sand-bentonite mixtures used for liners and covers. MSc Thesis. University of Saskatchewan, Saskatoon, SK, Canada.

Swan, R.H. Jr., Bonaparte, R., Bachus, R.C., Rivette, C.A., and Spikula, D.R. 1991. Effect of Soil Compaction Conditions on Geomembrane-Soil Interface Strength. Geotextiles and Geomembranes, **10** (5): pp. 523-529.

Taber, H.G. 2003. Tensiometer tips for vegetables. Department of Horticulture, Iowa State University , Ames, Iowa, USA.

Take, W.A. & Bolton, M.D. 2003. Tensiometer saturation and reliable measurement of soil suction. Géotechnique, **53** (2): pp. 159-172.

Vaid, Y.P. and Rinne, N. 1995. Geomembrane Coefficients of Interface Friction.. Geosynthetics International, **2**(1): pp. 309-325.

Van Genuchten, M.T. 1980. A closed form equation for predicting the hydraulic conductivity of unsaturated soils. Soil Science Society of America Journal, 44: pp 892-890.

Vanapalli, S.K., Fredlund, D.G., Pufhal, D. and Clifton, A.W., 1996. Model for prediction of shear strength with respect to soil suction. Canadian Geotechnical Journal, **33**: pp.379-392.

Von Pein, R.T. and Lewis, S.P. 1991. Composite lining system design issues. Geotextile and geomembranes, **10.** pp. 507-511

Williams, N.D. and Houlihan, M.F. 1986. Evaluation of friction coefficients between geomembranes, geotextiles and related products, proceedings from the 3rd International conference on Geotextles, 1986. OIAV Vienna, Austria.

Williams, N.D. and Houlihan, M.F. 1987, Evaluation of interface friction properties between geosynthetics and soils, proceedings of geosynthetics '87, IFAI, vol. 2, New Orleans, Lousiana, USA, February 1987, pp 616-627.

Zettler, T.E., DeJong, J.D. and Frost, J.T. 2000. Shear induced changes in smooth HDPE geomembrane surface topography. Geosynthetics International, **7**(3): pp. 243-267.